

TESIS DOCTORAL

Programa de doctorado:
Investigación Aplicada a las
Ciencias Sanitarias

Evaluación de potenciales compuestos antileucémicos de origen natural y sintéticos inspirados en productos naturales

Ester Gloria Saavedra Díaz

Las Palmas de Gran Canaria, 2020



ULPGC
Universidad de
Las Palmas de
Gran Canaria

UNIVERSIDAD DE LAS PALMAS DE GRAN CANARIA

ESCUELA DE DOCTORADO DE LA ULPGC

Bioquímica y Biología Molecular, Fisiología, Genética e Inmunología

PROGRAMA DE DOCTORADO

Investigación Aplicada a las Ciencias Sanitarias por La Universidad de Las Palmas de Gran Canaria y Universidad de León

Evaluación de potenciales compuestos antileucémicos de origen natural y sintéticos inspirados en productos naturales

Tesis Doctoral presentada por Dña Ester Gloria Saavedra Díaz

Dirigida por el Dr. Francisco Jesús Estévez Rosas y el Dr. José Martín Quintana Aguiar

La Doctoranda

El Director

El Director

Las Palmas de Gran Canaria, a 26 de noviembre de 2020

D. FRANCISCO JESÚS ESTÉVEZ ROSAS Y D. JOSÉ MARTÍN QUINTANA AGUIAR, CATEDRÁTICOS DE BIOQUÍMICA Y BIOLOGÍA MOLECULAR DE LA UNIVERSIDAD DE LAS PALMAS DE GRAN CANARIA

CERTIFICAN:

Que el trabajo de investigación titulado “Evaluación de potenciales compuestos antileucémicos de origen natural y sintéticos inspirados en productos naturales”, ha sido realizado por Dña. Ester Gloria Saavedra Díaz, en el Departamento de Bioquímica y Biología Molecular, Fisiología, Genética e Inmunología y en el Instituto de Investigaciones Biomédicas y Sanitarias (IUIBS) de la Universidad de Las Palmas de Gran Canaria, Unidad Asociada al CSIC, bajo su dirección y asesoramiento científico y técnico, y que una vez revisada la presente memoria, la encuentran apta para su defensa ante tribunal.

Y para que así conste y surta los efectos oportunos, extienden la presente certificación en Las Palmas de Gran Canaria a 26 de noviembre de 2020

El Director

El Director

Gracias a todos aquellos que hicieron de esta Tesis un bello camino que me cuesta dejar atrás, a los que me han enseñado a amar esta profesión y a los que han hecho posible este trabajo con su amor, apoyo y paciencia. Así mismo, hago extensivo este agradecimiento al Instituto Canario de Investigación del Cáncer por el contrato concedido como investigadora durante la realización de esta Tesis.

Índice

Abreviaturas.....	11
Resumen	15
Introducción.....	17
La leucemia	18
Importancia de los compuestos naturales y sus derivados.....	19
Flavonoides	20
Lactonas sesquiterpénicas	22
El ciclo celular.....	23
La apoptosis	25
Estrés oxidativo	29
El papel de los lisosomas y el retículo endoplasmático en la apoptosis.....	31
Proteínas quinasas activadas por mitógenos (MAPKs).....	33
Justificación	35
Objetivos.....	39
Publicaciones	41
1. 6-Benzoyloxy-4-bromo-2-hydroxychalcone is cytotoxic against human leukaemia cells and induces caspase-8- and reactive oxygen species dependent apoptosis	45
2. The synthetic flavanone 6-methoxy-2-(naphthalen-1-yl)chroman-4-one induces apoptosis and activation of the MAPK pathway in human U-937 leukaemia cells	55
3. Cytotoxicity of the sesquiterpene lactone spiciformin and its acetyl derivative against the human leukemia cell lines U-937 and HL-60	70

Conclusiones	85
Referencias.....	89

Abreviaturas

ADN	Ácido desoxirribonucleico
Apaf-1	Factor activador de proteasa apoptótica 1
ATP	Adenosín trifosfato
Bad	Proteína agonista de muerte celular asociada a Bcl-2
Bak	Proteína citotóxica antagonista de Bcl-2
Bax	Proteína pro-apoptótica X asociada a Bcl-2
Bfl-1/A1	Proteína anti-apoptótica A1 relacionada con Bcl-2 aislada de hígado fetal
Bcl-2	Proteína 2 de linfoma de células B
Bcl-xL	Proteína del linfoma de célula B extra larga
Bcl-W	Proteína anti-apoptótica de linfoma de células B-W
Bid	Agonista de muerte del dominio que interactúa con BH3
Bik	Proteína citotóxica que interactúa con Bcl-2
Bim	Mediador de muerte que interactúa con Bcl-2
Bmf	Factor modificador de Bcl-2
DR-4	Receptor de muerte 4
DR-5	Receptor de muerte 5
Fas	Receptor de muerte, también denominado Apo1 o CD95R
Fas-L	Ligando del receptor de muerte Fas
Hrk	Proteína pro-apoptótica de la familia Bcl-2 Harakiri
IAP	Proteína inhibidora de apoptosis
IC₅₀	Concentración de producto que inhibe la proliferación celular a la mitad

jun	Factor de transcripción de la familia AP-1
Mcl-1	Proteína anti-apoptótica de la familia Bcl-2
MEK	Proteína quinasa activada por mitógenos/ quinasa regulada por señales extracelulares
MLKL	Proteína similar al dominio de quinasa de linaje mixto
NOXA	Proteína pro-apoptótica de la familia Bcl-2 que inactiva a Mcl-1
p53	Proteína supresora de tumores
PMSF	Fluoruro de fenilmetilsulfonilo
Puma	Modulador de la apoptosis inducido por p53
RIP	Proteína de interacción con el receptor
ROS	Especies reactivas del oxígeno
Smac/DIABLO	Segundo activador de caspasas derivado de mitocondria
TNF	Factor de necrosis tumoral
TNFR	Receptor del factor de necrosis tumoral
TRADD	Dominio de muerte asociado al receptor de TNFR
TRAIL	Ligando inductor de apoptosis relacionado con TNF
XIAP	Proteína inhibidora de la apoptosis

Resumen

En la presente tesis doctoral se estudia la potencial actividad citotóxica de una selección de compuestos, mayoritariamente sintéticos, pertenecientes a dos grupos, los flavonoides y las lactonas sesquiterpénicas, frente a varias líneas celulares de leucemia humana.

Dentro del primer grupo de compuestos, se ha llevado a cabo el estudio de la citotoxicidad de una chalcona sintética seleccionada de una batería de casi cien compuestos analizados en estudios previos de nuestro grupo de investigación, y las relaciones estructura-citotoxicidad de naftil-chalconas y sus correspondientes compuestos cíclicos. En el grupo de las lactonas sesquiterpénicas analizamos los mecanismos de acción y de transducción de señales de la espiciformina presente en dos especies del género *Tanacetum* endémicas de las Islas Canarias, y su derivado acetilado.

Los productos seleccionados son potentes inductores de la apoptosis en la línea celular humana U-937. El proceso apoptótico estuvo asociado con el procesamiento y activación de las caspasas iniciadoras y ejecutoras, con la hidrólisis e inactivación de la poli(ADP-ribosa) polimerasa (PARP), y con la liberación de proteínas mitocondriales, incluidas el citocromo *c* y Smac/DIABLO. Las especies reactivas de oxígeno y las proteínas quinasas activadas por mitógenos están implicadas en la muerte celular. Las células mononucleares humanas aisladas de donantes sanos fueron más resistentes que las células tumorales a los efectos citotóxicos de los compuestos ensayados.

Introducción

La leucemia

La leucemia es un grupo heterogéneo de cánceres hematológicos que afecta predominantemente a la sangre periférica y la médula ósea. Ocurre debido a las alteraciones en los procesos reguladores celulares normales causando proliferación incontrolada de células madre hematopoyéticas en la médula ósea. La leucemia puede ser aguda o crónica, dependiendo de la velocidad de crecimiento y propagación del cáncer, y mieloide o linfoblástica, dependiendo del tipo de células a las que afecte. Es el tipo de cáncer más común en niños y adolescentes, aunque también puede desarrollarse en cualquier franja de edad. Los distintos tipos de leucemia presentan signos y síntomas generales como anemia, leucopenia, fatiga, debilidad y susceptibilidad a las infecciones.

Uno de los principales tratamientos en la mayoría de los tipos de leucemia es la quimioterapia [1], la cual se basa en el uso de fármacos. Los agentes quimioterapéuticos se incorporan al torrente sanguíneo y actúan sobre las células cancerosas por todo el organismo. A pesar de los recientes avances, que han potenciado significativamente el conocimiento de la biología de las células tumorales y de las estrategias de diagnóstico, la quimioterapia tiene serias limitaciones [2,3]. Los tratamientos quimioterapéuticos disponibles actualmente frente a los distintos tipos de cáncer son en general poco efectivos, presentan selectividad cuestionable y serios efectos adversos y, a menudo, generan resistencias y recaídas [1]. Por tanto, existe una necesidad urgente de desarrollar nuevas entidades químicas que mejoren la eficacia del tratamiento [4,5].

Importancia de los compuestos naturales y sus derivados

En los últimos años la investigación sobre nuevos medicamentos para ser utilizados en oncología se ha focalizado en los productos naturales [6]. Históricamente las plantas han jugado un papel fundamental en el descubrimiento de fármacos potencialmente efectivos contra el cáncer [7]. Las moléculas derivadas de la naturaleza han desempeñado y continúan ejerciendo un papel clave en el descubrimiento y desarrollo de medicamentos para el tratamiento de la mayoría de las enfermedades. De hecho, los productos naturales constituyen una fuente importante de fármacos antitumorales ya que el 65% de los tratamientos quimioterapéuticos actuales están basados en ellos. Los productos aislados de plantas son útiles porque se toleran mejor que los quimioterapéuticos sintéticos, exhiben mecanismos de acción más amplios y muestran una mayor afinidad contra las dianas del cáncer. Estos compuestos no solo ejercen efectos protectores, sino que también poseen un impacto en las características celulares distintivas del cáncer como son la señalización proliferativa sostenida y la resistencia a la apoptosis [8,9].

En particular, los metabolitos secundarios de origen vegetal han sido objeto de un impresionante número de estudios de investigación [7]. Estos productos son, en su mayoría, moléculas orgánicas pequeñas que no son esenciales para el crecimiento, desarrollo y reproducción de la planta pero que exhiben un amplio espectro de propiedades farmacológicas, incluidas las actividades anticancerígenas [3,10]. Estos compuestos están presentes, en gran medida, en la dieta humana, integrados en hierbas, frutas y verduras [10,11], muchas de las cuales se han utilizado durante siglos en la medicina tradicional [12].

Las modificaciones sintéticas de los productos naturales para mejorar su valor terapéutico a través de la optimización de la farmacocinética, la estabilidad, la potencia y/o la selectividad, han generado varios fármacos exitosos. La preparación de bibliotecas de análogos derivados de compuestos naturales también puede contribuir a una mejor comprensión de los mecanismos moleculares de acción de los compuestos naturales a través de estudios de las relaciones estructura-actividad (SAR). En algunos casos los análogos han mostrado mayor actividad, incluso a través de un mecanismo de acción diferente, y una efectividad superior con respecto al modelo natural. De los metabolitos aislados de la naturaleza se han desarrollado compuestos con actividad antiproliferativa potente frente a células tumorales y con otras propiedades adicionales como son la actividad anti-angiogénica, la actividad pro-apoptótica e inhibición de la multirresistencia a fármacos [13, 14].

Entre de los metabolitos secundarios con propiedades citotóxicas se encuentran los compuestos polifenólicos, como los flavonoides [12,15,16], y los terpenos, como las lactonas sesquiterpénicas [5,17].

Flavonoides

Los flavonoides son la familia más numerosa de compuestos fenólicos en vegetales, se encuentran presentes en casi todas las plantas y representan una de las clases más prevalentes de compuestos en la dieta humana. Son pigmentos vegetales comestibles responsables de gran parte de la coloración en la naturaleza [18]. Además, exhiben un amplio espectro de propiedades farmacológicas incluidas las actividades anticancerígenas. Los flavonoides pueden interferir en todas las fases de

la progresión del cáncer al modular proteínas clave involucradas en la proliferación, diferenciación, apoptosis, angiogénesis, metástasis y reversión de la multirresistencia a fármacos [13, 15, 19, 20].

Los flavonoides contienen un esqueleto de 15 carbonos que consta de dos anillos aromáticos, A y B, unidos a través de un anillo C heterocíclico de pirano o pirona (con un doble enlace) central. La modificación de esta estructura básica, a través de distintos niveles de oxidación y sustituyentes del anillo C, es responsable de las diferentes clases de flavonoides [17, 21] (Figura 1).

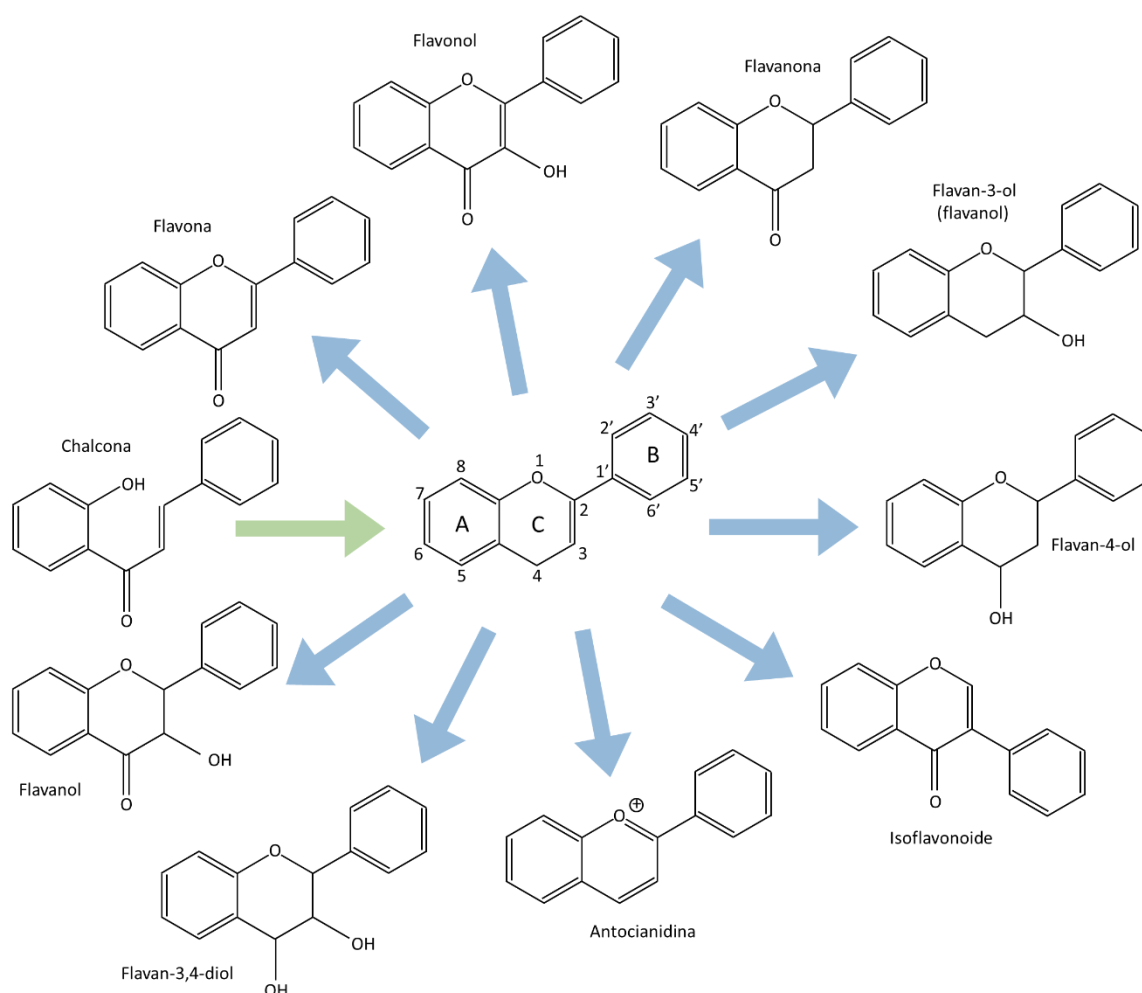


Figura 1. Estructuras básicas de los flavonoides. Las chalconas (1,3-difenil-2-propen-1-onas) son los precursores biosintéticos de los flavonoides con estructura abierta constan de dos anillos aromáticos unidos por un resto enona de tres carbonos.

Lactonas sesquiterpénicas

Las lactonas sesquiterpénicas son un grupo diverso de metabolitos secundarios biológicamente activos que se encuentran mayoritariamente en plantas (en particular en la familia *Asteraceae*) y en menor medida en hongos. Estas moléculas exhiben múltiples actividades biológicas incluyendo antioxidantes, antivíricas, antiinflamatorias y aquellas relacionadas con la apoptosis y el cáncer [3, 5, 22].

La actividad anticancerígena de las lactonas sesquiterpénicas se ha descrito para células tumorales de mama, ovario y páncreas, así como en gliomas y leucemia. La actividad antileucémica de estos compuestos se debe a la inducción de diferentes tipos de muerte celular de los cuales la vía apoptótica es uno de los principales mecanismos [5].

Las lactonas sesquiterpénicas son terpenoides de quince carbonos formados a partir de la condensación de tres unidades de isopreno y contienen un grupo lactona. El anillo de γ -lactona, generalmente con un grupo α -metileno, es esencial para los efectos biológicos mediados por las lactonas sesquiterpénicas. Según su esqueleto carbonado, se clasifican principalmente en lactonas de tipo germacranolida, eudesmanolida y guayanolida (Figura 2).

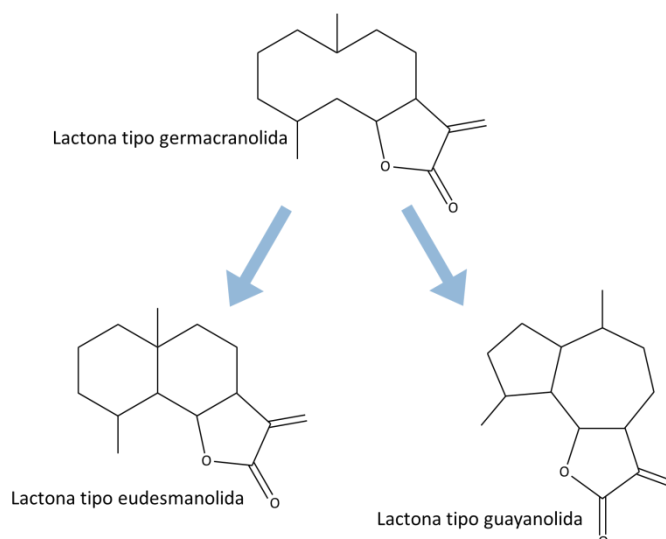


Figura 2. Tipos principales de lactonas sesquiterpénicas. Las lactonas de tipo eudesmanolida y guaianolida derivan de las germacranolidas.

El ciclo celular

La proliferación celular viene determinada normalmente por las señales extracelulares que controlan la expresión génica y la regulación proteica requerida para la división celular [23]. Durante la progresión tumoral, las células cancerosas poseen la capacidad de proliferar independientemente de las señales exógenas que promueven o inhiben la proliferación. Por lo tanto, el efecto antiproliferativo de sustancias químicas o fármacos sobre las células cancerosas es uno de los mecanismos para ejercer su actividad anti-carcinogénica.

El ciclo celular de una célula eucariota se divide en cuatro fases: i) Fase G_1 , que consiste en el intervalo entre la mitosis y el inicio de la replicación del ADN; durante esta fase la célula es metabólicamente activa y está creciendo. ii) Fase S o de síntesis, donde ocurre la duplicación del ADN. iii) Fase G_2 , que sigue a la fase S y en la que la célula prosigue su crecimiento y se sintetizan proteínas necesarias

para la mitosis. iv) Fase M, donde tiene lugar la mitosis con la consecuente división nuclear, en la cual ocurre la separación de los cromosomas hijos y que, normalmente, finaliza en la división celular (citoquinesis) [24].

La progresión de las células animales a través del ciclo celular se regula principalmente por factores de crecimiento extracelulares. Si estos factores no están disponibles en G_1 , las células entran en un estado de reposo denominado G_0 (células quiescentes). Las células en G_0 son metabólicamente activas y no proliferan; este estado es reversible y la mayoría de las células en humanos se encuentran en esta fase [24,25].

La progresión a través del ciclo celular se regula en distintos puntos de control. Los principales están al comenzar en la fase S (punto de control G_1 -S), antes de la mitosis (punto de control G_2 -M) y el punto de control en fase M que controla la progresión en anafase (Figura 3). Estos puntos de control están regulados por múltiples familias de proteínas como ciclinas, quinasas dependientes de ciclinas (CDK), inhibidores de CDK (CKI) y supresores de tumores, incluido p53 [26]. Estas proteínas favorecen o inhiben el avance del ciclo celular a la siguiente fase o detienen el ciclo en el punto de control [27].

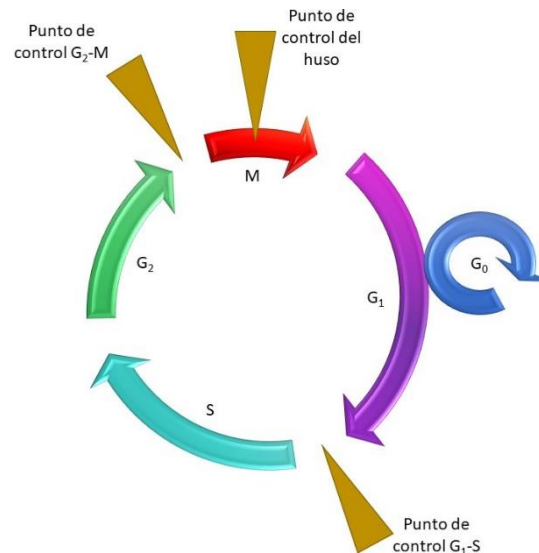


Figura 3. Puntos de control del ciclo celular.

La apoptosis

La apoptosis es una forma de muerte celular programada que conduce a la eliminación ordenada y eficiente de las células durante el desarrollo o debido al daño en el ADN. La desregulación de la muerte celular apoptótica es una característica distintiva del cáncer [28]. La alteración de la apoptosis es responsable no solo del desarrollo y la progresión del tumor, sino también de su resistencia a las terapias [19]. Por tanto, la inducción de la apoptosis está reconocida como un mecanismo eficiente para destruir células tumorales mediante quimioterapia.

La maquinaria de la apoptosis es compleja e involucra diferentes vías de señalización. La activación de la apoptosis requiere de las caspasas, una familia de cisteinproteasas que se expresan en las células como zimógenos inactivos denominados pro-caspasas [30]. Estas enzimas se clasifican en al menos dos tipos. Las caspasas iniciadoras (caspasa -2, -8, -9 y -10) son las responsables del comienzo

de la vía apoptótica y las caspasas ejecutoras (caspasa -3, -6 y -7) degradan múltiples sustratos que provocan alteraciones bioquímicas (exposición de la fosfatidilserina en la superficie celular, fragmentación del ADN) y finalmente morfológicos (formación de ampollas en la membrana y cuerpos apoptóticos). La translocación de fosfatidil serina desde la cara interna a la cara externa de la membrana plasmática permite el reconocimiento de las células apoptóticas por los macrófagos, permitiendo la fagocitosis sin la liberación de componentes celulares pro-inflamatorios [31]. Existen dos vías que desencadenan la activación de la apoptosis: la vía intrínseca y la vía extrínseca (Figura 4).

La vía apoptótica intrínseca es dependiente de las mitocondrias y está mediada por señales intracelulares en respuesta, tanto a la ausencia de factores de crecimiento, de hormonas y de citoquinas, como a diferentes tipos de estrés como radiación, toxinas, hipoxia, presencia de radicales libres o tratamientos con agentes quimioterapéuticos. Perturbaciones a nivel celular pueden activar a las proteínas pro-apoptóticas de la familia Bcl-2, que median apoptosis dependiente de estrés [31]. La familia de proteínas Bcl-2 comprende proteínas anti- y pro-apoptóticas que se clasifican en tres subfamilias dependiendo de la homología y las funciones de cada proteína: (i) Proteínas anti-apoptóticas que se caracterizan por la presencia de cuatro dominios de homología Bcl-2, BH (BH1, BH2, BH3 y BH4) y por poseer una región hidrofóbica C-terminal que localiza a estas proteínas en la superficie exterior de la membrana mitocondrial con el resto de la proteína orientada al citosol; éstas son Bcl-2, Bcl-xL, Bcl-w y Mcl-1. (ii) Proteínas pro-apoptóticas que contienen tres dominios BH (BH1, BH2 y BH3) y una región hidrofóbica C-terminal, como Bax, Bak, Bok y Bcl-Xs, esenciales para la liberación de citocromo

c. (iii) Proteínas que solo contienen un dominio BH3; estas proteínas son pro-apoptóticas y se subdividen en: activadoras (Bim y Bid), que actúan directamente sobre Bax/Bak aumentando la permeabilidad de la membrana externa mitocondrial, desplazando a las proteínas anti-apoptóticas que promueven la supervivencia celular, y sensibilizantes (Bad, Bik, Bmf, Hrk, Noxa y Puma), que no activan directamente a Bax/Bak sino que neutralizan a las proteínas anti-apoptóticas [32-34].

La activación de los miembros pro-apoptóticos de la familia Bcl-2 conducen al aumento de la permeabilidad de la membrana externa mitocondrial, de modo que las proteínas normalmente confinadas en el espacio intermembrana se liberan al citosol, como el citocromo *c* y Smac/DIABLO [30]. El citocromo *c* se une a Apaf-1 (factor de activación de la proteasa de apoptosis-1) y desencadena la formación de un complejo llamado apoptosoma, que recluta a la pro-caspasa-9, permitiendo su activación y favoreciendo su proteólisis [35]. Este procesamiento de la caspasa-9 a su vez activa a las caspasas ejecutoras -3, -6 y -7 que escinden múltiples sustratos que conducen a la muerte celular apoptótica. La liberación de Smac/DIABLO al citosol promueve la apoptosis al unirse a las proteínas inhibidoras de la apoptosis (IAPs) y facilitar su degradación [36] (figura 4). La expresión de niveles elevados de las proteínas anti-apoptóticas, como Bcl-2 o Bcl-xL ocurre en más de la mitad de todos los cánceres, lo que confiere resistencia a las células tumorales frente a múltiples estímulos pro-apoptóticos, incluidos los desencadenados por la mayoría de los fármacos citotóxicos frente al cáncer.

La vía extrínseca se inicia por perturbaciones del microambiente extracelular y activación de los receptores de muerte en la superficie celular mediante la

producción de ligandos de muerte por células citotóxicas naturales o macrófagos, que al unirse con los receptores de muerte en la membrana de la célula diana activan a la procaspasa-8 [30]. Los receptores de muerte son miembros de la superfamilia del factor de necrosis tumoral (TNF) e incluyen varios miembros (TNFR1, Fas, DR4, DR5) y cada receptor de muerte tiene su ligando correspondiente (TNF, Fas-L, TRAIL). La unión de un ligando de muerte a su correspondiente receptor resulta en el reclutamiento de procaspasa-8 monomérica a través de su dominio efector de muerte (DED) a un complejo de señalización inductor de muerte (DISC) ubicado en el dominio citoplasmático del receptor de muerte unido a su ligando. El DISC también incluye una proteína adaptadora, conocida como proteína con dominio de muerte asociado a FAS (FADD) o proteína con dominio de muerte asociado al receptor de TNF (TNFR) (TRADD), que facilita la interacción de la procaspasa-8 con el DISC [36]. El reclutamiento de varios monómeros de procaspasa-8 al DISC da como resultado su dimerización y activación y el posterior procesamiento de las caspasas efectoras -3, -6 y -7 cuya activación conduce a la escisión de sustratos esenciales para la viabilidad celular, induciendo la muerte celular [38] (Figura 4).

Algunas células no mueren solamente en respuesta a la activación de la vía extrínseca y requieren una etapa de amplificación inducida por la caspasa-8. Esta caspasa hidroliza a Bid y el producto resultante (tBid) activa a proteínas pro-apoptóticas multidominio de la familia Bcl-2 para aumentar la permeabilidad de la membrana externa mitocondrial [30,38].

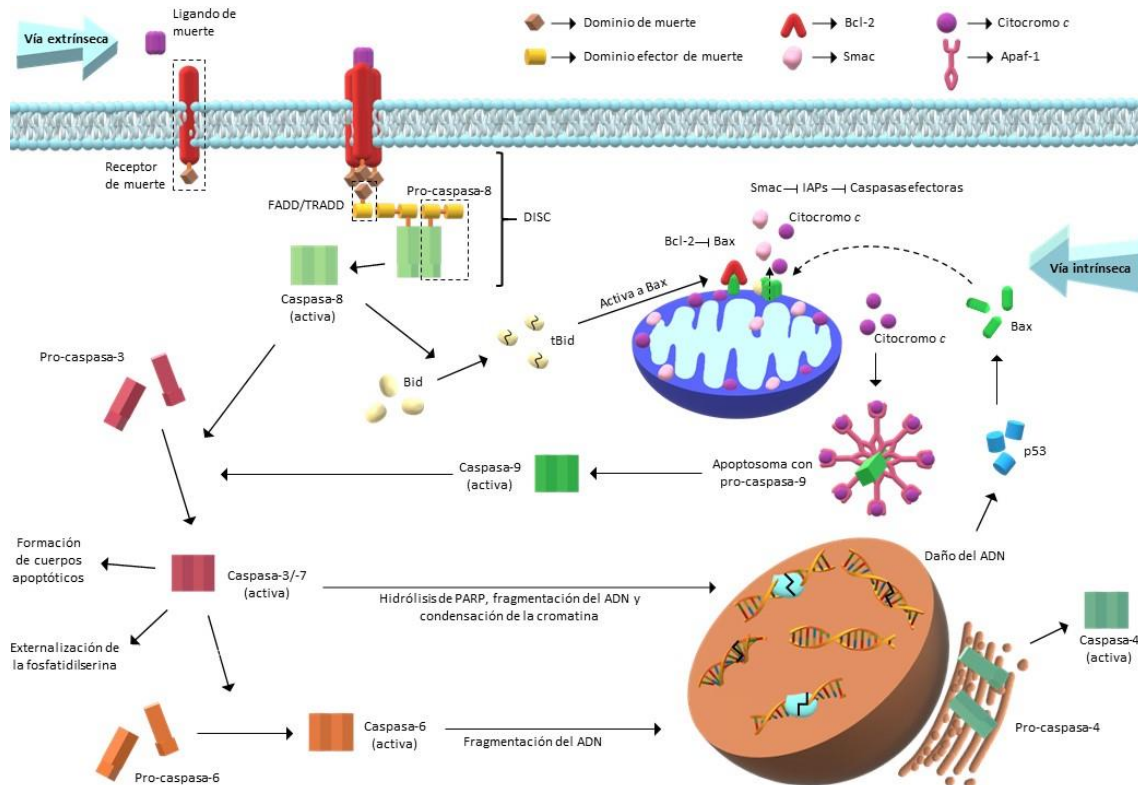


Figura 4. Representación esquemática de las dos vías principales de la apoptosis, la extrínseca y la intrínseca. Cada una requiere señales de activación específicas para comenzar una cascada de eventos moleculares dependientes de energía. Estas vías están conectadas y las moléculas de señalización de una vía pueden influir en la otra. Cada ruta activa sus propias caspasas iniciadoras que a su vez activarán a las caspasas ejecutoras.

Estrés oxidativo

El estrés oxidativo es un fenómeno causado por el desequilibrio entre la producción y la acumulación de especies reactivas de oxígeno (ROS) en células y tejidos y su capacidad para neutralizar estos productos reactivos [39]. Este desequilibrio puede producir apoptosis por activación de la vía mitocondrial mediante estímulos tanto exógenos como endógenos. Las mitocondrias son el lugar donde se producen la mayoría de estas especies químicas intracelulares, como resultado de la reducción parcial de la molécula de oxígeno durante el transporte de

electrones en la cadena respiratoria. Bajas concentraciones de H_2O_2 se han relacionado con la inducción de respuestas de supervivencia celular, mientras que concentraciones más altas activan procesos de muerte como la apoptosis. Si el daño es demasiado grave, p53 activa la transcripción de genes que codifican factores pro-apoptóticos cruciales para inducir la vía intrínseca de la apoptosis, como Bax, Bid, Puma, Noxa y Apaf-1, y proteínas que activan la vía extrínseca como Fas, DR-4 y DR-5. Además, p53 citosólico puede translocarse a las mitocondrias, donde puede interactuar directamente y regular negativamente a proteínas anti-apoptóticas como Bcl-2, Bcl-xL y Mcl-1 y favoreciendo la actividad de las proteínas pro-apoptóticas Bax y Bak, que aumentan la permeabilidad de la membrana mitocondrial externa permitiendo la liberación de factores pro-apoptóticos como citocromo *c*. Además, estas especies reactivas generadas en las mitocondrias pueden dañar al ADN mitocondrial y afectar a la biosíntesis de las proteínas involucradas en el transporte de electrones. La interrupción de la función de la cadena respiratoria, aumenta la generación de ROS, y conlleva a la disipación del potencial de la membrana mitocondrial e inhibición de la biosíntesis de ATP [40]. Estos eventos culminan en la activación de la apoptosis a través de la vía mitocondrial. La apoptosis independiente de las caspasas implica la liberación del factor inductor de apoptosis (AIF) de las mitocondrias y su translocación al núcleo [40]. Además, la activación de JNK por estrés oxidativo puede estimular la fosforilación e inactivar factores anti-apoptóticos como Bcl-2 y Bcl-xL, mientras que fosforila y activa a los miembros pro-apoptóticos de esta familia como Bid y Bax [41]. El estrés oxidativo y la acumulación mitocondrial de Ca^{2+} pueden desencadenar la apertura de poros en la membrana mitocondrial, mediante un proceso conocido como transición de permeabilidad mitocondrial [40,41].

El papel de los lisosomas y el retículo endoplasmático en la apoptosis

Los lisosomas son orgánulos dinámicos con múltiples funciones biológicas como reparación de la membrana plasmática, transducción de señales, presentación de antígenos y degradación de macromoléculas con el fin de mantener la homeostasis metabólica, y pueden desempeñar un papel crítico en el metabolismo de las células tumorales [42]. El interior de los lisosomas es ácido (pH 4,5 o inferior) y contiene proteasas de la familia de las catepsinas, las hidrolasas lisosómicas mejor caracterizadas [43]. Las células cancerosas dependen de la función de los lisosomas y se han observado cambios en el volumen lisosómico y localización subcelular durante la transformación oncogénica [44], lo que favorece que las células tumorales sean más sensibles a posibles roturas del lisosoma con la consecuente liberación de catepsinas al citosol. La lisis de los lisosomas está asociada a la muerte celular pero el citosol contiene reguladores de la actividad de las catepsinas llamadas cistatinas que inhiben las proteasas liberadas o activadas accidentalmente. El grado de permeabilidad lisosómica determinará la cantidad de catepsinas liberadas en el citosol. La descomposición completa de los lisosomas favorece la necrosis, mientras que si es parcial (suficiente para superar la protección de las cistatinas) puede desencadenar apoptosis [45]. Algunas catepsinas pueden favorecer la escisión de Bid, lo que favorece la activación de otros miembros pro-apoptóticos de la familia Bcl-2 [43,45].

El retículo endoplasmático es una red membranosa dinámica y especializada de túbulos alargados y discos aplanados, y abarca una gran área del citoplasma. Está involucrado en varios procesos celulares y desempeña un papel importante en la síntesis, plegamiento y maduración estructural de más de un tercio de todas las

proteínas producidas en la célula [46]. Después de la translocación cotraduccional en el retículo endoplasmático, estas proteínas deben plegarse correctamente mediante las chaperonas y modificarse (por *N*-glicosilación, por ejemplo). Al menos un tercio de todos los polipéptidos translocados se pliegan incorrectamente y, para algunas proteínas, la tasa de éxito es mucho menor [47]. La acumulación de proteínas mal plegadas por encima de un umbral crítico desencadena señales denominadas de estrés del retículo endoplasmático [43,48]. Si este es prolongado y severo puede provocar la muerte celular mediada por caspasas a través de varios mecanismos dependientes de proteínas transmembrana que regulan la respuesta al estrés del retículo endoplasmático, como IRE1 α (endorribonucleasa/quinasa transmembrana 1 α que requiere inositol) y PERK (proteína quinasa del retículo endoplasmático que fosforila al factor de iniciación eucariota de la traducción eIF2 α) [49,50]. La caspasa-4, localizada en el retículo endoplasmático, es escindida y participa en la apoptosis inducida por Fas y TRAIL [51]. La activación de JNK mediada por IRE1 α reprime la actividad de Bcl-2 y mejora la función de BIM (pro-apoptótica), favoreciendo así la muerte celular [49,52]. La liberación de Ca²⁺ desde el retículo endoplasmático da como resultado la activación de calpaínas activadas por Ca²⁺ que escinden sustratos intracelulares relacionados con la señalización apoptótica, incluidos Bid, Bax y caspasa-7 [44]. El Ca²⁺ liberado también es captado por las mitocondrias, lo que lleva a la apertura de poros y la despolarización de la membrana mitocondrial interna.

Proteínas quinasas activadas por mitógenos (MAPKs)

La ruta de señalización de las proteínas quinasas activadas por mitógenos (MAPKs) desempeña un papel clave en la proliferación y supervivencia celular y, también, en la apoptosis [53,54]. Hay al menos tres grupos principales de MAPKs; las proteínas quinasas reguladas por señales extracelulares (ERK 1/2), las proteínas quinasas activadas por mitógenos p38 (p38^{MAPKs}, isoformas α , β , γ , δ) y las proteínas quinasas NH₂ terminal de c-Jun (JNK 1/2/3). Estas vías pueden activarse mediante diversos estímulos celulares, incluidos factores de crecimiento, citoquinas y estrés celular [55]. Esto conduce a una cascada de eventos de fosforilación secuencial compuesta por al menos cinco niveles de familias de quinasas [MAP4K, MAP3K, MAP2K, MAPK, y proteínas quinasas activadas por MAPK (MK) u otras proteínas [56] (Figura 5).

La familia de proteínas MAPKs juega un papel diverso y a veces contradictorio en el desarrollo del cáncer. La vía ERK está implicada principalmente en la proliferación, la diferenciación y la supervivencia, mientras que las vías JNK y p38^{MAPK} están implicadas preferentemente en la inflamación, la apoptosis, la proliferación y la diferenciación. El resultado biológico de la activación de MAPKs depende de los estímulos, la intensidad/duración de la señal y la especificidad del tipo de célula o tejido. Por ejemplo, la activación transitoria de JNK promueve la supervivencia celular, mientras que si la activación es prolongada induce apoptosis [56].

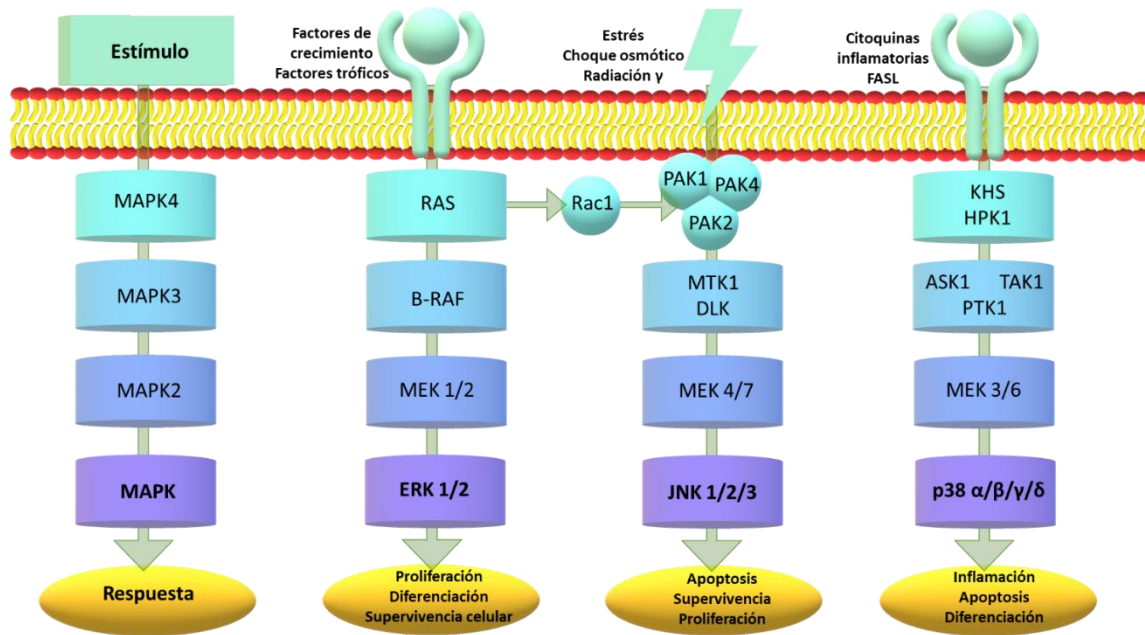


Figura 5. Cascadas de señalización de las proteínas quinasas activadas por mitógenos (MAPKs). Las rutas de señalización de las MAPKs median la transmisión de señales extracelulares hasta las proteínas efectoras que alteran la proliferación y la supervivencia celular.

Justificación

El cáncer se encuentra entre las principales causas de mortalidad a nivel global, representando un importante problema de salud pública. A pesar de los grandes esfuerzos en investigación para comprender los procesos y los mecanismos moleculares, la incidencia mundial del cáncer aumenta anualmente y la mortalidad total ha superado a muchas otras enfermedades, siendo la segunda causa de muerte en España. En el 2018 se notificaron 18 millones de nuevos casos en el mundo y 9,5 millones de fallecidos, y se prevé que en el año 2040 afecte a 29,5 millones de personas.

En particular, la leucemia es responsable de más de 300.000 muertes en el mundo en el año 2018, con casi 440.000 casos nuevos ese mismo año según la Organización Mundial de la Salud. La mayoría de leucemias que se producen en niños y adultos son agudas; y según la Sociedad Americana contra el Cáncer, tres de cada cuatro leucemias infantiles son leucemia linfocítica aguda, mientras que en adultos la leucemia mieloide aguda es el tipo más común. Solamente alrededor del 20% de las personas con más de 20 años que han sido diagnosticadas de leucemia aguda sobreviven cinco o más años, aumentando la supervivencia hasta aproximadamente el 70% en el caso de los niños.

En las últimas décadas se han conseguido grandes avances en el desarrollo de nuevos compuestos más selectivos contra el cáncer, pero los tratamientos actuales aún presentan graves inconvenientes. Por lo tanto, es necesaria la búsqueda de nuevos agentes quimioterapéuticos con mejores propiedades que los ya existentes.

El presente trabajo se ha enfocado en el estudio de nuevos productos potencialmente quimioterapéuticos que presentan citotoxicidad selectiva frente a las células leucémicas humanas. Los compuestos seleccionados surgieron de los conocimientos previos de su citotoxicidad y fueron escogidos, en todos los casos, mediante estudios SAR. La chalcona sintética 6'-benciloxi-4-bromo-2'-hidroxichalcona fue seleccionada de una colección de alrededor de 100 flavanonas y chalconas con distintos sustituyentes. La selección de la flavanona 6-metoxi-2-(naftalen-1-il) croman-4-ona se llevó a cabo a través de estudios de SAR de diez naftilchalconas y sus correspondientes flavanonas. En el caso de la lactona sesquiterpénica espiciformina y su derivado acetilado, fueron seleccionados de estudios fitoquímicos de endemismos canarios y de estudios previos sobre la citotoxicidad en células tumorales de compuestos conteniendo el grupo funcional α -metilen- γ -lactona.

Objetivos

OBJETIVO GENERAL

Estudiar la citotoxicidad e investigar las vías de transducción de señales de muerte celular de potenciales compuestos antileucémicos.

OBJETIVOS ESPECÍFICOS

Artículo 1

Estudiar los efectos citotóxicos de una serie de chalconas conteniendo como sustituyentes un átomo de bromo y/o un radical benciloxi y explorar las cascadas de señalización implicadas en la acción biológica del compuesto más potente, utilizando como modelo de estudio líneas celulares de leucemia humana.

Artículo 2

Evaluar la actividad antiproliferativa de un grupo de naftil-chalconas y sus correspondientes flavanonas sintéticas e investigar las vías de señalización activadas por el compuesto más potente, utilizando como modelo de estudio la línea celular leucémica de origen humano U-937.

Artículo 3

Investigar la potencial citotoxicidad de la espiciformina y su derivado acetilado, y caracterizar las vías de señalización implicadas en células tumorales humanas.

Publicaciones

En esta tesis doctoral se ha analizado el potencial papel citotóxico de compuestos de origen natural y sintéticos pertenecientes a dos grupos, los flavonoides y los terpenoides, frente a células leucémicas. Las líneas celulares utilizadas fueron de leucemia mieloide aguda (U-937 y HL-60), leucemia mieloide crónica (K-562) y leucemia linfoblástica aguda (NALM-6 y MOLT-3), y las líneas celulares U-937/Bcl-2 y K-562/ADR, que sobreexpresan Bcl-2 y la glicoproteína P, respectivamente, responsables de la resistencia a la quimioterapia. Se han investigado las vías de transducción de señales de muerte celular de los productos más potentes y elucidado los mecanismos moleculares implicados. Algunos de los compuestos estudiados bloquean la expresión de proteínas involucradas en la quimiorresistencia. Además, se analizó la citotoxicidad de los compuestos, no solo en células tumorales humanas, sino también en células mononucleares humanas aisladas de donantes sanos, siendo éstas últimas más resistentes.

Este trabajo de investigación se ha llevado a cabo en el Departamento de Bioquímica y Biología Molecular, Fisiología, Genética e Inmunología por el Grupo de Investigación Reconocido A+ “Bioquímica Farmacológica” del Instituto Universitario de Investigaciones Biomédicas y Sanitarias (IUIBS) de la ULPGC, Unidad Asociada al Consejo Superior de Investigaciones Científicas (CSIC) a través del Instituto de Productos Naturales y Agrobiología (IPNA).

Los productos orgánicos de esta Tesis han sido obtenidos tanto por los integrantes del Grupo de Investigación de la ULPGC como del IPNA del CSIC. Los trabajos realizados se han publicado en tres revistas internacionales indexadas en el *Journal Citation Reports*, situadas en el primer cuartil en las categorías de

Bioquímica y Biología Molecular y Toxicología, y que se relacionan a continuación:

Título: 6-Benzoyloxy-4-bromo-2-hydroxychalcone is cytotoxic against human leukaemia cells and induces caspase-8- and reactive oxygen species dependent apoptosis.

Autores: Ester Saavedra, Henoc Del Rosario, Ignacio Brouard, José Quintana, Francisco Estévez

Revista: Chemico-Biological Interactions, 2019 Jan 25;298:137-145

DOI: 10.1016/j.cbi.2018.12.010

Factor de impacto: 3.723

Cuartil: Q1 (Journal Citation Reports, 2019)

Categoría: Toxicología

Título: The synthetic flavanone 6-methoxy-2-(naphthalen-1-yl)chroman-4-one induces apoptosis and activation of the MAPK pathway in human U-937 leukaemia cells.

Autores: Ester Saavedra, Henoc Del Rosario, Ignacio Brouard, Judith Hernández-Garcés, Celina García, José Quintana, Francisco Estévez

Revista: Bioorganic Chemistry, 2020 Jan;94:103450

DOI: 10.1016/j.bioorg.2019.103450

Factor de impacto: 4.831

Cuartil: Q1 (Journal Citation Reports, 2019)

Categoría: Bioquímica y Biología Molecular

Título: Cytotoxicity of the sesquiterpene lactone spiciformin and its acetyl derivative against the human leukemia cell lines U-937 and HL-60.

Autores: Ester Saavedra, Francisco Estévez-Sarmiento, Mercedes Said, José Luis Eiroa, Sara Rubio, José Quintana, Francisco Estévez

Revista: International Journal of Molecular Sciences, 2020 Apr 16;21(8):2782

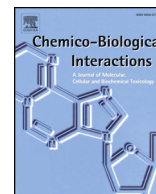
DOI:10.3390/ijms2108278

Factor de impacto: 4.556 (2019)

Cuartil: Q1 (Journal Citation Reports, 2019)

Categoría: Bioquímica y Biología Molecular

1. **6-Benzoyloxy-4-bromo-2-hydroxychalcone is cytotoxic against human leukaemia cells and induces caspase-8- and reactive oxygen species dependent apoptosis**



6'-Benzyloxy-4-bromo-2'-hydroxychalcone is cytotoxic against human leukaemia cells and induces caspase-8- and reactive oxygen species-dependent apoptosis

Ester Saavedra^a, Henoc Del Rosario^a, Ignacio Brouard^b, José Quintana^a, Francisco Estévez^{a,*}

^a Departamento de Bioquímica y Biología Molecular, Unidad Asociada al Consejo Superior de Investigaciones Científicas (CSIC), Instituto Universitario de Investigaciones Biomédicas y Sanitarias (IUIBS), Universidad de las Palmas de Gran Canaria, Spain

^b Instituto de Productos Naturales y Agrobiología, CSIC, La Laguna, Tenerife, Spain

ARTICLE INFO

Keywords:

Apoptosis
Caspases
Cytotoxicity
Chalcone

ABSTRACT

In this study, we investigated the effects of synthetic 6'-benzyloxy-4-bromo-2'-hydroxychalcone on viabilities of seven human leukaemia cells. It was cytotoxic against U-937, HL-60, K-562, NALM-6, MOLT-3 cells, and also against Bcl-2-overexpressing U-937/Bcl-2 cells and P-glycoprotein-overexpressing K-562/ADR, but had no significant cytotoxic effects against quiescent or proliferating human peripheral blood mononuclear cells. This chalcone is a potent apoptotic inducer in human leukaemia U-937 cells. Cell death was (i) mediated by the activation and the cleavage of initiator and executioner caspases and poly(ADP-ribose) polymerase; (ii) prevented by the pan-caspase inhibitor z-VAD-fmk, and by the selective caspase-3/7, -6 and -8 inhibitors, and by a cathepsins B/L inhibitor; (iii) associated with the release of mitochondrial proteins, including cytochrome c and Smac/DIABLO; (iv) accompanied by dissipation of the mitochondrial membrane potential, (v) partially blocked by the inhibition of p38^{MAPK} and (vi) mostly abrogated by catalase. In conclusion, the synthetic chalcone is cytotoxic against several types of human leukaemia cell with apoptosis being induced by activation of the extrinsic pathway and the generation of reactive oxygen species.

1. Introduction

Flavonoids are natural products that exhibit a wide array of pharmacological properties, including chemoprotective and chemotherapeutic activities [1]. Chalcones (1,3-diphenyl-2-propen-1-ones) are biosynthetic precursors of flavonoids and can be considered as flavonoids with an open structure. These compounds are commonly found in fruits and vegetables, and some of them are potential anticancer agents [2]. Two structural characteristics are important in determining their anti-proliferative effects on cancer cells: (i) the presence of hydroxy group/s in the chalcone skeleton and (ii) the conjugated enone system. Hydroxy derivatives of chalcone display more potent antiproliferative properties compared to the other chalcone derivatives and the presence of the central double bond plays a crucial role [3,4]. Naturally occurring and synthetic chalcones have been identified for modulating key pathways or molecular targets in cancer including apoptotic pathways [5]. Apoptosis induction is recognized as an efficient mechanism for

destroying malignant tumour cells using chemotherapy [6]. This kind of cell death can be executed by aspartate-specific cysteine proteases, the caspases, which are activated by two main pathways [7,8]. The extrinsic pathway is initiated with the activation of the tumour necrosis factor receptor superfamily (TNF) or Fas receptor, involved in the recruitment and activation of the initiator caspase-8 or -10, which activate the effector caspases (-3, -6 and -7) [9]. The intrinsic pathway involves permeabilization of the mitochondrial outer membrane by the activation of the pro-apoptotic proteins Bax and Bak of the Bcl-2 family proteins [10]. This induces cytochrome c release in the cytosol which associates with Apaf-1 (apoptotic protease-activating factor 1) in a multimeric complex called the apoptosome. Initiator caspase-9 is then activated which in turn activates the effector caspases [11].

Although chalcone derivatives exhibit cytotoxicity against different tumour cell lines, little is known about the mechanism of action of these compounds. It has recently been reported that flavonoids with halogen substituents in the B ring show improved cytotoxicity against cancer

Abbreviations: CHAL, 6'-benzyloxy-4-bromo-2'-hydroxychalcone; H₂-DCF-DA, 2',7'-dichlorodihydrofluorescein diacetate; IC₅₀, 50% inhibition of cell growth; MTT, 3-(4,5-dimethyl-2-thiazolyl)-2,5-diphenyl-2H-tetrazolium bromide; ROS, reactive oxygen species

* Corresponding author. Departamento de Bioquímica y Biología Molecular. Universidad de Las Palmas de Gran Canaria, Paseo Blas Cabrera Felipe s/n, Las Palmas de Gran Canaria, 35016, Spain.

E-mail address: francisco.estevez@ulpgc.es (F. Estévez).

<https://doi.org/10.1016/j.cbi.2018.12.010>

Received 25 July 2018; Received in revised form 23 November 2018; Accepted 14 December 2018

Available online 19 December 2018

0009-2797/ © 2018 Elsevier B.V. All rights reserved.

cells relative to methoxylated, methylated or hydroxylated analogues [12]. In a previous report we described a synthetic flavonol containing a bromine atom at position 4' of the B ring that showed cytotoxic properties against human myeloid HL-60 tumour cells [13]. In addition, we have recently described how the introduction of two benzyloxy groups at positions 3' and 4' on the B ring of the flavonol skeleton enhances the cytotoxicity of the polyphenolic structure [14]. Moreover, Bu and coworkers have shown how the *ortho*-aryl substitution in the A ring is likely to be very important [15]. Since the presence of a bromine atom as well as a benzyloxy group may play an important role in the cytotoxic properties of chalcones we decided to synthesize new derivatives and explore the impact on human myeloid U-937 tumour cells.

In this study we synthesized 6'-benzyloxy-4-bromo-2'-hydroxychalcone (CHAL) and studied i) its potential cytotoxic effects against a panel of human leukaemia cells and ii) the signal transduction pathways involved in the mechanism of cell death.

2. Materials and methods

2.1. Reagents

Compounds used as starting material and reagents were obtained from Aldrich Chemical Co. or other chemical companies and used without further purification. Nuclear Magnetic Resonance (NMR): ^1H and ^{13}C NMR spectra were obtained on a Bruker model AMX-400 spectrometer with standard pulse sequences operating at 500 in ^1H and 125 MHz in ^{13}C NMR. CDCl_3 was used as solvent. Chemical shifts (δ) are given in ppm relative to the residual solvent signals, and coupling constants (J) are reported in hertz. High resolution ESI mass spectra were obtained from a Fourier transform ion cyclotron resonance (FT-ICR) mass spectrometer, an RF-only hexapole ion guide, and an external electrospray ion source. IR spectra were recorded using a Bruker model IFS-55 spectrophotometer. Melting points were determined on a Büchi B-540 apparatus and are uncorrected. Analytical thin layer chromatography (TLC) was performed using silica gel 60 (230–400 mesh) aluminum sheets. All commercially available chemicals were used without further purification.

2'-Hydroxychalcone, 4-bromo-2'-hydroxychalcone and 6'-benzyloxy-2'-hydroxychalcone were obtained by synthesis following established protocols and have been previously described. The spectroscopic data were compared with those described in the literature in order to confirm the structures [12,16,17]. The inhibitors benzyloxycarbonyl-Val-Ala-Asp(OMe) fluoromethyl ketone (z-VAD-fmk), benzyloxycarbonyl-Val-Ala-Asp(OMe)-Val-Ala-Asp(OMe) fluoromethyl ketone (z-VDVAD-fmk), benzyloxycarbonyl-Asp(OMe)-Glu(O-Me)-Val-Ala-Asp(OMe) fluoromethyl ketone (z-DEVD-fmk), benzyloxycarbonyl-Ile-Glu-Thr-Asp(OMe) fluoromethyl ketone (z-IETD-fmk), benzyloxycarbonyl-Leu-Glu-His-Asp(OMe) fluoromethyl ketone (z-LEHD-fmk), Ac-LEVD-CHO (*N*-acetyl-Leu-Glu-Val-Ala-CHO), PD98059, U0126, SP600125, SB203580, MeOSuc-Phe-Homo-Phe-fluoromethyl ketone (Mu-Phe-HPH-fmk; cathepsins B and L inhibitor) and pepstatin A were purchased from Sigma (Saint Louis, MO, USA). The caspase inhibitor Ac-VEID-CHO (*N*-acetyl-AAVALLPAVLLALLAPVEID-CHO) was from Calbiochem (Darmstadt, Germany). Acrylamide, bisacrylamide, ammonium persulfate and *N,N,N',N'*-tetramethylethylenediamine were from Bio-Rad (Hercules, CA, USA). Antibodies for caspase-3, caspase-7, caspase-8 and caspase-9 were purchased from Stressgen-ENZO (Victoria, British Columbia, Canada). Anti-caspase-6 and anti-caspase-4 monoclonal antibodies were from Medical & Biological Laboratories (Nagoya, Japan). Monoclonal anti- β -Actin (clone AC-74) was purchased from Sigma (Saint Louis, MO, USA). Monoclonal anti-human Bcl-2 was from Santa Cruz Biotechnology (Santa Cruz, CA, USA). Polyclonal anti-human Bax and Bid antibodies and monoclonal anti-cytochrome c and poly(ADP-ribose) polymerase (PARP) antibodies were from BD Pharmingen (San Diego, CA, USA). Monoclonal antibody for Smac/DIABLO was from BD Transduction Laboratories. Secondary antibodies were

from GE Healthcare Bio-Sciences AB (Little Chalfont, UK). PVDF membranes were from Millipore (Temecula, CA, USA). All other chemicals were obtained from Sigma (Saint Louis, MO, USA).

2.1.1. General procedure for the synthesis of 6'-benzyloxy-4-bromo-2'-hydroxychalcone (3)

A mixture of the acetophenone **1** (5–10 mmol, 1 equiv.) and the corresponding aldehyde **2** (1 equiv.) in EtOH (20–40 ml) was stirred at room temperature. Then, a 50% aqueous solution of NaOH (5–8 ml) was added. The mixture was stirred at room temperature until the aldehyde had completely reacted. After that, HCl (10%) was added until neutrality. The solid was filtered and crystallized from MeOH. The chalcone **3** was isolated as an orange solid (80%), mp 146–147 °C. IR (KBr, cm^{-1}) ν_{max} : 3441, 3034, 1632, 1579, 1555, 1485, 1475, 1450, 1401, 1338, 1327, 1235, 1203, 1177, 1073, 1028, 1008, 972, 987, 816. ^1H NMR (500 MHz, CDCl_3) δ = 13.39 (s, 1H); 7.73 (d, J = 15.6 Hz, 1H); 7.53 (d, J = 15.6 Hz, 1H); 7.41–7.38 (m, 2H); 7.38–7.34 (m, 1H); 7.33–7.27 (m, 3H); 7.21 (d, J = 8.4 Hz, 2H); 6.80 (d, J = 8.7 Hz, 2H); 6.56 (dd, J = 8.4, 1.0 Hz, 1H); 6.45 (dd, J = 8.3, 1.0 Hz, 1H); 5.01 (s, 2H). ^{13}C NMR (125 MHz, CDCl_3) δ = 194.2, 165.6, 160.3, 141.7, 136.2, 135.5, 134.0, 131.9, 129.8, 128.9, 128.7, 128.6, 128.3, 124.2, 111.6, 111.4, 102.2, 71.4. HRMS (ESI-FT-ICR) m/z : 409.0263 [M-H] $^-$; calcd. for $\text{C}_{22}\text{H}_{16}\text{O}_3^{81}\text{Br}$: 409.0262.

2.2. Cell culture and cytotoxicity assays

U-937, HL-60, K-562, NALM-6 and MOLT-3 cells were from DSMZ (German Collection of Microorganisms and Cell Cultures, Braunschweig, Germany). U-937/Bcl-2 cells were kindly provided by Dr. Jacqueline Bréard (INSERM U749, Faculté de Pharmacie Paris-Sud, Châtenay-Malabry, France) and K-562/ADR, a cell line resistant to doxorubicin was provided by Dr. Lisa Oliver (INSERM, Nantes, France). The U-937 is a pro-monocytic, human myeloid leukaemia cell line which was isolated from a histiocytic lymphoma. HL-60 is an acute myeloid leukaemia cell line. K-562 is a chronic myeloid leukaemia cell line. NALM-6 is a human B cell precursor leukaemia. MOLT-3 is an acute lymphoblastic leukaemia cell line.

Cells were cultured in RPMI 1640 medium containing 10% (v/v) heat-inactivated fetal bovine serum, 100 $\mu\text{g}/\text{ml}$ streptomycin and 100 U/ml penicillin, incubated at 37 °C in a humidified atmosphere containing 5% CO_2 as described [18]. The doubling times of the cell lines were 30 h in U-937, U-937/Bcl-2, K-562 and K-562/ADR, 24 h in HL-60 and 40 h in NALM-6 and MOLT-3. K-562/ADR was cultured in presence of 200 ng/ml doxorubicin. Human peripheral blood mononuclear cells (PBMC) were isolated from heparin-anticoagulated blood of healthy volunteers by centrifugation with Ficoll-Paque Plus (GE Healthcare Bio-Sciences AB, Uppsala, Sweden). PBMC were also stimulated with phytohemagglutinine (2 $\mu\text{g}/\text{ml}$) for 48 h before the experimental treatment. The trypan blue exclusion method was used for counting the cells by a hemacytometer and the viability was always greater than 95% in all experiments. The cytotoxicity of chalcone **3** (6'-benzyloxy-4-bromo-2'-hydroxychalcone, CHAL) was evaluated by colorimetric 3-(4,5-dimethyl-2-thiazolyl)-2,5-diphenyl-2H-tetrazolium bromide (MTT) assay as previously described [19]. Chalcone **3** was dissolved in DMSO and kept under dark conditions at 25 °C. Before each experiment the chalcone was dissolved in culture media at 37 °C and the final concentration of DMSO did not exceed 0.3% (v/v).

2.3. DNA fragmentation

Cells were harvested by centrifugation, washed twice with PBS, resuspended in 30 μl of lysis buffer [50 mM Tris-HCl (pH 8.0) 10 mM EDTA and 0.5% SDS] and incubated sequentially with 1 $\mu\text{g}/\mu\text{l}$ of RNase A for 1 h at 37 °C and 1 $\mu\text{g}/\mu\text{l}$ of proteinase K for 1 h at 50 °C. Two μl of bromophenol blue (0.25%) was added and DNA was extracted with 100 μl of the mixture [phenol: chloroform: isoamyl alcohol (25: 24: 1)].

Samples were centrifuged at $12,000 \times g$ for 1 min at 25°C and the aqueous phases were extracted with 100 μl chloroform. Five μl of loading buffer [10 mM EDTA (pH 8.0), with 1% (w/v) of low melting point agarose, 0.25% bromophenol blue and 40% sucrose] was added and the mixture was incubated at 70°C during 10 min. The samples were separated in a 1.8% agarose gel by electrophoresis at 5 V/cm during 3–4 h, in TAE buffer (40 mM Tris-acetate, 1 mM EDTA, pH 8.0). The gel was stained with ethidium bromide (1 $\mu\text{g}/\text{ml}$) during 20 min, exposed to UV illumination and the image captured by the DC290 Zoom Digital Camera (Kodak, Rochester, NY, USA).

2.4. Fluorescent microscopy analysis

Cells were washed with PBS and fixed in 3% paraformaldehyde for 10 min at room temperature. The paraformaldehyde was removed by centrifugation ($12,000 \times g$, 1 min, 25°C) and the samples were stained with 20 $\mu\text{g}/\text{ml}$ of bisbenzimidazole trihydrochloride (Hoechst 33258) in PBS at 25°C during 15 min. An aliquot of 10 μl of the mixture was used to observe the stained nuclei with a fluorescent microscopy (Zeiss-Axiovert).

2.5. Quantification of hypodiploid cells and flow cytometry analysis of annexin V-FITC and propidium iodide-stained cells

Flow cytometric analysis of propidium iodide-stained cells was performed as previously described [20]. Briefly, cells (2.5×10^5) were centrifuged for 10 min at $500 \times g$, washed with cold PBS, fixed with ice-cold 75% ethanol and stored at -20°C for 1 h. Samples were then centrifuged at $500 \times g$ for 10 min at 4°C , washed with PBS, resuspended in 200 μl of PBS containing 100 $\mu\text{g}/\text{ml}$ RNase A and 50 $\mu\text{g}/\text{ml}$ propidium iodide and incubated for 1 h in the dark. The DNA content was analyzed by flow cytometry with a BD FACSVerser[™] cytometer (BD Biosciences, San Jose, CA, USA). Flow cytometric analysis of annexin V-FITC and propidium iodide-stained cells was performed as described [20].

2.6. Assay of caspase activity

Caspase activity was determined by measuring proteolytic cleavage of the chromogenic substrates Ac-DEVD-pNA (for caspase-3 like protease activity), Ac-IETD-pNA (for caspase-8 activity) and Ac-LEHD-pNA (for caspase-9 activity) as previously described [20].

2.7. Western blot analysis

Cells were harvested by centrifugation ($500 \times g$, 10 min, 4°C) and pellets were resuspended in lysis buffer [1% Triton X-100, 10 mM sodium fluoride, 2 mM EDTA, 20 mM Tris-HCl (pH 7.4), 2 mM tetrasodium pyrophosphate, 10% glycerol, 137 mM NaCl, 20 mM sodium β -glycerophosphate], with the protease inhibitors phenylmethylsulfonyl fluoride (PMSF, 1 mM), aprotinin, leupeptin, and pepstatin A (5 $\mu\text{g}/\text{ml}$ each) and kept on ice during 15 min. Cells were sonicated on ice five times (5 s each, with intervals between each sonication of 5 s) with a Braun Labsonic 2000 microtip sonifier and centrifuged ($11,000 \times g$, 10 min, 4°C). Bradford's method was used to determine protein concentration. The samples that were loaded in sodium dodecyl sulphate-polyacrylamide gel (from 7.5 to 15% depending on the molecular weight of interest) were prepared with the same amount of protein and boiled for 5 min. The proteins were transferred to a poly(vinylidene difluoride) membrane for 20 h at 20 V. The membrane was blocked with 10% nonfat milk in Tris-buffered saline [50 mM Tris-HCl (pH 7.4), 150 mM NaCl] containing 0.1% Tween-20 (TBST) for 1 h, followed by incubation with specific antibodies against caspase-3, caspase-4, caspase-6, caspase-7, caspase-8, caspase-9, Bax, Bcl-2, β -actin and poly (ADP-ribose)polymerase overnight at 4°C . Membranes were washed three times with TBST and incubated for 1 h with the specific secondary

antibody and the antigen-antibodies complexes were visualized by enhanced chemiluminescence using the manufacturer's protocol.

2.8. Subcellular fractionation

Cells were harvested by centrifugation ($500 \times g$, 10 min, 4°C) and washed two times with cold PBS at 4°C . The pellets were resuspended in buffer [20 mM HEPES (pH 7.5), 1 mM EDTA, 0.1 mM phenylmethylsulfonyl fluoride, 1.5 mM MgCl_2 , 1 mM EGTA, 10 mM KCl, 1 mM dithiothreitol, and 5 $\mu\text{g}/\text{ml}$ leupeptin, aprotinin, and pepstatin A] with 250 mM sucrose. The samples were incubated during 15 min on ice and lysed 10 times with a 22-gauge needle. The lysates were centrifuged ($1,000 \times g$, 5 min, 4°C). The supernatants were centrifuged at $105,000 \times g$ for 45 min at 4°C , and the resulting supernatant was used as the soluble cytosolic fraction and analysed by immunoblotting with specific antibodies against Smac/DIABLO and cytochrome c.

2.9. Analysis of mitochondrial membrane potential ($\Delta\Psi_m$) and intracellular reactive oxygen species (ROS) determination

The mitochondrial membrane potential was measured by flow cytometry using the fluorochrome 5,5',6,6'-tetrachloro-1,1',3,3'-tetraethylbenzimidazolylcarbocyanine iodide (JC-1) and intracellular ROS were detected by flow cytometry using the probe 2',7'-dichlorodihydrofluorescein diacetate (H_2 -DCF-DA). Flow cytometric analysis was carried out using a BD FACSVerser[™] cytometer (BD Biosciences, San Jose, CA, USA). All of the methods have been described in detail elsewhere [21].

2.10. Statistical methods

Statistical differences between means were tested using (i) Student's *t*-test (two samples) or (ii) one-way analysis of variance (ANOVA) (3 or more samples) with Tukey's test used for *a posteriori* pairwise comparisons of means. A significance level of $P < 0.05$ was used.

3. Results

3.1. The synthetic chalcone, 6'-benzyloxy-4-bromo-2'-hydroxychalcone, inhibits the viability of human leukaemia cells

Preliminary studies on U-937 cells revealed that the 2'-hydroxychalcone derivative containing a bromine atom at position 4 and a benzyloxy at position 6' (CHAL) displays a higher cytotoxic potency [IC_{50} (50% inhibition of cell growth) = $4.4 \pm 1.1 \mu\text{M}$] than the 2'-hydroxychalcone ($\text{IC}_{50} = 42.0 \pm 6.5 \mu\text{M}$) and also than the analogue containing a bromine atom at position 4 ($\text{IC}_{50} = 17.0 \pm 2.0 \mu\text{M}$). The 2'-hydroxychalcone containing a benzyloxy group at position 6' displays a similar cytotoxic potency than CHAL ($\text{IC}_{50} = 5.0 \pm 2.6 \mu\text{M}$). Since we were interested in the study of halogen chalcones, CHAL was selected to determine its cytotoxic properties in several human leukaemia cells. In addition, the precursor 4-bromobenzaldehyde for CHAL synthesis is more stable than benzaldehyde itself used in the synthesis of 6'-benzyloxy-2'-hydroxychalcone. Synthesis of CHAL was carried out using a standard strategy for the generation of chalcones and involved an aldol condensation reaction in basic media to generate the desired chalcone 3 (Fig. 1A) [22,23].

CHAL was found to have strong cytotoxic properties with IC_{50} values of approximately $5 \mu\text{M}$ against the seven human leukaemia cell lines tested (Table 1), including the human histiocytic lymphoma U-937, the human chronic myeloid leukaemia K-562, the human acute myeloid leukaemia HL-60, the human B cell precursor leukaemia NALM-6, the acute lymphoblastic leukaemia MOLT-3 and cell lines over-expressing Bcl-2 (U-937/Bcl-2) and the glycoprotein P (K-562/ADR). For comparison, the standard antitumor agent etoposide was included as a positive control for U-937 ($\text{IC}_{50} = 1.2 \pm 0.3 \mu\text{M}$), HL-60

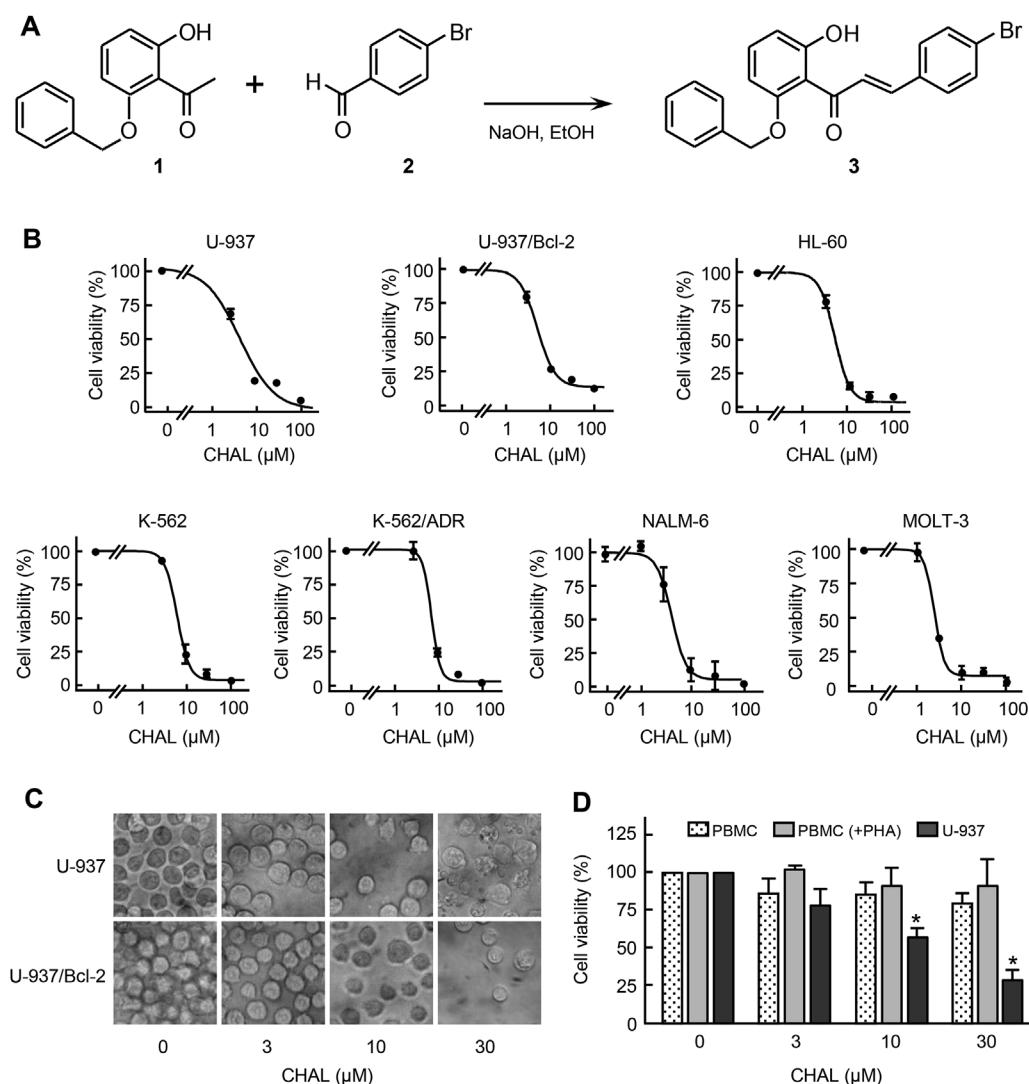


Fig. 1. Synthesis and effects on cell viability of CHAL. (A) Synthesis and chemical structure of CHAL. (B) Dose-response study of CHAL on human leukaemia cells viability. Cells were cultured in the presence of increasing concentrations of CHAL for 72 h, and thereafter cell viability was determined by the MTT assay. (C) Photomicrographs of morphological changes visualized with an inverted phase contrast microscope after treatment with CHAL for 24 h. (D) Differential effects of CHAL on cell viability of normal peripheral blood mononuclear cells (PBMC) versus U-937 cells. Human leukaemia, and quiescent and phytohemagglutinine-activated PBMC [PBMC (+PHA)] cells from healthy human origin were cultured in the presence of the specified concentrations of CHAL for 24 h. Values represent means \pm SE for three independent experiments each performed in triplicate. * $P < 0.05$, significantly different from the corresponding control.

($IC_{50} = 0.3 \pm 0.1 \mu\text{M}$) and MOLT-3 ($IC_{50} = 0.2 \pm 0.1 \mu\text{M}$). Treatment with this chalcone resulted in a concentration-dependent inhibition of cell viability (Fig. 1B) and induced significant morphological changes and an important reduction in the number of cells (Fig. 1C). In addition, quiescent and proliferating peripheral blood mononuclear cells were more resistant than U-937 cells, even at $30 \mu\text{M}$ CHAL (Fig. 1D). These results indicate that CHAL displays strong cytotoxic properties against leukaemia cells but has only weak cytotoxic effects against peripheral blood mononuclear cells (PBMCs) and also that the overexpression of the Bcl-2 protein and glycoprotein P did not confer resistance to CHAL-induced cytotoxicity.

3.2. CHAL induces apoptosis on human leukaemia cells

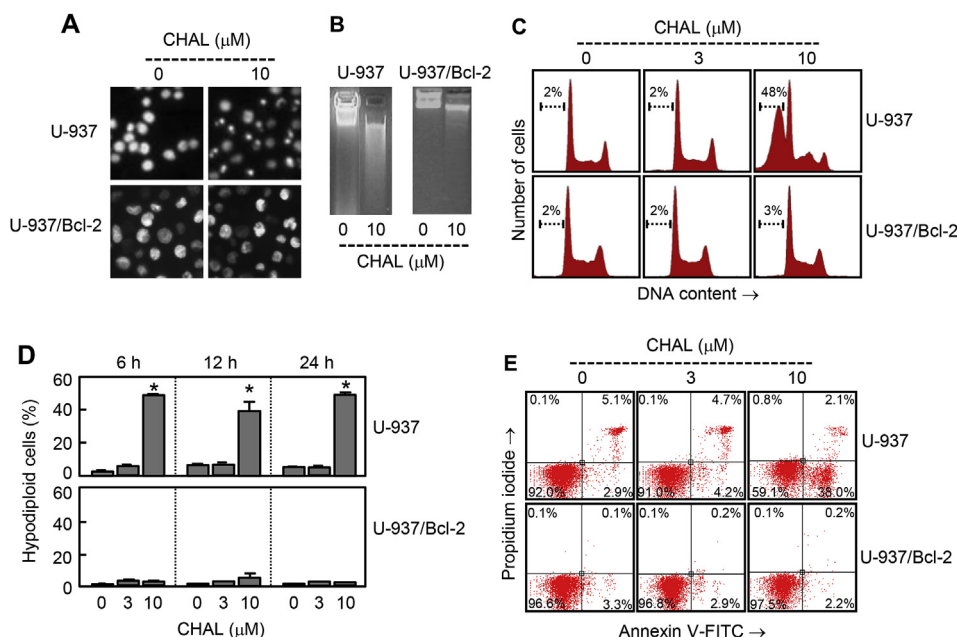
To elucidate the mechanism responsible for inhibition of cell viability, we investigated whether CHAL induces apoptosis. To this end,

we analysed the nuclei of treated cells ($10 \mu\text{M}$ CHAL for 24 h) using fluorescent microscopy after staining with the fluorochrome bisbenzimidazole trihydrochloride (Hoechst 33258) and observed condensation and fragmentation of chromatin in U-937 cells but not in U-937/Bcl-2 cells (Fig. 2A). Agarose gel electrophoresis showed typical DNA fragmentation caused by internucleosomal hydrolysis of chromatin after treatment with $10 \mu\text{M}$ CHAL for 24 h (Fig. 2B). Evaluation of the percentage of sub- G_1 (hypodiploid) cells by flow cytometry showed that the percentage of apoptotic cells increased approximately 25-fold in CHAL-treated U-937 compared with control cells after 24 h exposure at concentration as low as $10 \mu\text{M}$. In contrast, $3 \mu\text{M}$ CHAL for 24 h was not sufficient to trigger apoptosis (Fig. 2C). Interestingly, treatment with $10 \mu\text{M}$ CHAL for 24 h did not induce apoptosis in PBMC (results not shown). Time-course experiments revealed that apoptotic cells were already detected at 6 h of treatment, however, in U-937/Bcl-2 cells, the percentage of sub- G_1 cells did not increase significantly after 24 h of

Table 1
Effects of CHAL on cell viability of human leukaemia cell lines.

IC_{50} (μM)						
U-937	U-937/Bcl-2	HL-60	K-562	K-562/ADR	NALM-6	MOLT-3
4.4 ± 1.1	5.0 ± 0.2	4.9 ± 0.5	7.2 ± 0.8	8.9 ± 1.8	4.3 ± 0.1	2.7 ± 0.3

Cells were cultured for 72 h and the IC_{50} values were calculated as described in the Experimental Section. The data shown represent the mean \pm SE of 3–5 independent experiments with three determinations in each.



indicated concentrations of CHAL for 24 h. Cells appearing in the lower right quadrant show positive annexin V-FITC staining, which indicates phosphatidylserine translocation to the cell surface, and negative PI staining, which demonstrates intact cell membranes, both features of early apoptosis. Cells in the top right quadrant are double positive for annexin V-FITC and PI and are undergoing necrosis. Representative data from three separate experiments are shown.

treatment with 10 μM CHAL (Fig. 2D). CHAL (10 μM, for 24 h) also led to the exposure of phosphatidylserine on the outside of the plasma membrane as detected by annexin V-FITC staining in U-937 cells (Fig. 2E). The results indicate that CHAL is a potent apoptotic inducer in human myeloid leukaemia cells and that the overexpression of Bcl-2 does not confer protection against apoptosis induction.

To assess whether cell growth inhibition is also mediated by alterations in the cell cycle, cells were incubated with CHAL for different time periods (6–24 h), stained with propidium iodide and analyzed by flow cytometry. There were no obvious changes in the different phases of the cell cycle after treatment with different concentrations of CHAL (3–10 μM) across the different time periods (results not shown).

3.3. CHAL-induced apoptosis is mediated by a caspase-dependent pathway

U-937 and U-937/Bcl-2 cells were cultured for 24 h with 10 μM CHAL in order to investigate the influence of caspases in their responses to this chalcone. Lysates were analyzed by Western blot using specific antibodies (Fig. 3A). The results showed that CHAL induced the cleavage of the initiator caspases-8 and -9, in U-937 but not in U-937/Bcl-2 cells. The chalcone also induced hydrolysis of pro-caspase-6 and -7, as well as the proteolytic processing of pro-caspase-3 only in U-937 cells. Pro-caspase-4 which has been involved in the endoplasmic reticulum stress was also processed. Poly(ADP-ribose) polymerase was effectively hydrolysed to the 85 kDa fragment after CHAL treatment, in accordance with the pro-caspase-3 activation. These results indicate that CHAL induces the processing of multiple caspases in U-937 but not in U-937/Bcl-2 cells.

The enzymatic activities of caspases-3/7, -8 and -9 were also evaluated since they are not always associated with pro-caspase processing. Cells were treated with CHAL (10 μM, 24 h) and lysates were assayed for the cleavage of the tetrapeptide substrates Ac-DEVD-pNA, Ac-IETD-pNA and Ac-LEHD-pNA as specific substrates of caspase-3/7, caspase-8 and caspase-9, respectively. The results showed a significant activation of these caspases after 24 h of treatment in U-937 but not in U-937/Bcl-2 cells (Fig. 3B), in accordance with the immunoblot experiments. These results indicate that CHAL is able to induce activation of caspases in leukaemia cells.

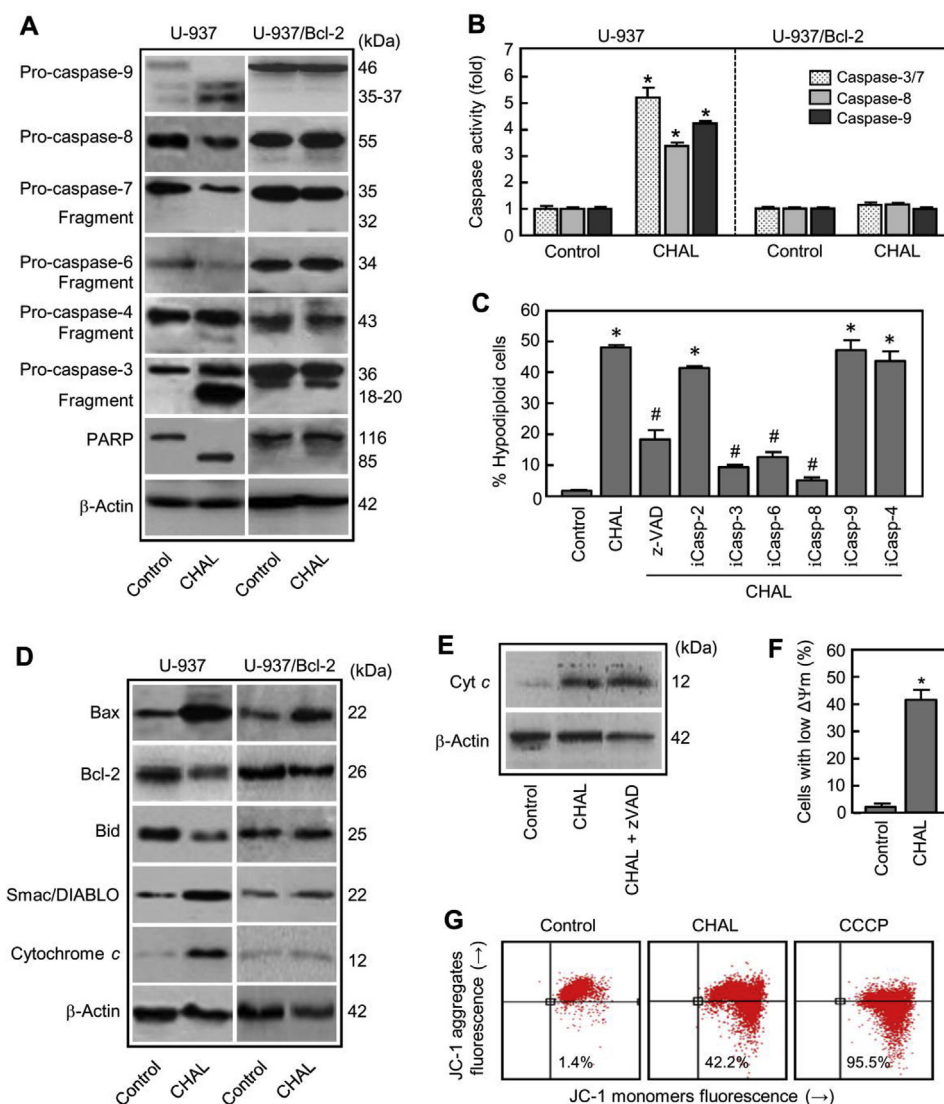
Fig. 2. Effects of CHAL on apoptosis induction in human myeloid leukaemia cells. (A) Photomicrographs of representative fields of cells stained with bisbenzamide trihydrochloride to evaluate nuclear chromatin condensation after treatment with 10 μM CHAL for 24 h. (B) Cells were incubated with 10 μM CHAL for 24 h and genomic DNA was extracted, separated on an agarose gel and visualized under UV light after ethidium bromide staining. (C) Cells were incubated in the presence of the indicated concentrations of CHAL and subjected to DNA flow cytometry using propidium iodide labelling. Representative histograms and the percentage of hypodiploid cells (apoptotic cells) are shown. (D) Cells were incubated in the presence of the specified concentrations of CHAL for different periods of time and the percentage of hypodiploid cells was determined by flow cytometry using the propidium iodide labelling method. Values represent means ± SE from three different experiments performed in triplicate. * indicates $P < 0.05$ for comparison with untreated control. (E) Flow cytometry analysis of annexin V-FITC and propidium iodide (PI)-stained U-937 and U-937/Bcl-2 cells after treatment with the

To determine whether caspases were involved in the apoptosis, U-937 cells were pretreated with the general caspase inhibitor z-VAD-fmk (100 μM) and cultured in the presence of CHAL for 24 h. As shown in Fig. 3C, apoptosis was significantly reduced, suggesting a caspase-dependent pathway. To identify which caspases were important in CHAL-induced apoptosis, the effect of specific cell-permeable caspase inhibitors was examined. The caspase-3/7 inhibitor (z-DEVD-fmk, 50 μM), the caspase-6 inhibitor (Ac-VEID-CHO, 25 μM) and the caspase-8 inhibitor (z-IETD-fmk, 50 μM) blocked the apoptosis induced by CHAL (10 μM) in U-937 cells. In contrast, neither the caspase-4 inhibitor (Ac-LEVD-CHO), nor caspase-9 inhibitor (z-LEHD-fmk, 50 μM) nor the caspase-2 inhibitor (z-VDVAD-fmk, 50 μM) blocked the apoptosis in U-937 cells (Fig. 3C). These experiments demonstrate that the extrinsic apoptotic pathway played the main role in U-937 cells death induced by CHAL.

To determine the mitochondrial proteins release, cytosolic preparations were analyzed by Western blot after 24 h treatment with 10 μM CHAL. As shown (Fig. 3D) cytochrome c levels increased in the cytosolic fraction in accordance with the processing and activation of pro-caspase-9 and also the substantial release of the proapoptotic mitochondrial protein Smac/DIABLO. Moreover, Bcl-2 levels clearly decreased after treatment with CHAL, while there was an increase in the proapoptotic factor Bax. CHAL also induced a decrease in Bid levels suggesting the processing of this protein due to caspase-8 activation (Fig. 3D).

To determine whether cytochrome c release precedes caspase activation, U-937 cells were preincubated with the pancaspase inhibitor z-VAD-fmk (1 h, 100 μM) and then followed with 10 μM CHAL for 24 h. The broad-spectrum caspase inhibitor was unable to prevent cytochrome c release, which suggests that cytochrome c release is independent of caspase activation (Fig. 3E).

To examine whether a disruption of the mitochondrial membrane potential ($\Delta\Psi_m$) is associated with the release of mitochondrial proteins, cells were stained with the fluorescent probe JC-1 and analysed by flow cytometry. It was found that the $\Delta\Psi_m$ dropped at 6 h of treatment, indicating that the dissipation of $\Delta\Psi_m$ is an early event in CHAL-induced apoptosis (Fig. 3F). Representative dot plots of these experiments are shown, including the experiment that used protonophore



metry after staining with the JC-1 probe. *indicates $P < 0.05$ for comparison with untreated control. (G) Representative dot plots after staining with the JC-1 probe; as a positive control, cells were stained in the presence of 50 μ M of CCCP (carbonyl cyanide *m*-chlorophenylhydrazone).

CCCP as a positive control (Fig. 3G).

3.4. Effect of cathepsins and mitogen-activated protein kinases (MAPKs) inhibitors and dependence on reactive oxygen species in CHAL-induced cell death

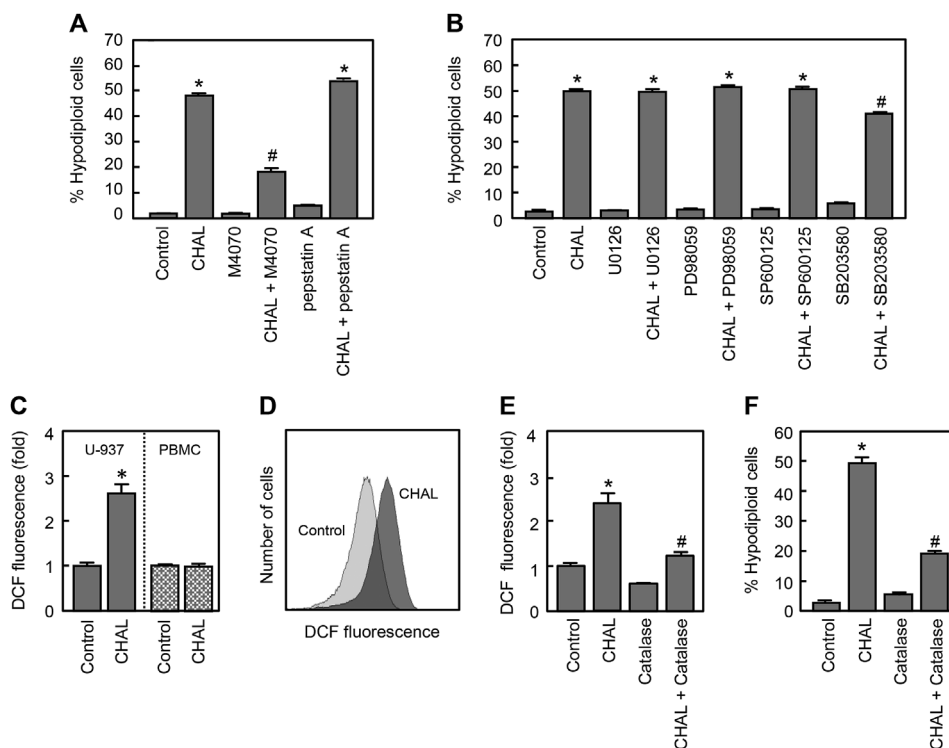
Since lysosomal cathepsins have been associated with caspase-dependent and -independent apoptotic cell death and with the activation of the intrinsic apoptotic pathway, their involvement was investigated using the cathepsin inhibitors Mu-Phe-HPh-fmk (M4070, cathepsins B/L inhibitor) and pepstatin A (cathepsin D inhibitor). As shown in Fig. 4A, cathepsins B/L inhibition significantly decreased apoptosis stimulated by CHAL suggesting that these types of proteases might be involved in cell death.

The mitogen-activated protein kinases (MAPKs) cascades play important roles in the regulation of apoptosis and growth of malignant hematopoietic cells. To determine whether activation of MAPKs plays a key role in CHAL-induced apoptosis, the effect of pharmacological inhibitors of MAPKs was investigated. Treatment of cells with inhibitors of mitogen-activated extracellular kinases 1/2 (MEK1/2), namely PD98059 or U0126 and the specific JNK/SAPK (c-Jun N-terminal kinases/stress activated protein kinase) inhibitor SP600125, had no

Fig. 3. Processing, activation and role of caspases and mitochondrial proteins in CHAL-induced apoptosis on leukaemia cells. (A) Cells were incubated with 10 μ M CHAL for 24 h and the cleavage of caspases and PARP was analyzed by immunoblotting. The protein β -actin was used as a loading control. (B) Caspase activation induced by CHAL on leukaemia cells. Cells were treated as above and cell lysates were assayed for caspase-3/7, -8 and -9 activities. Results are expressed as n-fold increases in caspase activity compared with control. Values represent the means \pm SE of three independent experiments each performed in triplicate. *indicates $P < 0.05$ for comparison with untreated control. (C) Cells were pretreated with z-VAD-fmk (100 μ M) or the selective caspase inhibitors z-VDVAD-fmk (iCasp-2, 50 μ M), z-DEVD-fmk (iCasp-3, 50 μ M), VEID-CHO (iCasp-6, 25 μ M), z-IETD-fmk (iCasp-8, 50 μ M), z-LEHD-fmk (iCasp-9, 50 μ M) or LEVD-CHO (iCasp-4, 50 μ M) for 1 h before the addition of CHAL (10 μ M) during 24 h, and apoptotic cells were analyzed by flow cytometry. Bars represent the mean \pm SE of three independent experiments each performed in triplicate. *indicates $P < 0.05$ for comparison with untreated control. # indicates $P < 0.05$ for comparison with CHAL treatment alone. (D) Effect of CHAL on mitochondrial cytochrome c and Smac/DIABLO release and on Bcl-2 family members. Cells were treated with 10 μ M CHAL and cytosolic fractions (in the case of cytochrome c and Smac/DIABLO) or whole cell lysates (for Bax, Bcl-2 and Bid) were analyzed by Western blot. β -Actin was used as a loading control. (E) Cytochrome c release is not inhibited by z-VAD-fmk. U-937 cells were pretreated with the caspase inhibitor z-VAD-fmk (100 μ M, 1 h) and then with CHAL (10 μ M, 24 h) and cytosolic fractions were subjected to immunoblotting. (F) CHAL reduces the mitochondrial membrane potential ($\Delta\Psi_m$). U-937 cells were treated with 10 μ M CHAL, harvested at 6 h and $\Delta\Psi_m$ analyzed by flow cytometry.

influence on the percentage of hypodiploid cells induced by CHAL. In contrast, the p38^{MAPK} (p38 mitogen-activated protein kinase) inhibitor SB203580 partially decreased the percentage of hypodiploid cells (Fig. 4B).

Increased reactive oxygen species (ROS) production may lead to cell death in leukaemia cells [24]. To determine whether CHAL induces ROS, U-937 cells were treated with the chalcone, stained with the fluorescent dye 2', 7'-dichlorodihydrofluorescein diacetate (H₂-DCF-DA) and analysed by flow cytometry. As shown in Fig. 4C, in U-937 cells but not in PBMC, treatment with 10 μ M CHAL induced a 2.5-fold increase in the H₂-DCF-DA-derived fluorescence as indicated by a rightward shift in fluorescence (Fig. 4D). These results suggest that CHAL induces the generation of H₂O₂ and other peroxides. To investigate whether ROS is involved in the apoptosis induced by CHAL, U-937 cells were preincubated with the antioxidants *N*-acetyl-L-cysteine (10 mM), α -tocopherol (20 μ M), trolox (2 mM), the NADPH oxidase inhibitor diphenyleneiodonium chloride (1 μ M), superoxide dismutase (400 units/ml) and catalase (500 units/ml). None of these antioxidants, except catalase, blocked ROS generation (Fig. 4E) or cell death (Fig. 4F) as assessed by flow cytometry indicating that CHAL-induced apoptosis is dependent on ROS production.



24 h with 10 μ M CHAL and the fluorescence of oxidized H_2DCF (E) and the percentage of hypodiploid cells (F) were determined by flow cytometry. Bars represent the means \pm SE of three independent experiments each performed in triplicate. *indicates $P < 0.05$ for comparison with untreated control. # indicates $P < 0.05$ for comparison with CHAL treatment alone.

4. Discussion

Chemotherapy drugs used in the treatment of cancer are expensive, toxic and show limited efficacy in treating these diseases. Naturally occurring compounds or compounds inspired in natural products have attracted the attention as potential anticancer agents. Chalcones are compounds that can be easily obtained by synthetic methods and, in general, are less toxic than current chemotherapy. These compounds display a vast array of pharmacological and biological activities, including antitumor properties. Chalcones have been described as Notch signalling inhibitors. This signal transduction pathway is considered a rational target in potential anticancer therapy because Notch inhibition triggers antiproliferative and pro-apoptotic effects in several human T-cell acute lymphoblastic leukaemia cells [25]. Recently, anthraquinone-chalcone hybrids have been reported as strong cytotoxic and apoptotic inducers in human leukaemia cell lines [26]. The naturally occurring chalcone brousssochalcone A has been described as a human cytochrome P450 2J2 inhibitor that is cytotoxic against human hepatoma HepG2 cells [27].

In this study, we designed a specific chalcone, 6'-benzyloxy-4-bromo-2'-hydroxychalcone, to examine the hypothesis that the introduction of one benzyloxy group at position 6' in the A ring might enhance cytotoxicity against cancer cell lines (due to an increase in lipid solubility that would facilitate cell penetration). Neither the effects on cell viability nor the mechanism involved in cell death induction of this specific chalcone have been investigated to date. Synthetic chalcone was screened for cytotoxicity against human tumour cells and found to be a potent cytotoxic compound against seven human leukaemia cell lines, including cells that overexpress the anti-apoptotic protein Bcl-2 and the glycoprotein P. Since P-glycoprotein-mediated multidrug resistance is a major limitation of the clinical efficacy of microtubule-targeting agents, it is necessary to find new compounds that may overcome this resistance. Experiments using P-glycoprotein-overexpressing K-562/ADR cells indicate that CHAL was also cytotoxic

in these cells, showing similar IC_{50} values in both the multidrug resistant K-562/ADR ($IC_{50} = 7.2 \pm 0.8 \mu$ M) and the corresponding parent K-562 cells ($IC_{50} = 8.9 \pm 1.8 \mu$ M). Interestingly, dose-response studies revealed that quiescent PBMC and proliferating PBMC were resistant toward CHAL. One possible explanation why normal cells are resistant to CHAL could be that this chalcone targets the transcription factor nuclear factor κ B (NF- κ B) which is the major molecular target affected by some chalcones [2,28]. For example, the naturally occurring butein (2',3,4,4'-tetrahydroxychalcone) blocks NF- κ B through I κ B kinase inhibition, avoiding its nuclear translocation and therefore deregulating its downstream biomolecules. This inactivation of NF- κ B is involved in apoptosis induction and the inhibition of proliferation, cell cycle progression, angiogenesis, invasion, metastasis and chemoresistance of various cancers [28]. NF- κ B signalling is elevated in leukemic stem cells but not in the normal hematopoietic stem cells. The ability to target the NF- κ B pathway could be the reason why CHAL selectively kills cancer and not normal cells. Normal cells might not be sensitive to CHAL because their basal NF- κ B activity is often low or sometimes required for cell differentiation rather than oncogenesis [29,30]. In addition, the modulation of ROS production could explain the preferential toxicity towards cancer cells, since CHAL was unable to induce ROS generation in PBMC. NF- κ B is involved in the processes of oxidative stress response and the increase in intracellular ROS in U-937 cells, as described here, could activate this transcription factor. Further studies are needed to determine whether NF- κ B signalling is a target of CHAL.

A recent report describes how a novel 3',5'-diprenylated chalcone inhibits the growth of the human leukaemia cells HEL and K-562 with IC_{50} values that were comparable with the chalcone described in this paper. However, this chalcone was also cytotoxic against human normal hepatocyte (LO2) cells. The authors concluded that 3',5'-diprenylated chalcone may inhibit the growth of leukaemia cells by inducing apoptosis and autophagy [31].

The experiments described here support apoptosis as the main cytotoxicity pathway induced by CHAL in U-937 cells and that

overexpression of the anti-apoptotic protein Bcl-2 does not confer resistance to apoptosis. The effects of CHAL in U-937 cells include condensation and fragmentation of chromatin, an increase in hypodiploid DNA content, caspase activation and a significant reduction in apoptosis by the pan-caspase inhibitor z-VAD-fmk, supporting a caspase dependent cell death mechanism. An effective blockage of CHAL-induced apoptosis by z-IETD-fmk was observed supporting a mechanism mediated by the initiator caspase-8. In contrast, the selective inhibitor against caspase-9 (z-LEHD-fmk) was unable to significantly block cell death suggesting a minor role of this initiator caspase in CHAL-induced cell death. Future experiments will be necessary to confirm the role of caspase-9 in the mechanism of cell death. Recently, we have described an effective block of cell death induced by the synthetic flavonoid 3',4'-dibenzoyloxyflavonol by the selective inhibitor of caspase-9 but not by the selective inhibitor of caspase-8 [14]. Although CHAL is able to induce caspase-4 cleavage, the endoplasmic reticulum stress signalling pathway does not appear to be involved since apoptosis was not blocked by a caspase-4 inhibitor. However it is important to note that the experiments of caspase activation reveal inductions of both initiator caspases, caspase-8 and -9, activities in U-937 cells but there was not a significant activation of caspases in U-937/Bcl-2. Moreover, the results demonstrate i) that caspase-3/7 is activated in response to CHAL and ii) the inhibitors against caspase-3/7 (z-DEVD-fmk) and caspase-6 (VEID-CHO) were able to block cell death.

Overexpression of Bcl-2 protein protects the cells, because it prevents the release of the pro-apoptotic protein cytochrome *c* from the mitochondria to the cytosol, apoptosome formation and the consequent activation of caspase-9 [32]. Our experiments demonstrate that CHAL is cytotoxic against human leukaemia U-937 cells that overexpress Bcl-2, as determined by the MTT assay. We emphasize that the cytotoxicity experiments were performed with long incubation times (72 h), while those that evaluated apoptosis were carried out for much shorter times. It is possible that CHAL might affect the cell viability in U-937/Bcl-2 by a different mechanism to apoptosis. Although we did not observe any change in the percentages of cells in each phase of the cell cycle up to 24 h in both cell lines, U-937 and U-937/Bcl-2, one explanation might be the increase in the duration of each phase of the cell cycle, as described for the electron transport chain complex II inhibitor 2-thienyltrifluoroacetone [33]. Further studies will be necessary to determine how inactivation or avoidance of Bcl-2 protein protection is achieved to yield similar IC₅₀ values in both cell lines (U-937 and U-937/Bcl-2). In U-937 cells, this chalcone induces the release of the proapoptotic mitochondrial proteins cytochrome *c* and Smac/DIABLO, a decrease in Bcl-2 levels and up-regulation of Bax. A decrease in the ratio Bcl-2/Bax has been also observed in K-562 cells treated with the 3'-geranyl-mono-substituted chalcone xanthoangelol, however the concentrations of this chalcone (up to 30 µM) and exposure durations (up to 48 h) were higher than those used here [34].

Several death stimuli can induce the lysosomal pathway which is characterized by a partial rupture of lysosome membrane and subsequent release of cathepsins into the cytosol [35]. Experiments with cathepsins inhibitors revealed that these cysteine proteases are also involved in the mechanism of cell death. The effective blockage of apoptosis induction by an inhibitor of cathepsins B/L supports a model in which CHAL also induces cell death by a cathepsins B/L mediated mechanism. Future studies will be necessary to determine whether additional pathways of cell death are involved in U-937 cells.

The mitogen activated protein kinase signalling pathway is involved in the control of cell proliferation, differentiation and apoptosis. The ERK1/2 (extracellular signal-regulated kinase) pathway is involved in cell proliferation and differentiation, whereas JNK/SAPK and p38^{MAPK} pathways are activated in response to stress and growth factors and mediate signals that regulate apoptosis [36]. Neither the specific MEK 1/2 inhibitors nor the selective JNK/SAPK inhibitor SP600125 influenced or attenuated cell death, suggesting that activation of these protein kinases is not required for apoptosis triggered by CHAL.

However, inhibition of p38^{MAPK} was found to decrease partially cell death suggesting that activation of this protein kinase is involved in part in CHAL induced-apoptosis. The activation of p38 mitogen-activated protein kinase signalling plays a key role not only in inhibiting but in promoting proliferation and in increasing resistance to chemotherapeutic agents [37]. It has been shown that inhibition of p38^{MAPK} using the pharmacologic inhibitor SB203580 enhances all-*trans*-retinoic acid-dependent growth inhibition of acute promyelocytic leukaemia [38] and also reduces the apoptosis induced by the combination of arsenic trioxide and the isoflavone genistein in U-937 cells [39]. A similar attenuation of apoptosis by SB203580 has been observed in U-937 cells treated with cadmium, suggesting that p38^{MAPK} activation is required, at least in part, for cadmium-induced apoptosis [40].

Reactive oxygen species (ROS) display a variety of biological effects including, among others, enhanced cell proliferation and cell death. Many antitumor compounds exhibit cytotoxic properties via ROS-dependent activation of apoptotic cell death in cancer cells including leukemic cells [41]. We demonstrate that the synthetic chalcone induced a fast ROS generation in U-937 cells. This elevated ROS production may affect the activity of a variety of apoptotic effectors such as the Bcl-2 family of proteins and the mitochondrial cytochrome *c* [42]. In addition, the increased levels of ROS might trigger the activation of death receptors [43]. The results shown here demonstrate that ROS play a key role in the mechanism of cell death triggered by CHAL, since the enzymatic antioxidant catalase was able to block ROS generation and cell death. Further experiments will be needed to determine whether CHAL is able to induce death receptors, including Fas, TNF receptor 1, TNF-related apoptosis inducing ligand receptor 1 and TNF-related apoptosis inducing ligand receptor 2.

5. Conclusions

CHAL displays potent cytotoxic properties against human leukaemia cells (U-937, HL-60, K-562, NALM-6 and MOLT-3) including Bcl-2-overexpressing U-937/Bcl-2 and P-glycoprotein-overexpressing K-562/ADR, but has only weak cytotoxic effects on peripheral blood mononuclear cells (PBMCs). Growth inhibition of U-937 cells was caused by induction of apoptotic cell death and the overexpression of Bcl-2 conferred resistance to apoptosis. Cell death was associated with the activation of multiple caspases and was dependent on the generation of reactive oxygen species. It was prevented by the selective caspase-3/7, -6 and -8 inhibitors, and by a cathepsins B/L inhibitor. CHAL is a potent apoptotic inducer in human leukaemia cells that might be useful in the development of new strategies for targeted cancer therapies.

Conflicts of interest

We declare no conflict of interest.

Acknowledgments

We thank Dr. Jacqueline Bréard (INSERM U749, Faculté de Pharmacie Paris-Sud., Châtenay-Malabry, France) and Dr. Lisa Oliver (INSERM, Nantes, France) for supplying U-937/Bcl-2 and K-562/ADR, respectively.

Funding: This research was supported in part by the Spanish Ministerio de Economía y Competitividad (MINECO) and the European Regional Development Fund (CTQ2015-63894-P).

Transparency document

Transparency document related to this article can be found online at <https://doi.org/10.1016/j.cbi.2018.12.010>.

Appendix A. Supplementary data

Supplementary data to this article can be found online at <https://doi.org/10.1016/j.cbi.2018.12.010>.

References

- [1] D. Ravishanker, A.K. Rajora, F. Greco, H.M. Osborn, Flavonoids as prospective compounds for anti-cancer therapy, *Int. J. Biochem. Cell Biol.* 45 (2013) 2821–2831, <https://doi.org/10.1016/j.biocel.2013.10.004>.
- [2] B. Orlikova, D. Tasdemir, F. Golais, M. Dicato, M. Diederich, The aromatic ketone 4'-hydroxychalcone inhibits TNF α -induced NF- κ B activation via proteasome inhibition, *Biochem. Pharmacol.* 82 (2011) 620–631, <https://doi.org/10.1016/j.bcp.2011.06.012>.
- [3] J. Loa, P. Chow, K. Zhang, Studies of structure-activity relationship on plant polyphenol-induced suppression of human liver cancer cells, *Cancer Chemother. Pharmacology* 63 (2009) 1007–1016, <https://doi.org/10.1007/s00280-008-0802-y>.
- [4] M. Cabrera, M. Simoes, G. Falchi, M.L. Lavaggi, O.E. Piro, E.E. Castellano, A. Vidal, A. Azqueta, A. Monge, A.L. de Cer  n, G. Sagrera, G. Seoane, H. Cerecetto, M. Gonz  lez, Synthetic chalcones, flavanones, and flavones as antitumoral agents: biological evaluation and structure-activity relationships, *Bioorg. Med. Chem.* 15 (2007) 3356–3367, <https://doi.org/10.1016/j.bmc.2007.03.031>.
- [5] D.D. Jandial, C.A. Blair, S. Zhang, L.S. Krill, Y.B. Zhang, X. Zi, Molecular targeted approaches to cancer therapy and prevention using chalcones, *Curr. Cancer Drug Targets* 14 (2014) 181–200, <https://doi.org/10.2174/1568009614666140122160515>.
- [6] T.G. Cotter, Apoptosis and cancer: the genesis of a research field, *Nat. Rev. Canc.* 9 (2009) 501–507, <https://doi.org/10.1038/nrc2663>.
- [7] D.R. Green, F. Llambi, Cell death signaling, *Cold Spring Harb. Perspect. Biol.* 7 (2015), <https://doi.org/10.1101/cshperspect.a006080> pii: a006080.
- [8] S. Shalini, L. Dorstyn, S. Dawar, S. Kumar, Old, new and emerging functions of caspases, *Cell Death Differ.* 22 (2015) 526–539, <https://doi.org/10.1038/cdd.2014.216>.
- [9] A. Ashkenazi, Targeting the extrinsic apoptotic pathway in cancer: lessons learned and future directions, *J. Clin. Invest.* 125 (2015) 487–489, <https://doi.org/10.1172/JCI80420>.
- [10] A.R. Delbridge, A. Strasser, The BCL-2 protein family, BH3-mimetics and cancer therapy, *Cell Death Differ.* 22 (2015) 1071–1080, <https://doi.org/10.1038/cdd.2015.50>.
- [11] C. Wang, R.J. Youle, The role of mitochondria in apoptosis, *Annu. Rev. Genet.* 43 (2009) 95–118, <https://doi.org/10.1146/annurev-genet-102108-134850>.
- [12] T.A. Dias, C.L. Duarte, C.F. Lima, M.F. Proen  a, C. Pereira-Wilson, Superior anticancer activity of halogenated chalcones and flavonols over the natural flavonol quercetin, *Eur. J. Med. Chem.* 65 (2013) 500–510, <https://doi.org/10.1016/j.ejmech.2013.04.064>.
- [13] O. Burmistrova, M.T. Marrero, S. Est  vez, I. Welsch, I. Brouard, J. Quintana, F. Est  vez, Synthesis and effects on cell viability of flavonols and 3-methyl ether derivatives on human leukemia cells, *Eur. J. Med. Chem.* 84 (2014) 30–41, <https://doi.org/10.1016/j.ejmech.2014.07.010>.
- [14] M. Said, I. Brouard, J. Quintana, F. Est  vez, Antiproliferative activity and apoptosis induction by 3',4'-dibenzoyloxyflavonol on human leukemia cells, *Chem. Biol. Interact.* 268 (2017) 13–23, <https://doi.org/10.1016/j.cbi.2017.02.010>.
- [15] C. Zhu, Y. Zuo, R. Wang, B. Liang, X. Yue, G. Wen, N. Shang, L. Huang, Y. Chen, J. Du, X. Bu, Discovery of potent cytotoxic *ortho*-aryl chalcones as new scaffold targeting tubulin and mitosis with affinity-based fluorescence, *J. Med. Chem.* 57 (2014) 6364–6382, <https://doi.org/10.1021/jm500024v>.
- [16] J. Mai, E. Hoxha, C.E. Morton, B.M. Muller, M.J. Adler, Towards a dynamic covalent molecular switch: substituent effects in chalcone/flavanone isomerism, *Org. Biomol. Chem.* 11 (2013) 3421–3423.
- [17] J.A. Smith, D.J. Maloney, S.M. Hecht, D.A. Lannigan, Structural basis for the activity of the RSK-specific inhibitor, SL0101, *Bioorg. & Med. Chem.* 15 (2007) 5018–5034.
- [18] O. Burmistrova, J. Perdomo, M.F. Sim  es, P. Rijo, J. Quintana, F. Est  vez, The abietane diterpenoid parvifloron D from *Plectranthus ecklonii* is a potent apoptotic inducer in human leukemia cells, *Phytomedicine* 22 (2015) 1009–1016, <https://doi.org/10.1016/j.phymed.2015.06.013>.
- [19] T. Mosmann, Rapid colorimetric assay for cellular growth and survival: application to proliferation and cytotoxicity assays, *J. Immunol. Methods* 65 (1983) 55–63, [https://doi.org/10.1016/0022-1759\(83\)90303-4](https://doi.org/10.1016/0022-1759(83)90303-4).
- [20] S. Est  vez, M.T. Marrero, J. Quintana, F. Est  vez, Eupatorin-induced cell death in human leukemia cells is dependent on caspases and activates the mitogen-activated protein kinase pathway, *PLoS One* 9 (2014) e112536, <https://doi.org/10.1371/journal.pone.0112536>.
- [21] F. Est  vez-Sarmiento, E. Hern  ndez, I. Brouard, F. Le  n, C. Garc  a, J. Quintana, F. Est  vez, 3'-Hydroxy-3,4'-dimethoxyflavone-induced cell death in human leukemia cells is dependent on caspases and reactive oxygen species and attenuated by the inhibition of JNK/SAPK, *Chem. Biol. Interact.* 288 (2018) 1–11, <https://doi.org/10.1016/j.cbi.2018.04.006>.
- [22] N. De Meyer, A. Haemers, L. Mishra, H.K. Pandey, L.A. Pieters, D.A. Vanden Berghe, A.J. Vlietinck, 4'-Hydroxy-3-methoxyflavones with potent anticoronavirus activity, *J. Med. Chem.* 34 (1991) 736–746, <https://doi.org/10.1021/jm00106a039>.
- [23] F.A. van Acker, J.A. Hageman, G.R. Haenen, W.J. van Der Vijgh, A. Bast, W.M. Menge, Synthesis of novel 3,7-substituted-2-(3',4'-dihydroxyphenyl)flavones with improved antioxidant activity, *J. Med. Chem.* 43 (2000) 3752–3760, <https://doi.org/10.1021/jm000951n>.
- [24] S. Zhuang, J.T. Demirs, I.E. Kochevar, p38 mitogen-activated protein kinase mediates bid cleavage, mitochondrial dysfunction, and caspase-3 activation during apoptosis induced by singlet oxygen but not by hydrogen peroxide, *J. Biol. Chem.* 275 (2000) 25939–25948, <https://doi.org/10.1074/jbc.M001185200>.
- [25] M. Mori, L. Tottone, D. Quaglio, N. Zhdanovskaya, C. Ingallina, M. Fusto, F. Ghirga, G. Peruzzi, M.E. Crestoni, F. Simeoni, F. Giulimondi, C. Talora, B. Botta, I. Screpanti, R. Palermo, Identification of a novel chalcone derivative that inhibits Notch signaling in T-cell acute lymphoblastic leukemia, *Sci. Rep.* 7 (2017) 2213, <https://doi.org/10.1038/s41598-017-02316-9>.
- [26] T. Stanojkovi  , V. Markovi  , I.Z. Mat  , M.P. Mladenovi  , N. Petrovi  , A. Krivoku  a, M. Petkovi  , M.D. Joksovi  , Highly selective anthraquinone-chalcone hybrids as potential antileukemia agents, *Bioorg. Med. Chem. Lett.* 28 (2018) 2593–2598, <https://doi.org/10.1016/j.bmcl.2018.06.048>.
- [27] S.H. Park, J. Lee, J.C. Shon, N.M. Phuc, J.G. Jee, K.H. Liu, The inhibitory potential of Broussonchalcone A for the human cytochrome P450 2J2 isoform and its anti-cancer effects via FOXO3 activation, *Phytomedicine* 42 (2018) 199–206, <https://doi.org/10.1016/j.phymed.2018.03.032>.
- [28] G. Padmnavathi, N.K. Roy, D. Bordoloi, F. Arfuso, S. Mishra, G. Sethi, A. Bishayee, A.B. Kunnammakkara, Butein in health and disease: a comprehensive review, *Phytomedicine* 25 (2017) 118–127, <https://doi.org/10.1016/j.phymed.2016.12.002>.
- [29] C.T. Jordan, The leukemic stem cell, *Best Pract. Res. Clin. Haematol.* 20 (2007) 13–18, <https://doi.org/10.1016/j.beha.2006.10.005>.
- [30] F.H. Sarkar, Y. Li, NF-kappaB: a potential target for cancer chemoprevention and therapy, *Front. Biosci.* 13 (2008) 2950–2959.
- [31] Y.Q. Zhang, Z.H. Wen, K. Wan, D. Yuan, X. Zeng, G. Liang, J. Zhu, B. Xu, H. Luo, A novel synthesized 3', 5'-diprenylated chalcone mediates the proliferation of human leukemia cells by regulating apoptosis and autophagy pathways, *Biomed. Pharmacother.* 106 (2018) 794–804, <https://doi.org/10.1016/j.bipha.2018.06.153>.
- [32] C. Correia, S.H. Lee, X.W. Meng, N.D. Vincelette, K.L. Knorr, H. Ding H, G.S. Nowakowski, H. Dai, S.H. Kaufmann, Emerging understanding of Bcl-2 biology: implications for neoplastic progression and treatment, *Biochim. Biophys. Acta* 1853 (2015) 1658–1671, <https://doi.org/10.1016/j.bbamer.2015.03.012>.
- [33] H.O. Byun, H.Y. Kim, J.J. Lim, Y.-H. Seo, G. Yoon, Mitochondrial dysfunction by complex II inhibition delays overall cell cycle progression via reactive oxygen species production, *J. Cell. Biochem.* 104 (2008) 1747–1759, <https://doi.org/10.1002/jcb.21741>.
- [34] Y. Teng, L. Wang, H. Liu, Y. Yuan, Q. Zhang, M. Wu, L. Wang, H. Wang, Z. Liu, P. Yu, 3'-Geranyl-mono-substituted chalcone Xanthoangelol induces apoptosis in human leukemia K562 cells via activation of mitochondrial pathway, *Chem. Biol. Interact.* 261 (2017) 103–107, <https://doi.org/10.1016/j.cbi.2016.11.025>.
- [35] M.E. Guicciardi, M. Leist, G.J. Gores, Lysosomes in cell death, *Oncogene* 23 (2004) 2881–2890, <https://doi.org/10.1038/sj.onc.1207512>.
- [36] M. Raman, W. Chen, M.H. Cobb, Differential regulation and properties of MAPKs, *Oncogene* 26 (2007) 3100–3112, <https://doi.org/10.1038/sj.onc.1210392>.
- [37] Y. Feng, J. Wen, C.C. Chang, p38 Mitogen-activated protein kinase and hematologic malignancies, *Arch. Pathol. Lab Med.* 133 (2009) 1850–1856, <https://doi.org/10.1043/1543-2165-133.11.1850>.
- [38] Y. Alsayed, S. Uddin, N. Mahmud, F. Lekmine, D.V. Kalkavolanu, S. Minucci, G. Bokoch, L.C. Platanias, Activation of Rac1 and the p38 mitogen-activated protein kinase pathway in response to all-trans-retinoic acid, *J. Biol. Chem.* 276 (2001) 4012–4019, <https://doi.org/10.1074/jbc.M007431200>.
- [39] Y. S  nchez, D. Amr  n, C. Fern  ndez, E. de Blas, P. Aller, Genistein selectively potentiates arsenic trioxide-induced apoptosis in human leukemia cells via reactive oxygen species generation and activation of reactive oxygen species-inducible protein kinases (p38-MAPK, AMPK), *Int. J. Canc.* 123 (2008) 1205–1214, <https://doi.org/10.1002/ijc.23639>.
- [40] A. Gal  n, M.L. Garc  a-Bermejo, A. Troyano, N.E. Vilaboa, E. de Blas, M.G. Kazanietz, P. Aller, Stimulation of p38 mitogen-activated protein kinase is an early regulatory event for the cadmium-induced apoptosis in human promonocytic cells, *J. Biol. Chem.* 275 (2000) 11418–11424, <https://doi.org/10.1074/jbc.275.15.11418>.
- [41] J. Fang, H. Nakamura, A.K. Iyer, Tumor-targeted induction of oxystress for cancer therapy, *J. Drug Target.* 15 (2007) 475–486, <https://doi.org/10.1080/10611860701498286>.
- [42] G. Groeger, C. Quiney, T.G. Cotter, Hydrogen peroxide as a cell-survival signalling molecule, *Antioxidants Redox Signal.* 11 (2009) 2655–2671, <https://doi.org/10.1089/ARS.2009.2728>.
- [43] S. Yodkeeree, B. Sung, P. Limtrakul, B.B. Aggarwal, Zerubone enhances TRAIL-induced apoptosis through the induction of death receptors in human colon cancer cells: evidence for an essential role of reactive oxygen species, *Cancer Res.* 69 (2009) 6581–6589, <https://doi.org/10.1158/0008-5472.CAN-09-1161>.

2. The synthetic flavanone 6-methoxy-2-(naphthalen-1-yl)chroman-4-one induces apoptosis and activation of the MAPK pathway in human U-937 leukaemia cells



The synthetic flavanone 6-methoxy-2-(naphthalen-1-yl)chroman-4-one induces apoptosis and activation of the MAPK pathway in human U-937 leukaemia cells

Ester Saavedra^a, Henoc Del Rosario^a, Ignacio Brouard^b, Judith Hernández-Garcés^c,
Celina García^c, José Quintana^a, Francisco Estévez^{a,*}

^a Departamento de Bioquímica y Biología Molecular, Unidad Asociada al Consejo Superior de Investigaciones Científicas (CSIC), Instituto Universitario de Investigaciones Biomédicas y Sanitarias (IUIBS), Universidad de las Palmas de Gran Canaria, Spain

^b Instituto de Productos Naturales y Agrobiología, CSIC, La Laguna, Tenerife, Spain

^c Instituto Universitario de Bio-organica AG, Departamento de Química Orgánica, Universidad de La Laguna, Tenerife, Spain

ARTICLE INFO

Keywords:

Apoptosis
Structure-activity relationship
Caspase
Cell cycle
Cytotoxicity
Flavanone

ABSTRACT

Synthetic flavonoids containing a naphthalene ring have attracted attention as potential cytotoxic compounds. Here, we synthesized ten chalcones and their corresponding flavanones and evaluated their antiproliferative activity against the human tumour cell line U-937. This series of chalcone derivatives was characterized by the presence of a naphthalene ring which was kept unaltered- and attached to the β carbon of the 1-phenyl-2-propen-1-one framework. The structure-activity relationship of these chalcone derivatives and their corresponding cyclic compounds was investigated by the introduction of different substituents (methyl, methoxy, benzyloxy, chlorine) or by varying the position of the methoxy or benzyloxy groups on the A ring. The results revealed that both the chalcone containing the methoxy group at 5' position of the A ring as well as its corresponding flavanone [6-methoxy-2-(naphthalen-1-yl)chroman-4-one] were the most cytotoxic compounds, with IC_{50} values of 2.8 ± 0.2 and $1.3 \pm 0.2 \mu M$, respectively, against U-937 cells. This synthetic flavanone was as cytotoxic as the antitumor etoposide in U-937 cells and displayed strong cytotoxicity against additional human leukaemia cell lines, including HL-60, MOLT-3 and NALM-6. Human peripheral blood mononuclear cells were more resistant than leukaemia cells to the cytotoxic effects of the flavanone. Treatment of U-937 cells with this compound induced G₂-M cell cycle arrest, an increase in sub-G₁ ratio and annexin-V positive cells, mitochondrial cytochrome *c* release, caspase activation and poly(ADP-ribose)polymerase processing. Apoptosis induction triggered by this flavonoid was blocked by overexpression of the anti-apoptotic protein Bcl-2. This flavanone induces phosphorylation of p38 mitogen-activated protein kinases, extracellular-signal regulated kinases and *c-jun* N-terminal kinases/stress-activated protein kinases (JNK/SAPK) following different kinetics. Moreover, cell death was attenuated by the inhibition of mitogen-activated extracellular kinases and JNK/SAPK and was independent of reactive oxygen species generation.

1. Introduction

Cancer is the second most common cause of death among children aged 1 to 14 years in the United States and leukaemia accounts for 29% for all childhood cancers. Cancer survival has improved especially for hematopoietic and lymphoid malignancies due to improvements in

treatment protocols, including the discovery of targeted therapies. The 5-year relative survival rate for all cancers combined improved from 58% during the mid-1970s to 83% during 2007 through 2013 for children. The lowest survival rate corresponds to acute myeloid leukaemia with a value of 65.1% between 2007 and 2013 [1]. In accordance with the GLOBOCAN estimates of incidence and mortality

Abbreviations: ERK, extracellular signal-regulated kinase; FL, 6-methoxy-2-(naphthalen-1-yl)chroman-4-one; IC_{50} , 50% inhibition of cell growth; JNK/SAPK, *c-jun* N-terminal kinases/stress-activated protein kinases; MAPK, mitogen-activated protein kinases; MEK, mitogen-activated extracellular kinases; MTT, 3-(4,5-dimethyl-2-thiazolyl)-2,5-diphenyl-2H-tetrazolium bromide; p38^{MAPK}, p38 mitogen-activated protein kinases; ROS, reactive oxygen species

* Corresponding author at: Departamento de Bioquímica y Biología Molecular, Universidad de Las Palmas de Gran Canaria, Paseo Blas Cabrera Felipe s/n, Las Palmas de Gran Canaria 35016, Spain.

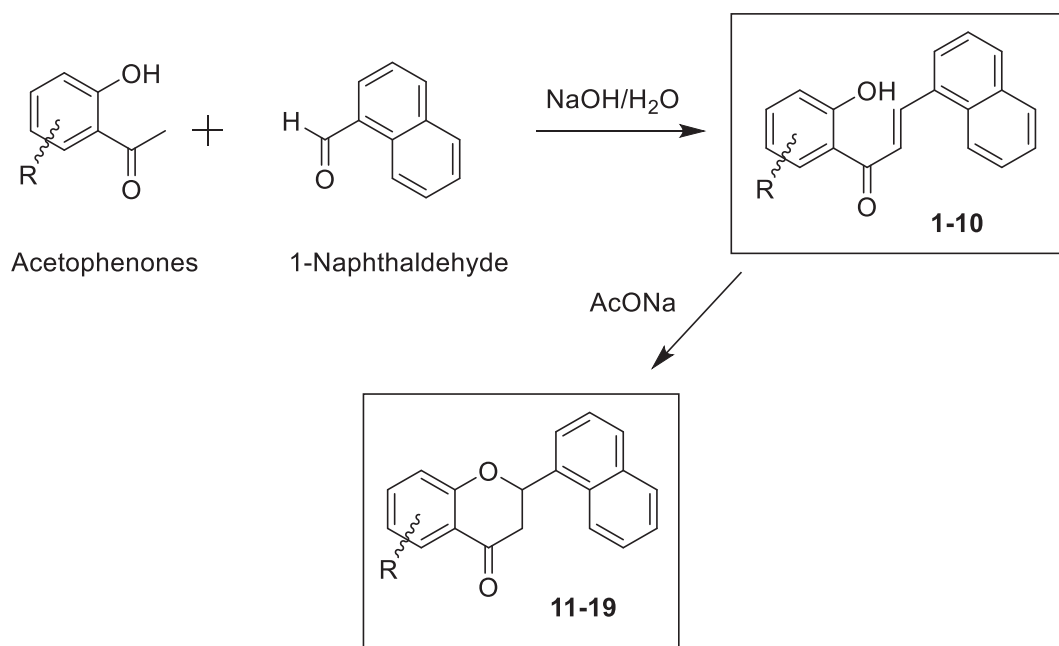
E-mail address: francisco.estevez@ulpgc.es (F. Estévez).

<https://doi.org/10.1016/j.bioorg.2019.103450>

Received 14 June 2019; Received in revised form 19 September 2019; Accepted 14 November 2019

Available online 21 November 2019

0045-2068/ © 2019 Elsevier Inc. All rights reserved.



Scheme 1. Synthesis of chalcones and flavanones.

worldwide for 2018, the estimated numbers of new cases and deaths from leukaemia were 437,033 and 309,006, respectively, indicating that mortality rates for this disease are still very high [2], and providing an urgent need for improved treatments.

Natural products represent realistic options as potential cytotoxic compounds against cancer cells [3]. Flavonoids are secondary polyphenolic metabolites present in almost all plants and the human diet. These compounds exhibit a wide spectrum of pharmacological properties that have been recently reviewed [4,5]. Flavonoids are able to interfere in all phases of cancer progression by modulating key proteins involved in proliferation, differentiation, apoptosis, angiogenesis, metastasis and reverse multidrug resistance process. Apoptosis is a form of regulated cell death which results in destruction of target cell with minimal inflammatory response. Essential executioners of apoptosis are the caspases, a family of cysteine proteases which are expressed in cells as inactive zymogens known as procaspases. These enzymes predominantly cleave their substrates on the C-terminal side of aspartate. Proteolytic cleavage leads to important changes in cell morphology such as membrane blebbing, DNA fragmentation, phosphatidylserine exposure at the cell surface, and formation of apoptotic vesicles. Two main apoptotic pathways have been described, the mitochondrial and the extrinsic pathways [6]. The mitochondrial or intrinsic pathway is initiated by perturbations of the intracellular or extracellular microenvironment, demarcated by mitochondrial outer membrane permeabilization and precipitated mainly by caspase-3. The extrinsic pathway is initiated by perturbations of the extracellular microenvironment that are detected by plasma membrane receptors (propagated by caspase-8 and precipitated by executioner caspases, mainly caspase-3).

It is well established that mutual molecular recognition of host and guest depends on non-covalent interactions (H-bonding, stacking interactions, cation- π interactions, ionic interactions and hydrophobic interactions) which are the basis of the functional properties of most molecules. Inter and intramolecular interactions involving aromatic ring systems are key processes in chemical and biological recognition and knowledge of these helps explain and predict the functionality of different structures.

Interactions between aromatic platforms and sugar and amino acid residues play a crucial role in determining the specificity of drug-receptor interaction processes. The planarity of the aromatic systems together with their polarizability and their multipolar moment are

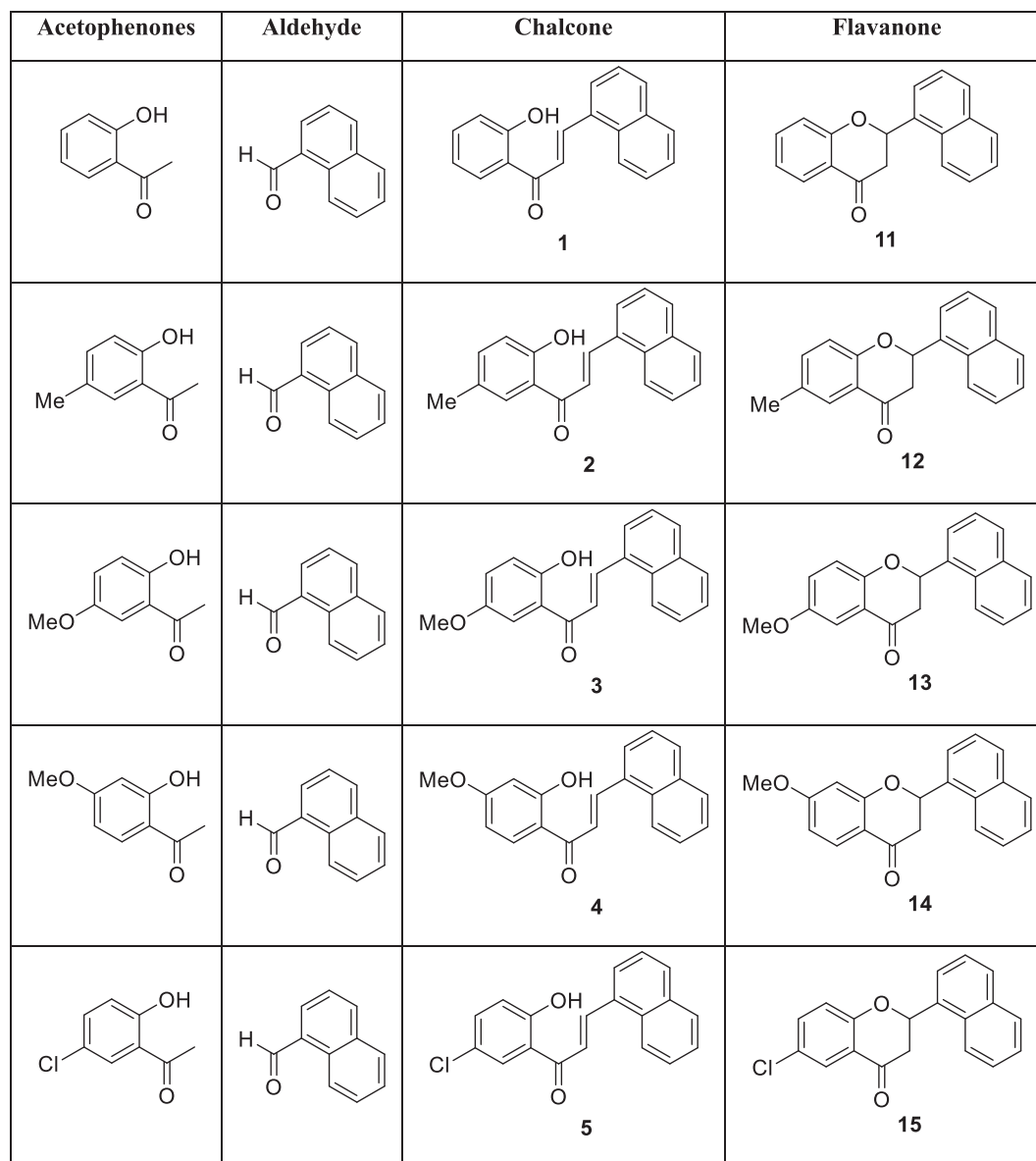
properties that illustrate the capacity of these systems to form functional complexes [7–9]. In particular, recent studies using small molecules carrying naphthalene groups describe the interaction of such a ring system with a hydrophobic pocket located in the Ras oncogene as causing the inhibition of that oncogene. Naphthalene also has the ability to generate strong π - π stacking interactions, providing high affinity ligands for more than one type of receptor, and making it a privileged scaffold. These findings suggest that the naphthalene ring could become a propitious building block for the development of new therapeutic agents [10].

Naphthalene-based chalcones, in which one of the aryl rings is replaced by naphthalene, have been explored as potential anticancer agents. The aim of this study was to synthesize a series of chalcone derivatives and their corresponding cyclic compounds containing a naphthalene ring to explore the effect of different substituents (methyl, methoxy, benzyloxy, chlorine) or changes in the position of the methoxy or benzyloxy groups on the phenyl ring on cytotoxicity against the human tumour U-937 cells. This cell line was selected as it is the most frequently used cell line in biomedical research for the study of neoplasia and therapeutics and has made important contributions to the disciplines of cancer, hematology, and immunology [11,12]. In addition, we investigated the signal transduction pathways of cell death triggered by one of the most cytotoxic compounds, the flavanone 6-methoxy-2-(naphthalen-1-yl)chroman-4-one (FL).

2. Results

2.1. Chemistry

In the present study, we explored the cytotoxic effects of a collection of 19 chalcones and flavanones containing a naphthalene core against human U-937 leukaemia cells. The chalcones (1–10) were prepared by a standard aldolic condensation procedure involving pH > 12 conditions. The aldolic condensation is one of the most versatile of organic chemical reactions because of its ability to use small molecules in the synthesis of larger ones under Claisen-Schmidt conditions. If this reaction is performed at lower pH (9–10) a reversible interconversion between the chalcone and its constitutional isomer flavanone is observed depending on the range of pH and on the substitution on the A ring [13]. The flavanones (11–19) were subsequently synthesized by



Scheme 2. Acetophenone derivatives and 1-naphthaldehyde used in the synthesis of the chalcones (1–10) and flavanones (11–19).

cyclization reactions of the above-mentioned chalcones in the presence of an excess of sodium acetate under reflux (Scheme 1). In the particular case of chalcone 10, it was not possible to isolate the desired flavanone. Chalcones (1–10) and their corresponding flavanones were designed to contain one or two substituents in the A ring (Scheme 2).

2.2. Biology

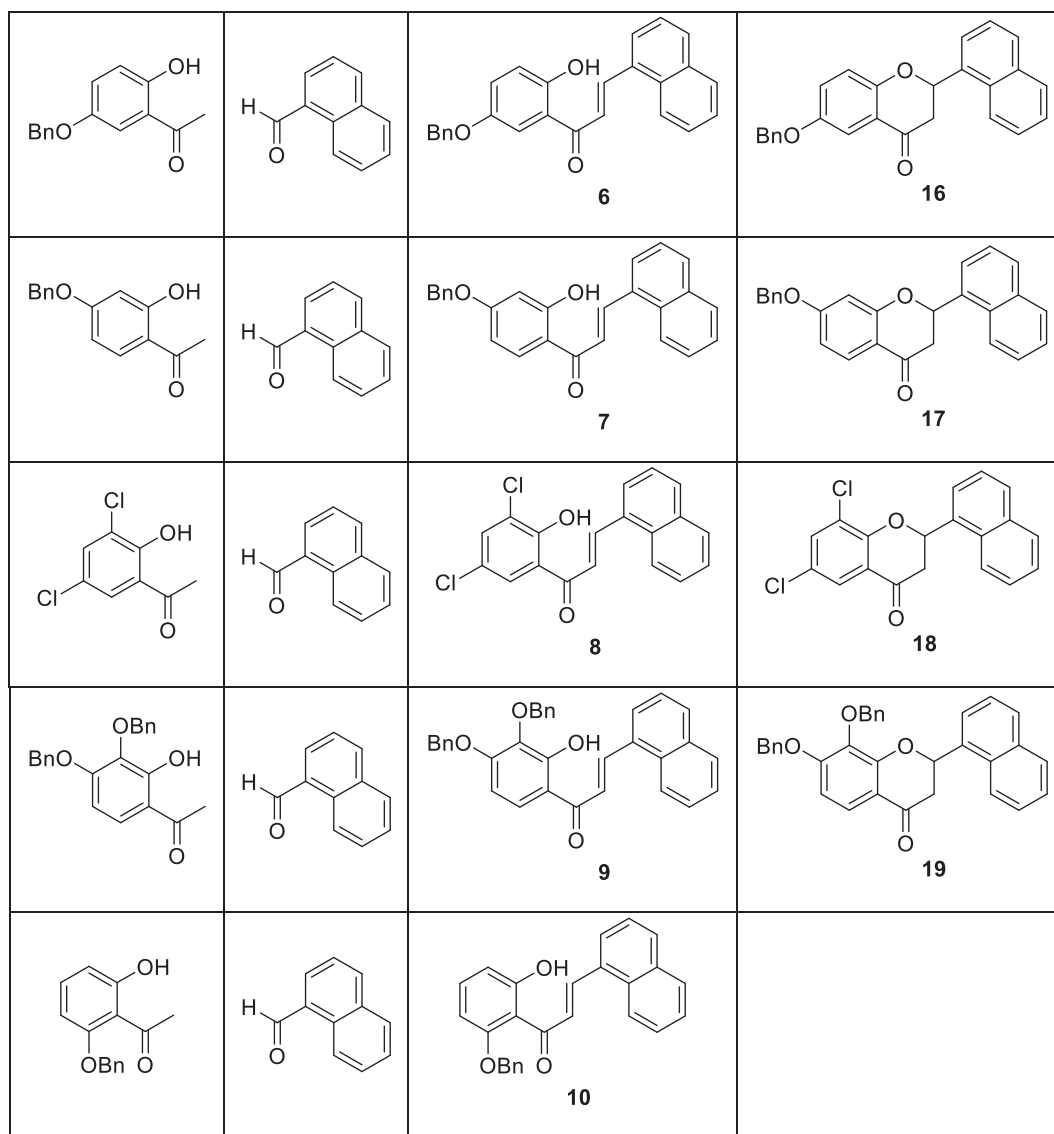
2.2.1. Screening of synthetic flavonoids. The synthetic 6-methoxy-2-(naphthalen-1-yl)chroman-4-one (FL) inhibits the viability of human leukaemia cells

The SARs (structure-activity relationship) of naphthalene-based chalcones and their corresponding flavanones were investigated by varying the substituent on the A ring or the location of the methoxy and/or benzyloxy groups at the 4' or 5' position on the A ring. In this series of naphthalene-chalcones we maintained the naphthyl ring attached to the β carbon of the 2-propen-1-one system and added various substituents (hydrogen, methyl, chlorine, methoxy or benzyloxy) at the 5' position on the phenyl ring. In addition, we included another chlorine atom or another benzyloxy group and changed the position of

the methoxy or the benzyloxy group at the 6' position. To this end, U-937 cells were treated with increasing concentrations of each compound and the IC_{50} values (the concentration that induces a 50% inhibition of cell growth) were determined by the MTT assay.

The results indicated that the introduction of a methoxy group at position 5' on the A ring (chalcone 3) or at position 6 in the A ring of the corresponding flavanone (flavanone 13) led to a significant improvement in cytotoxic activity, both in chalcones [$IC_{50} = 9.7 \pm 2.0 \mu M$ for chalcone 1 vs $IC_{50} = 2.8 \pm 0.2 \mu M$ for chalcone 3]; 3.5-fold increase in cytotoxicity] and flavanones [$IC_{50} = 10.4 \pm 3.1 \mu M$ for flavanone 11 vs. $IC_{50} = 1.3 \pm 0.2 \mu M$ for flavanone 13]; 8-fold increase in cytotoxicity]. In contrast, the introduction of the methyl group or an atom of chlorine in this position appears to be irrelevant in determining cytotoxicity against U-937 cells. The presence of an additional chlorine atom at position 3' did not change the cytotoxicity of the chalcone (8, $IC_{50} = 13.4 \pm 7.2 \mu M$) or the flavanone (18, $IC_{50} = 8.2 \pm 3.0 \mu M$) skeleton. Moreover, the introduction of a methoxy group at position 4' of the chalcone skeleton (chalcone 4) did not enhance the potency against cell growth inhibition compared with chalcone 1.

The introduction of one or two benzyloxy groups at the 4' and 5'



Scheme 2. (continued)

positions on the A ring of chalcones or at positions C6 or C7 and C8 of flavanones significantly decreased cytotoxic activity (chalcones: $IC_{50} > 30 \mu M$ for **7** and **9** and $IC_{50} = 20.3 \pm 9.0 \mu M$ for **6**, flavanones: $IC_{50} > 30 \mu M$ for **17**, **16** and **19**). The bulky groups on the A ring appear to interfere with the cytotoxic activity and might be explained for their low solubility due to the presence of the aromatic rings and exacerbated by the naphthyl group.

Since there are no large differences in cytotoxic activity between chalcones and flavanones, these results suggest that the major determinant of cytotoxicity is the presence and the position of a methoxy group on the A ring, and that the most cytotoxic compounds were the

chalcone **3** and the flavanone **13** with IC_{50} values of 2.8 ± 0.2 and $1.3 \pm 0.2 \mu M$, respectively for U-937 cells (Table 1).

Since flavanone **13** [6-methoxy-2-(naphthalen-1-yl)chroman-4-one, FL] was found to be one of the most cytotoxic compounds, it was selected for further experiments. Comparison with additional human leukaemia cells revealed that FL displays strong cytotoxic properties against three human leukaemia cell lines, including the human acute myeloid leukaemia HL-60, the human B cell precursor leukaemia NALM-6 and the acute lymphoblastic leukaemia MOLT-3, with IC_{50} values between 1 and $3 \mu M$ (Table 2). For comparison, the standard antitumor agent etoposide was included as a positive control for U-937

Table 1
Effects of flavonoids on the growth of human tumour cell line U-937.

Chalcone	1	2	3	4	5	6	7	8	9	10
IC_{50} (μM)	9.7 ± 2.0	8.3 ± 2.2	2.8 ± 0.2	8.5 ± 0.9	7.5 ± 1.6	20.3 ± 9.0	> 30	13.4 ± 7.2	> 30	12.6 ± 3.9
Flavanone	11	12	13	14	15	16	17	18	19	
IC_{50} (μM)	10.4 ± 3.1	22.6 ± 3.0	1.3 ± 0.2	15.3 ± 5.0	5.7 ± 2.1	> 30	> 30	8.2 ± 3.0	> 30	

Cells were cultured for 72 h in presence of the indicated compounds and the IC_{50} values were calculated as described in the Experimental Section. The data shown represent the mean \pm SEM of 3 independent experiments with three determinations in each.

Table 2
Effects of FL on cell viability of human leukaemia cell lines.

IC ₅₀ (μM)		
HL-60	NALM-6	MOLT-3
2.0 ± 1.5	3.1 ± 1.0	1.1 ± 0.2

Cells were cultured for 72 h and IC₅₀ values were calculated as described in the Experimental Section. Representative values are means ± SE from 3 to 5 independent experiments with determinations performed in triplicate.

(IC₅₀ = 1.2 ± 0.2 μM), HL-60 (IC₅₀ = 0.4 ± 0.1 μM) and MOLT-3 (IC₅₀ = 0.2 ± 0.1 μM).

Treatment of the human histiocytic lymphoma U-937 cells with this flavanone resulted in a concentration-dependent inhibition of cell viability (Fig. 1A), induced significant morphological changes and caused an important reduction in the number of cells (Fig. 1B). Studies using the trypan blue exclusion method showed that FL displays cytotoxicity but it is not cytostatic against U-937 cells. Fig. 1C–E show the number of total cells, live cells and the percentage of live cells after treatment

with 10 μM FL during increasing periods of time. In addition, quiescent and proliferating peripheral blood mononuclear cells isolated from healthy volunteers were more resistant to the cytotoxic effects of FL than human leukaemia U-937 cells (Fig. 1F). These results indicate that FL exhibits strong cytotoxic properties against leukaemia cells but has only weak cytotoxic effects against peripheral blood mononuclear cells (PBMCs).

2.2.2. FL induces G₂-M arrest and apoptosis in human myeloid leukaemia cells

To determine whether the effects of FL on cell viability were due to alterations in cell cycle progression, cells were incubated with increasing concentrations for different time periods (6–24 h), stained with propidium iodide and analyzed by flow cytometry. As shown (Table 3, Fig. 2A) an exposure at a concentration as low as 3 μM FL caused a significant G₂-M arrest at the expense of G₁ phase cell population which was evident after 6 h of treatment. The percentage of cells in G₂-M phase increased from ~21% in control cells to ~36% after treatment with FL for 12 h. Moreover, the percentage of hypodiploid cells (i.e.

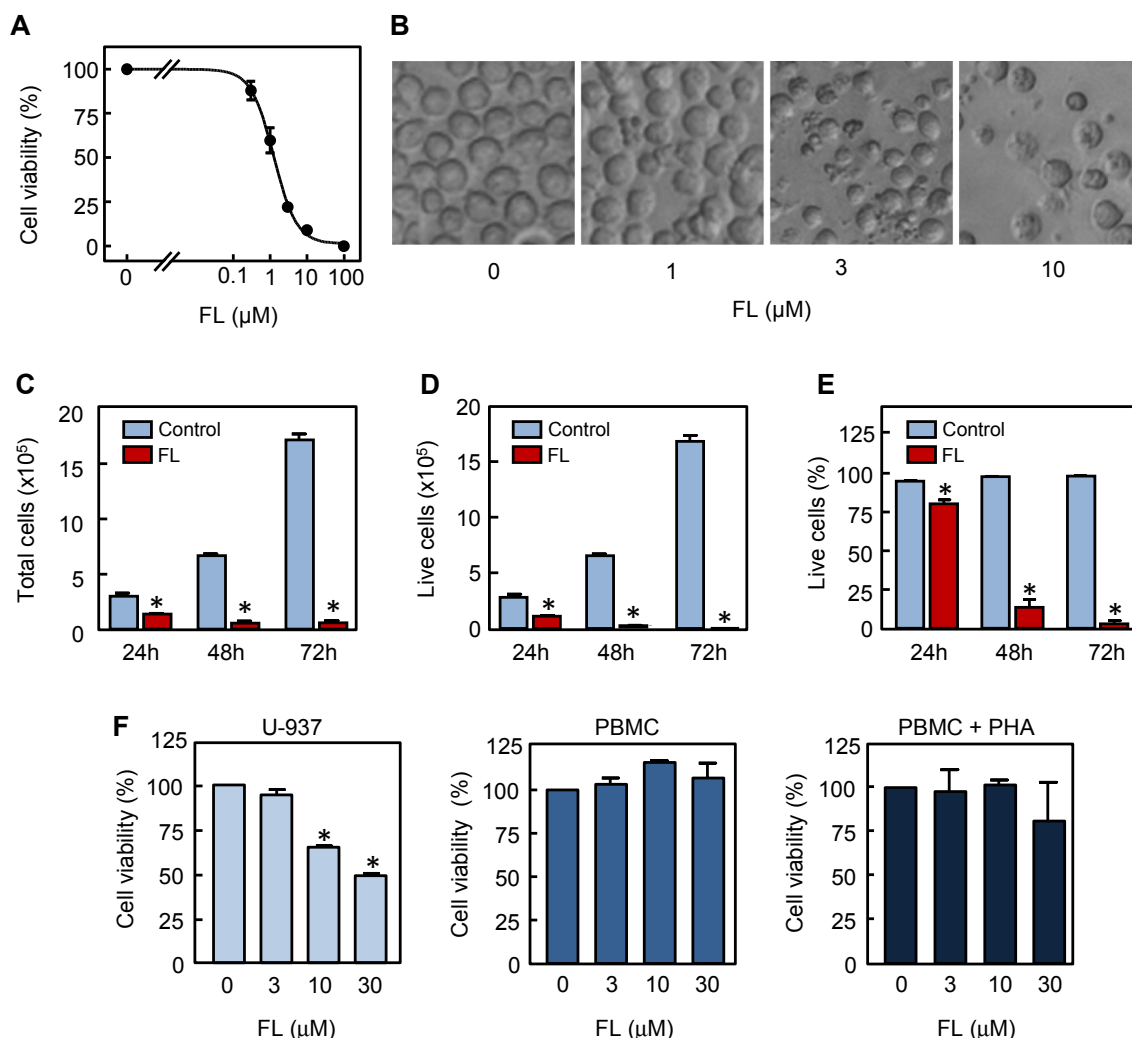


Fig. 1. FL is cytotoxic against human leukaemia U-937 cells but not against peripheral blood mononuclear cells. (A) Dose-response study of FL on U-937 cells viability. Cells were incubated with increasing concentrations of FL for 72 h, and thereafter cell viability was determined by the MTT assay. (B) Photomicrographs of morphological changes visualized with inverted phase contrast microscopy after treatment with the indicated concentrations of FL for 24 h. (C–E) Time-course of FL-mediated cell death. Cells were incubated with FL (10 μM) for the indicated times and the number of total cells (C), live cells (D) and the percentage of live cells were determined by the trypan blue exclusion method using a TC10 counter (Bio-Rad, Hercules, CA). (F) Differential effects of FL on cell viability of U-937 and quiescent and phytohemagglutinine (PHA)-activated healthy human peripheral blood mononuclear cells (PBMC). Cells were incubated in the presence of the specified concentrations of FL for 24 h and thereafter cell viability was determined by the MTT assay. Values represent means ± SE of two independent experiments each performed in triplicate. **P* < 0.05, significantly different from the untreated control.

Table 3
Effect of FL on cell cycle phase distribution of U-937 leukaemia cells.

	(μM)	% Sub-G ₁	%G ₁	%S	%G ₂ -M
6 h	0	1.4 \pm 0.2	52.5 \pm 2.2	24.4 \pm 1.0	21.7 \pm 3.3
	1	2.9 \pm 0.2	45.6 \pm 1.0	26.7 \pm 0.4	24.7 \pm 1.1
	3	4.2 \pm 0.4	29.0 \pm 1.1*	33.4 \pm 0.4*	33.3 \pm 1.4*
	10	3.3 \pm 0.3	19.8 \pm 0.7*	34.5 \pm 1.2*	42.3 \pm 2.0*
12 h	0	0.9 \pm 0.1	51.5 \pm 0.8	26.5 \pm 0.6	21.0 \pm 0.9
	1	1.5 \pm 0.2	50.6 \pm 0.4	24.7 \pm 0.1	23.1 \pm 0.4
	3	8.0 \pm 1.8*	29.0 \pm 1.5*	27.4 \pm 3.4	35.6 \pm 3.7*
	10	7.4 \pm 0.5*	7.3 \pm 0.5*	31.7 \pm 1.2*	53.6 \pm 2.1*
24 h	0	1.4 \pm 0.1	55.6 \pm 0.2	27.6 \pm 0.9	15.8 \pm 0.9
	1	2.6 \pm 0.3	51.0 \pm 0.6	29.4 \pm 0.1	17.0 \pm 0.4*
	3	25.9 \pm 3.4*	17.0 \pm 0.6*	45.8 \pm 2.6*	11.1 \pm 1.9*
	10	39.2 \pm 9.2*	17.3 \pm 0.6*	24.5 \pm 1.4	18.6 \pm 4.9

Cells were cultured with the four concentrations of FL (0, 1, 3, 10 μM) over three time periods (6, 12, 24 h) and the percentages of cells in the four phases of the cell cycle (%Sub-G₁, %G₁, %S, %G₂-M) were determined by flow cytometry. The values are means \pm S.E. of two independent experiments with three determinations in each. Asterisks indicate a significant difference ($P < 0.05$) compared with the corresponding controls.

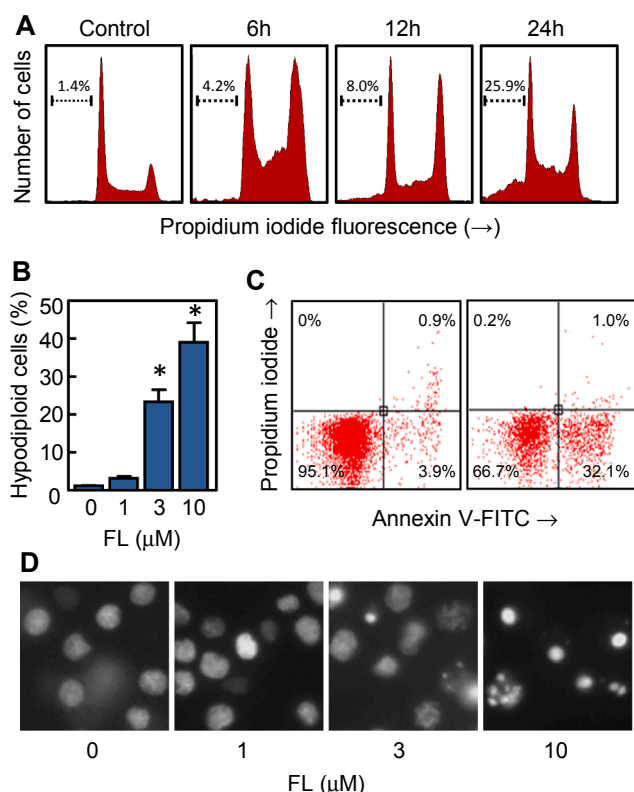


Fig. 2. Effect of FL on apoptosis on human myeloid leukaemia U-937 cells. (A) Cells were incubated in the presence/absence of 3 μM FL for the indicated times and subjected to flow cytometric analysis using propidium iodide labeling. The percentages of hypodiploid cells (apoptotic cells) are shown. (B) U-937 cells were incubated in the presence of the indicated concentrations of FL for 24 h and percentages of hypodiploid cells were quantified by flow cytometry. (C) Cells were treated with 10 μM FL for 24 h and subjected to flow cytometry analysis after annexin V-FITC and propidium iodide staining. (D) Photomicrographs of representative fields of U-937 cells stained with Hoechst 33,258 to evaluate nuclear chromatin condensation after treatment with the specified concentrations of FL for 24 h.

sub-G₁ fraction) increased about 18-fold in FL-treated U-937 compared with control cells after 24 h (Fig. 2A).

Maximal levels of apoptotic cells (approximately 30-fold increase

with respect to control) were observed at 24 h with 10 μM FL in U-937 (Table 3, Fig. 2B). FL treatment also led to the exposure of phosphatidylserine on the outside of the plasma membrane as detected by Annexin V-FITC staining in U-937 cells (Fig. 2C). In addition, fluorescence microscopy experiments clearly demonstrate increases in condensed and fragmented chromatin, which is typical of apoptotic cells in U-937 (Fig. 2D). Taken together, these results indicate that FL induces cell cycle arrest in the G₂-M phase and apoptosis on human myeloid leukaemia U-937 cells.

2.2.3. Effects of FL on caspases- and PARP cleavage

To determine whether caspases were associated with the cell death triggered by FL, we examined the proteolytic processing of these proteases and PARP [poly(ADP-ribose) polymerase] cleavage. To this end, U-937 cells were treated with increasing concentrations of FL for 24 h, and caspases were determined by western blot (Fig. 3A). The results indicate that FL stimulates the cleavage of the main effector pro-caspase (pro-caspase-3) into 18–20 kDa fragments as well as the other executioner pro-caspases (pro-caspases-6 and -7). These effector caspases perform downstream execution of apoptosis. Interestingly, FL stimulated pro-caspase-4 processing as determined by a significant decrease in the zymogen levels. Processing of the main initiator caspases (pro-caspases-8 and -9) - involved in the extrinsic and the intrinsic apoptotic pathways - was detected by the visualization of the active 35–37 kDa fragment (pro-caspase-9) and a decrease of pro-caspase-8 levels. This flavanone also induced poly(ADP-ribose) polymerase (PARP) cleavage in accordance with caspase activation, generating the 85 kDa fragment. Protein loading was checked by reprobing the membranes with β -actin antibody.

To confirm that caspases processing correlates with activity, enzymatic activities of caspase-3-like protease (caspase-3/7), caspase-8 and caspase-9 were also investigated in extracts of U-937 cells treated with increasing concentrations of FL during 24 h. To this end, cell lysates were assayed for cleavage of the tetrapeptide substrates DEVD-pNA, IETD-pNA and LEHD-pNA as specific substrates for caspase-3/7, -8 and -9, respectively. As shown (Fig. 3B), dose-response experiments showed that a low concentration (1 μM) of FL was sufficient to induce caspases activation. A 2-fold increase in caspases-8 and -9 activities was observed in cells treated with 3 μM FL.

Confirmation that FL-triggered apoptosis requires the activation of caspases was carried out with cells pre-treated with the broad-spectrum caspase inhibitor z-VAD-fmk (100 μM). The results (Fig. 3C) showed that apoptosis was significantly suppressed in the presence of the inhibitor, which suggests that FL induces cytotoxicity by a caspase dependent mechanism. To determine which caspases are important in the mechanism of cell death triggered by this flavanone, we determined the effect of two sets of caspase inhibitors, including -CHO and -fmk derivatives. The -CHO derivatives included DEVD-CHO, LEVD-CHO, IETD-CHO and LEHD-CHO (all at 10 μM , except z-LEHD-CHO which was assayed at 50 μM , results not shown) and the -fmk derivatives included DEVD-fmk, IETD-fmk and LEHD-fmk (all at 50 μM , Fig. 3C). None of these inhibitors was able to decrease the percentage of hypodiploid cells induced by the flavanone. Fig. 3D shows the representative histograms of annexin V-FITC and propidium iodide-stained U-937 cells to confirm the effect of the pan-caspase inhibitor z-VAD-fmk. The lack of effect of the specific caspase inhibitors (z-DEVD-fmk, caspase-3/7 inhibitor; z-LEVD-CHO, caspase-4 inhibitor; z-IETD-fmk, caspase-8 inhibitor and z-LEHD-fmk, caspase-9 inhibitor) was also confirmed by flow cytometry after double staining with annexin V-FITC and propidium iodide (results not shown).

2.2.4. Effects of FL on mitochondrial proteins release and on Bcl-2 family members

Release of cytochrome *c* from mitochondria to cytosol is a central event in apoptotic signalling. To determine whether FL-induced apoptosis involves release of mitochondrial proteins, cytosolic preparations

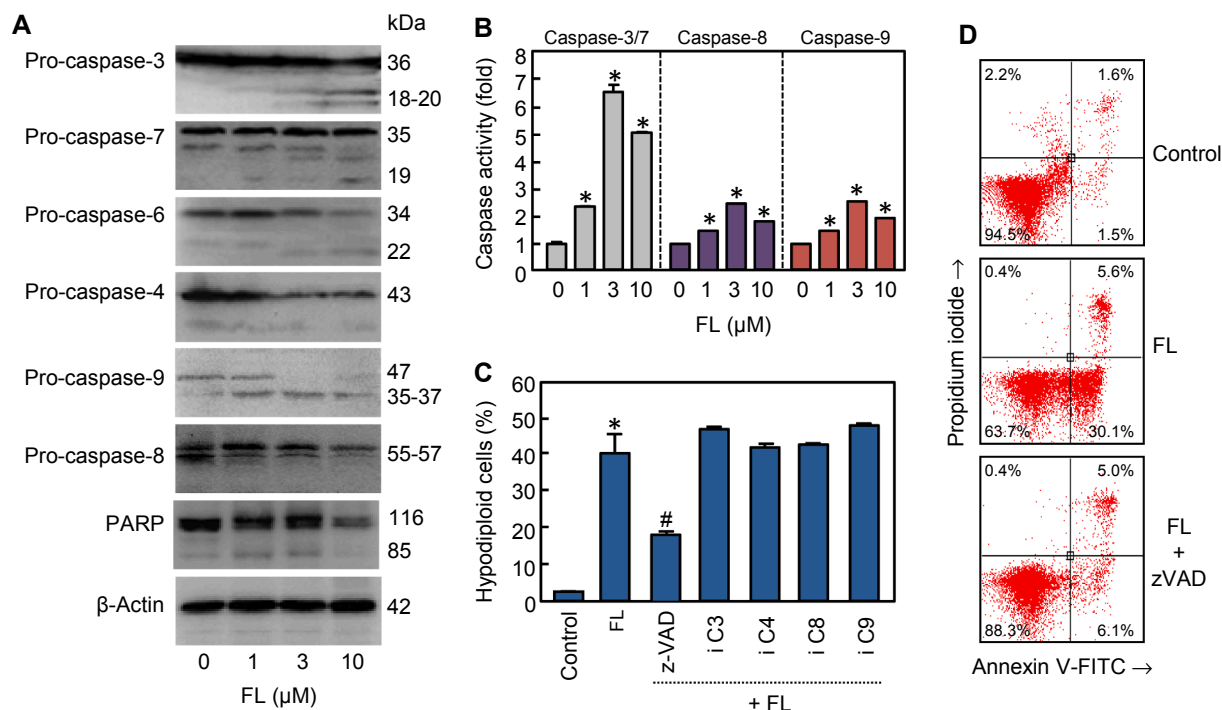


Fig. 3. Involvement of caspases in the mechanism of cell death triggered by FL in U-937 cells. (A) Immunoblotting for the cleavage of caspases and PARP after 24 h of treatment with the specified concentrations of FL. The protein β -actin was used as a loading control. (B) Activation of caspases in response to FL. Cells were incubated as above and cell lysates were assayed for caspase-3/7, caspase-8 and caspase-9 activities using the colorimetric substrates DEVD-pNA, IETD-pNA and LEHD-pNA, respectively. Results are expressed as the fold-increase in caspase activity compared with control. (C) Effect of cell-permeable caspase inhibitors on FL-induced apoptosis. Cells were incubated with 10 μ M FL for 24 h, in presence or absence of the broad-spectrum caspase inhibitor z-VAD-fmk (z-VAD, 100 μ M), the caspase-3/7 inhibitor z-DEVD-fmk (iC3, 50 μ M), the caspase-4 inhibitor z-LEVD-CHO (iC4, 50 μ M), the caspase-8 inhibitor z-IETD-fmk (iC8, 50 μ M) and the caspase-9 inhibitor z-LEHD-fmk (iC9, 50 μ M) and percentages of hypodiploid cells were quantified by flow cytometry. Bars represent the mean \pm SE of two independent experiments each performed in triplicate. * P < 0.05, significantly different from untreated control. # P < 0.05, significantly different from FL treatment alone. (D) Flow cytometry analysis of Annexin V-FITC and propidium iodide-stained cells after 24 h of treatment with 10 μ M FL in absence or in presence of the pan-caspase inhibitor z-VAD-fmk (100 μ M). Representative data from two independent experiments are presented.

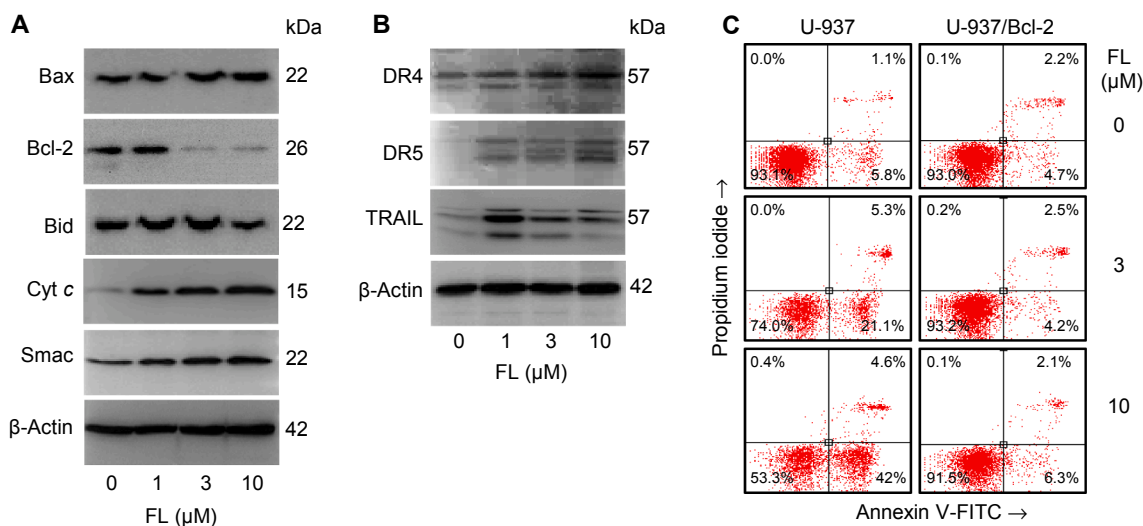


Fig. 4. Effect on Bcl-2 family proteins, release of mitochondrial proteins and expression of death receptors. (A) Cells were incubated with increasing concentrations of FL and the expression of Bcl-2 family members and release of cytochrome c and Smac/DIABLO were analyzed by western blot in U-937 cells. (B) Cells were treated as in (A) and expression of death receptors was detected by immunoblotting. β -Actin was used as a loading control. (C) U-937 and the cell line overexpressing Bcl-2, U-937/Bcl-2, were incubated with the specified concentrations of FL and apoptosis was determined by flow cytometry after double staining with annexin V-FITC and propidium iodide. The experiment was replicated twice.

were analyzed by immunoblotting of U-937 cells. The results showed a significant increase in the amount of cytochrome c in the cytosol in a concentration-dependent manner (Fig. 4A). There was also a concentration-dependent release of the mitochondrial apoptogenic factor

Smac/DIABLO (second mitochondrial activator of caspases/Diablo IAP-binding mitochondrial protein).

We also investigated the expression of the Bcl-2 family proteins in FL-treated cells. The results revealed that flavanone induces

downregulation of Bcl-2 and a clear increase in Bax levels (Fig. 4A). In addition, there was a clear decrease in Bid protein, which is a substrate of caspase-8, indicating processing of this protein.

Since FL induces activation of caspase-8, it is possible that death receptors and/or their ligand might be involved in cell death. Therefore, we explored the effects of FL on the expression of DR4 (death receptor 4), DR5 (death receptor 5) and TRAIL (tumor necrosis factor-related apoptosis-inducing ligand) in U-937 cells. Cells were treated during 24 h and cell lysates were subjected to immunoblot analysis. As shown in Fig. 4B, FL up-regulates the expression of DR4, DR5 and TRAIL.

To clarify whether the anti-apoptotic protein Bcl-2 is involved in the activation of intrinsic pathway by FL treatment, we compared the effect on apoptosis in the U-937 cell line overexpressing human Bcl-2 protein (U-937/Bcl-2) and the parental U-937 cell line. As shown in Fig. 4C, Bcl-2 over-expression blocked apoptosis triggered by FL, suggesting that Bcl-2 is involved in FL-induced apoptosis.

2.2.5. FL activates MAPKs (mitogen-activated protein kinases) and cell death is independent on ROS (reactive oxygen species) generation

Whether FL induces the activation of the MAPK pathway or not was investigated because this signal transduction pathway plays a crucial role in cell fate. Incubation of U-937 cells with FL leads to a fast phosphorylation (0.5 h) of JNK/SAPK (c-jun N-terminal kinases/stress-activated protein kinases) and p38^{MAPK} while the activation of ERK1/2 (extracellular signal-regulated kinase) was not detected until 6 h (Fig. 5A). The activation of p38^{MAPK} decreased after 1 h, while the level of phosphorylated JNK/SAPK occurs in a biphasic manner. These results indicate that FL treatment of U-937 cells leads to activation of JNK/SAPK, p38^{MAPK} and ERK1/2 following different kinetics. To determine whether the phosphorylation of MAPKs plays a key role in FL-induced apoptosis, we examined the effects of p38^{MAPK}, JNK/SAPK, and mitogen-activated extracellular kinases 1/2 (MEK 1/2) inhibitors (Fig. 5B). Pretreatment of U-937 cells with the specific p38^{MAPK} inhibitor SB 203,580 (2 μ M) did not affect the rate of FL-mediated apoptosis. These results suggest that activation of p38^{MAPK} is not involved in FL-induced cell death. Treatment of cells with U0126 or PD98059, inhibitors of MEK1/2, and with the JNK/SAPK inhibitor SP600125 significantly decreased FL-induced cell death. The percentage of apoptotic cells (hypodiploid cells) decreased from ~37% in FL-treated cells to 17% and 22% with U0126 and PD98059, respectively. The JNK/SAPK inhibitor attenuated FL-induced cell death from ~37% of apoptotic cells to 22% in the combination group (FL + SP600125).

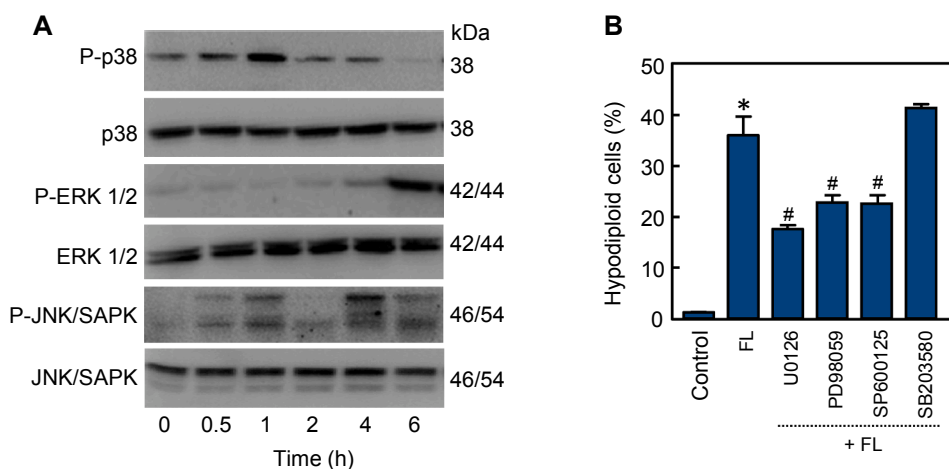


Fig. 5. Role of the MAPK pathway on FL-induced apoptosis in U-937 cells. (A) Representative Western blots show the time-dependent phosphorylation of p38^{MAPK}, ERK1/2 and JNK/SAPK by FL. Cells were incubated with 10 μ M FL for the time periods shown. Protein extracts were prepared and analysed on Western blots probed with specific antibodies to ascertain the phosphorylation of MAPKs. Membranes were stripped and reprobed with total MAPK antibodies as loading controls. (B) Effect of MAPK inhibitors on FL-induced cell death. Cells were preincubated with the MEK1/2 inhibitors U0126 (10 μ M) and PD98059 (10 μ M), the JNK/SAPK inhibitor SP600125 (10 μ M) and the p38^{MAPK} inhibitor SB203580 (2 μ M) for 1 h and then treated with FL. Apoptosis was quantified by flow cytometry as described in Materials and Methods. Bars represent the mean \pm S.E. of three independent experiments each performed in triplicate. * P < 0.05, significantly different from untreated control. # P < 0.05, significantly different from FL treatment alone.

These results suggest that activation of ERK1/2 and JNK/SAPK is involved in FL-induced apoptosis.

Activation of the MAPK pathway can be mediated by the generation of reactive oxygen species (ROS). Hence the ability of FL to increase ROS levels was investigated using the fluorescent dye 2', 7'-dichlorodihydrofluorescein diacetate after 1, 2 and 3 h of incubation, as well as the effect of different antioxidants [20 μ M vitamin E, 2 mM trolox, 10 mM N-acetyl-L-cysteine, 0.5–1 μ M diphenyleneiodonium chloride (a NADPH oxidase inhibitor); 500 units/ml catalase; 400 units/ml superoxide dismutase]. However, ROS were not generated at assayed times and the antioxidants did not reduce the cell death, either (results not shown). These results suggest that cell death is not dependent on ROS generation.

3. Discussion

Despite the potential of flavonoids in human medicine its clinical use is limited due to challenges associated with their effective use, including, among others, their pharmacokinetic and pharmacodynamic properties. Low solubility, poor oral absorption and extensive hepatic metabolism are responsible for the unfavorable pharmacokinetics of flavonoids. The modification of the flavonoid structure to generate new derivatives constitutes an important strategy to optimize their pharmacokinetic and pharmacodynamic properties. Previous studies have shown that methylation and/or the introduction of some lipophilic moieties in specific flavonoids significantly increase the potency and bioavailability and also enhance the stability and effectiveness by preventing chemical and metabolic hydrolysis [14–16].

In the present report, we attempted to find new potent anti-proliferative molecules inspired by natural products. The results revealed that both the chalcone containing the methoxy group at 5' position of the A ring as well as its corresponding flavanone were the most cytotoxic compounds, with IC₅₀ values of 2.8 \pm 0.2 and 1.3 \pm 0.2 μ M, respectively, against U-937 cells. This is the first time to date that the effects on cell viability and the mechanism involved in cell death induction have been investigated for this specific flavanone.

In a previous study, we showed that the synthetic chalcone 6'-benzyloxy-4-bromo-2'-hydroxychalcone is cytotoxic against seven human leukaemia cells and induces caspase-8- and reactive oxygen species-dependent apoptosis [17]. These results prompted us to design additional analogues of chalcone containing additional substituents other than halogen chalcones. When the 4-bromobenzyl group was replaced by a naphthyl group, the chalcone was unexpectedly cyclized

to generate a flavanone (FL). This cyclic compound was found to have strong cytotoxic properties with IC_{50} values of approximately 2 μ M against the four human leukaemia cell lines tested, including U-937, HL-60, NALM-6 and MOLT-3. Dose-response experiments revealed that U-937 cells were more sensitive to FL than quiescent and proliferating PBMC, as determined by the MTT assay. This flavanone is able to induce a fast cell cycle arrest at the G₂-M phase, starting at 6 h, and a delayed (later) increase in the percentage of hypodiploid cells. The arrest of cells in the G₂-M phase of the cell cycle by FL could be explained by microtubule formation or by changes in the expression and/or activity of G₂-M cell cycle regulators. Previous studies have shown that some flavonoids exert their anti-proliferative activity by targeting microtubules through tubulin binding [18] and we have reported that some naturally occurring and synthetic cytotoxic flavonoids block tubulin polymerization [19–21]. Further studies are needed to determine the effect of FL on tubulin polymerization and on G₂-M cell cycle regulators such as the cyclin-dependent kinases (Cdk) inhibitor p21^{Cip1/WAF1}, Cdk1, Cdc25C phosphatase and B-type cyclin isoforms.

Our results indicate that FL induces cell death by apoptosis, a process of programmed cell death that can occur with or without activation of caspases, but in this case cell death was dependent on caspases since the pan-caspase inhibitor z-VAD-fmk was able to significantly reduce both the percentage of hypodiploid cells and the percentage of annexin V-FITC positive cells. Our results showed that the flavanone induces the activation and processing of multiple caspases in U-937 cells. Caspase-6 which is believed to be an effector caspase that is activated downstream of caspase-3 and -7 in apoptosome-mediated apoptosis [22] and the effector caspase-7 which is substrate for initiator caspases in extrinsic or intrinsic apoptotic pathways were also processed. However, the specific caspase inhibitors against caspase-3/7, -4, -8 and -9 were unable to block the cell death. This raises the possibility that other specific caspases such as caspase-6 and/or additional pathways may play a key role in the mechanism of cell death. The potential involvement of caspase-6 is supported by recent data which indicate that caspase-6 may be involved in regulated cell death initiation [23–25].

The synthetic flavanone induced the release of mitochondrial apoptogenic proteins including cytochrome *c* and Smac/DIABLO. Cytochrome *c* in the cytosol binds to apoptotic peptidase activating factor 1 (Apaf-1) and pro-caspase-9 to form the apoptosome which is responsible for caspase-9 activation [26]. Smac/DIABLO in the cytosol precipitates apoptosis by binding with members of the inhibitor of apoptosis (IAP) protein family [27]. Although the specific caspase-9 inhibitor was unable to significantly block the cell death triggered by FL, the results seem to indicate that the intrinsic pathway, which is activated in response to cellular stress and is controlled by the Bcl-2 protein family, plays a key role. Treatment with the flavanone induced a strong downregulation of Bcl-2 protein in U-937. In addition, overexpression of Bcl-2 was able to block the cell death triggered by FL suggesting that Bcl-2 itself is a potential target in the mechanism of cell death. Furthermore, the Bax protein that promotes apoptosis was increased in U-937 cells, demonstrating that the ratio between proapoptotic and anti-apoptotic Bcl-2 members plays a major role in determining susceptibility of cells to apoptotic stimuli, as suggested by previous studies [28].

We found that FL also induces activation of caspase-8 which is involved in death receptor-mediated apoptosis. Caspase-8 cleaves Bid to a truncated form (tBid), which engages the mitochondrial pathway to amplify the apoptotic response. We did not observe a truncated form of Bid but the Western blot experiments revealed a clear decrease in Bid levels mainly at 10 μ M FL in accordance with caspase-8 processing and activation. Since caspase-8 activation is mediated by ligand-binding and activation of the death-domain-containing tumor necrosis receptor superfamily we explored the involvement of death receptors. FL was found to effectively stimulate the expression of TRAIL, DR4 and DR5.

Although further experiments are needed to determine whether FL is able to amplify the sensitivity to TRAIL these results are of potential importance because they demonstrate that FL is a death receptor inducer.

The mitogen activated protein kinase (MAPK) signalling pathway regulates the expression of a large number of proteins involved in the control of cell proliferation, differentiation and apoptosis. Activation of the MAPK signalling pathway is known to cause the transformation of normal cells to tumor phenotype [29,30]. Therefore, targeting any component in the MAPK signalling pathway has the potential to arrest tumor growth. Here we found that FL effectively activates the MAPK pathway and interestingly the activation of ERK1/2 and JNK/SAPK is involved in FL-induced apoptosis, since the MEK1/2 and JNK/SAPK inhibitors were able to block partially cell death. These results indicate a key role for the MAPK signalling cascade in the mechanism of cytotoxicity triggered by this flavanone. We have previously shown that betuletol 3-methyl ether, a naturally occurring flavonoid, induces the activation of mitogen-activated protein kinases. However, FL is a greater apoptotic inducer than betuletol 3-methyl ether and induces a fast phosphorylation of JNK/SAPK [31]. In addition, we have described that a flavonoid derivative, trifolin acetate, induces cell death in human leukaemia cells and that this was attenuated by MEK1/2 inhibition. However, this was different to the flavanone described here: the JNK/SAPK inhibitor SP600125 amplified cell death [32]. These results reveal that these flavonoid derivatives differentially modulate the MAPK pathways and could be used to enhance the cell death triggered by these specific compounds. An amplification of the cleavage of caspase-3 and PARP by JNK/SAPK inhibition has been also described in the mechanism of cell death triggered by the prenylated flavonoid daphnegiravone D in human hepatocellular carcinoma cells [33].

Future studies addressing the bioavailability – including the development of micro- and nanodelivery systems – as well as efficacy of *in vivo* concentrations of this specific compound are necessary to determine its potential beneficial effects for human health.

4. Conclusions

The SAR of naphthalene-based chalcones and their corresponding flavanones are displayed graphically in Fig. 6. The most relevant results are (i) some chalcones are more potent than their corresponding flavanones, while other chalcones show similar potency to flavanones, indicating that flexible structures are important in determining cytotoxicity; (ii) the introduction of a methoxy group at a specific position (position 5' on the A ring in chalcone or at position 6 on the A ring of the corresponding flavanone) improved the cytotoxicity against U-937 cells and (iii) the introduction of a methyl group or an atom of chlorine appears to be irrelevant, while the presence of one or two benzyloxy groups on the A ring completely abrogates cytotoxicity, except for the 6'-benzyloxy derivative in the chalcone skeleton that showed a similar potency to the parent chalcone.

We show that the synthetic flavanone FL is cytotoxic against four human leukaemia cells but not against human peripheral blood mononuclear cells. FL-induced cytotoxicity (i) involves the activation and processing of the initiator (caspase-8 and -9) and the executioner caspases (caspases-3, -6 and -7); (ii) is attenuated by the pan-caspase inhibitor z-VAD-fmk; (iii) is associated with the phosphorylation of the mitogen-activated protein kinases ERK1/2, JNK/SAPK and p38^{MAPK}, and (iv) is reduced by the inhibition of MEK1/2 and JNK/SAPK. The IC_{50} values in human leukaemia cells were comparable with those obtained with the antitumor compound etoposide. The studies shown here open new avenues of research into the potential of this compound or derivatives in the development of new therapeutic strategies against leukaemia cells.

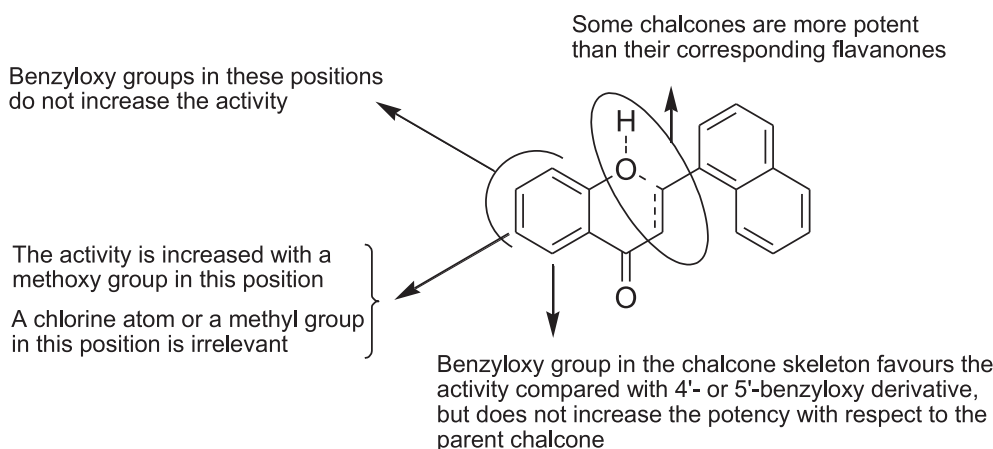


Fig. 6. Structure-activity relationship of naphthyl-chalcone/flavanone analogues.

5. Experimental

5.1. General method and reagents

^1H and ^{13}C NMR spectra were obtained on a Bruker model AMX-500 spectrometer with standard pulse sequences operating at 500 MHz in ^1H and 126 MHz in ^{13}C NMR. Chemical shifts (δ) are given in ppm upfield from tetramethylsilane as internal standard, and coupling constants (J) are reported in hertz. IR spectra were recorded using a Bruker model IFS-55 spectrophotometer. Melting points were determined on a Büchi B-540 apparatus and are un-corrected. EIMS and HREIMS were recorded on a Micromass model Autospec (70 eV) spectrometer. Column chromatography was carried out on silica gel 60 (Merck 230–400 mesh) and analytical thin layer chromatography (TLC) was performed using silica gel aluminum sheets. HPLC analyses were performed on a Waters 600 Controller using a Chiralcel OD-H column (iPrOH:hexane) and a Silica gel 100 Å LC column (250 × 4.6 mm – Hexane:ethyl acetate). Elemental analyses were performed on a Leco TruSpec Micro equipment. The purity of compounds used in biological testing was > 98%, as determined by elemental analysis or high-performance liquid chromatography. The inhibitors benzyloxycarbonyl-Val-Ala-Asp(OMe) fluoromethyl ketone (z-VAD-fmk), benzyloxycarbonyl-Asp(OMe)-Glu(O-Me)-Val-Asp(O-Me) fluoromethyl ketone (z-DEVD-fmk), benzyloxycarbonyl-Ile-Glu-Thr-Asp(OMe) fluoromethyl ketone (z-IETD-fmk), benzyloxycarbonyl-Leu-Glu-His-Asp(OMe) fluoromethyl ketone (z-LEHD-fmk), Ac-LEVD-CHO (N-acetyl-Leu-Glu-Val-Asp-CHO), PD98059, U0126, SP600125 and SB203580 were purchased from Sigma (Saint Louis, MO, USA). Acrylamide, bisacrylamide, ammonium persulfate and N,N,N',N'-tetramethylethylenediamine were from Bio-Rad (Hercules, CA, USA). Antibodies for caspase-3, caspase-7, caspase-8 and caspase-9 were purchased from Stressgen-ENZO (Victoria, British Columbia, Canada). Anti-caspase-6 and anti-caspase-4 monoclonal antibodies were from Medical & Biological Laboratories (Nagoya, Japan). Monoclonal anti- β -Actin (clone AC-74) was purchased from Sigma (Saint Louis, MO, USA). Monoclonal anti-human Bcl-2 was from Santa Cruz Biotechnology (Santa Cruz, CA, USA). Polyclonal anti-human Bax and Bid antibodies and monoclonal anti-cytochrome c and poly(ADP-ribose) polymerase (PARP) antibodies were from BD Pharmingen (San Diego, CA, USA). Monoclonal antibody for Smac/DIABLO was from BD Transduction Laboratories. Anti-JNK/SAPK, anti-phospho-JNK/SAPK (T183/Y185), anti-p44/42 MAP kinase (ERK1/2), anti-phospho-p44/42 MAP kinase (T202/Y204), anti-p38MAPK and a phosphorylated form (T180/Y182) of p38MAPK were purchased from New England BioLabs (Cell Signaling Technology, Inc, Beverly, MA, USA). Secondary antibodies were from GE Healthcare Bio-Sciences AB (Little Chalfont, UK). PVDF membranes were from Millipore (Temecula,

CA, USA). All other chemicals were obtained from Sigma (Saint Louis, MO, USA).

5.2. General procedure for the synthesis of chalcones (1–10)

A mixture of the acetophenone (5–10 mmol, 1 equiv.) and the corresponding aldehyde (1 equiv.) in EtOH (20–40 mL) was stirred at room temperature and a 50% aqueous solution of NaOH (5–8 mL) was added. The reaction mixture was stirred at room temperature until the starting materials had been consumed. HCl (10%) was then added until neutrality was reached. Precipitated chalcones were generally filtered and crystallized from MeOH although in some cases, the product was purified using column chromatography.

5.2.1. (E)-1-(2-hydroxyphenyl)-3-(naphthalen-1-yl)prop-2-en-1-one (1)

Yellow amorphous solid (65%). IR (cm^{-1}): 1694, 1640, 1607, 1581, 1566, 1491, 1472, 1462, 1439, 1365, 1342, 1304, 1278, 1209, 1159, 1072, 1024, 977, 901. ^1H NMR (500 MHz, CDCl_3): δ = 12.86 (s, 1H); 8.79 (d, J = 15.2 Hz, 1H); 8.29 (dd, J = 8.5, 1.0 Hz, 1H); 8.01–7.89 (m, 4H); 7.76 (d, J = 15.3 Hz, 1H); 7.62 (ddd, J = 8.4, 6.8, 1.5 Hz, 1H); 7.60–7.47 (m, 3H); 7.06 (dd, J = 8.4, 1.1 Hz, 1H); 6.97 (ddd, J = 8.2, 7.2, 1.2 Hz, 1H). ^{13}C NMR (126 MHz, CDCl_3): δ = 193.6, 163.7, 142.4, 136.5, 133.8, 132.1, 131.8, 131.2, 129.7, 128.8, 127.2, 126.4, 125.4, 125.3, 123.4, 122.8, 120.0, 118.9, 118.7. HRMS (ESI-FT-ICR) m/z : 297.0895 [M + Na]; calcd. for $\text{C}_{19}\text{H}_{14}\text{NaO}_2$: 297.0891.

5.2.2. (E)-1-(2-hydroxy-5-methoxyphenyl)-3-(naphthalen-1-yl)prop-2-en-1-one (2)

Orange crystalline solid (82%), mp 112–113 °C. IR (cm^{-1}): 1635, 1566, 1479, 1396, 1337, 1323, 1289, 1273, 1249, 1207, 1176, 1162, 1020, 1001, 979, 849. ^1H NMR (500 MHz, CDCl_3): δ = 12.68 (s, 1H); 8.77 (d, J = 15.2 Hz, 1H); 8.32–8.24 (m, 1H); 7.95 (t, J = 7.7 Hz, 2H); 7.93–7.86 (m, 1H); 7.75 (d, J = 15.3 Hz, 1H); 7.73 (s, 1H); 7.62 (ddd, J = 8.4, 6.8, 1.5 Hz, 1H); 7.59–7.50 (m, 2H); 7.34 (dd, J = 8.6, 2.2 Hz, 1H); 6.97 (d, J = 8.5 Hz, 1H); 2.36 (s, 3H). ^{13}C NMR (126 MHz, CDCl_3): δ = 193.5, 161.6, 142.1, 137.6, 133.8, 132.2, 131.8, 131.1, 129.4, 128.8, 128.0, 127.1, 126.4, 125.4, 125.3, 123.4, 122.9, 119.7, 118.4, 20.6. HRMS (ESI-FT-ICR) m/z : 311.1043 [M + Na]; calcd. for $\text{C}_{20}\text{H}_{16}\text{NaO}_2$: 311.1048.

5.2.3. (E)-1-(2-hydroxy-5-methoxyphenyl)-3-(naphthalen-1-yl)prop-2-en-1-one (3)

Orange crystalline solid (78%), mp 111–112 °C. IR (cm^{-1}): 1644, 1581, 1566, 1495, 1417, 1346, 1271, 1188, 1166, 1048, 1017, 975, 960, 844. ^1H NMR (500 MHz, CDCl_3): δ = 12.42 (s, 1H); 8.78 (d, J = 15.2 Hz, 1H); 8.32–8.24 (m, 1H); 7.96 (d, J = 8.2 Hz, 1H);

7.94–7.88 (m, 2H); 7.69 (d, $J = 15.2$ Hz, 1H); 7.62 (ddd, $J = 8.5, 6.8, 1.4$ Hz, 1H); 7.60–7.51 (m, 2H); 7.40 (d, $J = 3.0$ Hz, 1H); 7.17 (dd, $J = 9.1, 3.0$ Hz, 1H); 7.01 (d, $J = 9.1$ Hz, 1H); 3.84 (s, 3H). ^{13}C NMR (126 MHz, CDCl_3): $\delta = 193.2, 158.1, 151.8, 142.5, 133.8, 132.1, 131.8, 131.2, 128.8, 127.2, 126.4, 125.4, 125.3, 124.1, 123.4, 122.9, 119.6, 119.4, 112.8, 56.1$. HRMS (ESI-FT-ICR) m/z : 327.0999 [M+Na]; calcd. for $\text{C}_{20}\text{H}_{16}\text{NaO}_3$: 327.0997.

5.2.4. (E)-1-(2-hydroxy-4-methoxyphenyl)-3-(naphthalen-1-yl)prop-2-en-1-one (4)

Pale yellow crystalline solid (58%), mp 114–115 °C. IR (cm^{-1}): 1583, 1573, 1500, 1356, 1249, 1204, 1171, 1121, 1088, 1020, 1005, 958, 849, 828. ^1H NMR (500 MHz, CDCl_3): $\delta = 13.48$ (s, 1H); 8.74 (d, $J = 15.2$ Hz, 1H); 8.28 (d, $J = 8.5$ Hz, 1H); 8.00–7.82 (m, 4H); 7.72–7.64 (m, 1H); 7.61 (ddt, $J = 8.3, 6.9, 1.4$ Hz, 1H); 7.58–7.46 (m, 2H); 6.50 (ddd, $J = 4.6, 2.5, 1.3$ Hz, 2H); 3.87 (d, $J = 1.2$ Hz, 3H). ^{13}C NMR (126 MHz, CDCl_3): $\delta = 191.7, 166.8, 166.3, 141.4, 133.7, 132.3, 131.8, 131.3, 130.9, 128.8, 127.0, 126.3, 125.4, 125.2, 123.5, 123.0, 114.1, 107.8, 101.1, 55.6$. HRMS (ESI-FT-ICR) m/z : 327.1000 [M+Na]; calcd. for $\text{C}_{20}\text{H}_{16}\text{NaO}_3$: 327.0997.

5.2.5. (E)-1-(5-chloro-2-hydroxyphenyl)-3-(naphthalen-1-yl)prop-2-en-1-one (5)

Yellow crystalline solid (88%), mp 165–165 °C. IR (cm^{-1}): 1642, 1556, 1462, 1403, 1365, 1358, 1332, 1327, 1275, 1242, 1207, 1190, 1024, 1013, 984, 826. ^1H NMR (500 MHz, CDCl_3): $\delta = 12.77$ (s, 1H); 8.82 (d, $J = 15.1$ Hz, 1H); 8.28 (d, $J = 8.9$ Hz, 1H); 8.02–7.94 (m, 2H); 7.92 (dt, $J = 3.4, 1.9$ Hz, 2H); 7.72–7.60 (m, 2H); 7.60–7.50 (m, 2H); 7.46 (dd, $J = 8.9, 2.5$ Hz, 1H); 7.02 (d, $J = 8.9$ Hz, 1H). ^{13}C NMR (126 MHz, CDCl_3): $\delta = 192.7, 162.2, 143.4, 136.3, 133.8, 131.8, 131.7, 131.6, 128.9, 128.9, 127.3, 126.5, 125.6, 125.4, 123.6, 123.3, 122.0, 120.6, 120.3$. HRMS (ESI-FT-ICR) m/z : 307.0522 [M–H]; calcd. for $\text{C}_{19}^{35}\text{ClH}_{12}\text{O}_2$: 307.0526; m/z : 309.0499 [M–H]; calcd. for $\text{C}_{19}^{37}\text{ClH}_{12}\text{O}_2$: 309.0496.

5.2.6. (E)-1-(5-benzyloxy)-2-hydroxyphenyl)-3-(naphthalen-1-yl)prop-2-en-1-one (6)

Orange crystalline solid (76%), mp 140–141 °C. IR (cm^{-1}): 1637, 1566, 1486, 1415, 1358, 1339, 1327, 1282, 1235, 1214, 1192, 1176, 1013, 965, 849, 837. ^1H NMR (500 MHz, CDCl_3): $\delta = 12.41$ (s, 1H); 8.76 (d, $J = 15.2$ Hz, 1H); 8.27 (d, $J = 8.4$ Hz, 1H); 7.97 (d, $J = 8.2$ Hz, 1H); 7.90 (dd, $J = 13.9, 7.6$ Hz, 2H); 7.67–7.51 (m, 4H); 7.51–7.30 (m, 6H); 7.23 (dd, $J = 9.1, 2.9$ Hz, 1H); 7.00 (d, $J = 9.0$ Hz, 1H); 5.08 (s, 2H). ^{13}C NMR (126 MHz, CDCl_3): $\delta = 193.2, 158.2, 150.9, 142.4, 136.8, 133.8, 132.1, 131.8, 131.3, 128.8, 128.7, 128.2, 127.6, 127.2, 126.4, 125.4, 125.3, 125.0, 123.4, 122.8, 119.6, 119.4, 114.6, 71.3$. HRMS (ESI-FT-ICR) m/z : 403.1314 [M+Na]; calcd. for $\text{C}_{26}\text{H}_{20}\text{NaO}_3$: 403.1310.

5.2.7. (E)-1-(4-benzyloxy)-2-hydroxyphenyl)-3-(naphthalen-1-yl)prop-2-en-1-one (7)

Yellow amorphous solid (60%). IR (cm^{-1}): 1633, 1566, 1507, 1363, 1289, 1254, 1218, 1190, 1128, 1020, 970, 830. ^1H NMR (500 MHz, CDCl_3): $\delta = 13.45$ (s, 1H); 8.75 (d, $J = 15.2$ Hz, 1H); 8.28 (d, $J = 8.5$ Hz, 1H); 7.98–7.84 (m, 4H); 7.67 (d, $J = 15.2$ Hz, 1H); 7.64–7.49 (m, 3H); 7.49–7.32 (m, 5H); 6.64–6.53 (m, 2H); 5.13 (s, 2H). ^{13}C NMR (126 MHz, CDCl_3): $\delta = 191.7, 166.7, 165.4, 141.4, 135.8, 133.7, 132.3, 131.8, 131.4, 130.9, 128.8, 128.7, 128.3, 127.6, 127.0, 126.4, 125.4, 125.2, 123.5, 123.0, 114.3, 108.3, 102.1, 70.3$. HRMS (ESI-FT-ICR) m/z : 403.1007 [M+Na]; calcd. for $\text{C}_{26}\text{H}_{20}\text{NaO}_3$: 403.1310.

5.2.8. (E)-1-(3,5-dichloro-2-hydroxyphenyl)-3-(naphthalen-1-yl)prop-2-en-1-one (8)

Orange crystalline solid (83%), mp 188–189 °C. IR (cm^{-1}): 1633, 1557, 1436, 1339, 1320, 1271, 1240, 1211, 1166, 1128, 1048, 1029,

975, 968, 866, 844, 821. ^1H NMR (500 MHz, CDCl_3): $\delta = 13.41$ (s, 1H); 8.87 (d, $J = 15.1$ Hz, 1H); 8.27 (dd, $J = 8.5, 1.1$ Hz, 1H); 8.03–7.94 (m, 2H); 7.92 (dd, $J = 8.5, 1.2$ Hz, 1H); 7.85 (d, $J = 2.5$ Hz, 1H); 7.69–7.60 (m, 3H); 7.60–7.52 (m, 2H). ^{13}C NMR (126 MHz, CDCl_3): $\delta = 192.4, 158.1, 144.4, 135.8, 133.8, 132.0, 131.8, 131.4, 128.9, 127.5, 127.4, 126.5, 125.7, 125.4, 124.2, 123.3, 123.2, 121.3, 121.0$. HRMS (ESI-FT-ICR) m/z : 341.0136 [M–H]; calcd. for $\text{C}_{19}^{35}\text{Cl}_2\text{H}_{11}\text{O}_2$: 341.0136; m/z : 343.0121 [M–H]; calcd. for $\text{C}_{19}^{35}\text{Cl}^{37}\text{ClH}_{11}\text{O}_2$: 343.0107.

5.2.9. (E)-1-(3,4-bis(benzyloxy)-2-hydroxyphenyl)-3-(naphthalen-1-yl)prop-2-en-1-one (9)

Yellow amorphous solid (54%). IR (cm^{-1}): 1635, 1564, 1500, 1453, 1431, 1342, 1306, 1294, 1259, 1228, 1128, 1091, 1060, 1017, 986, 972. ^1H NMR (500 MHz, CDCl_3): $\delta = 13.28$ (s, 1H); 8.75 (d, $J = 15.2$ Hz, 1H); 8.28 (d, $J = 8.4$ Hz, 1H); 7.94 (d, $J = 8.2$ Hz, 1H); 7.92–7.87 (m, 2H); 7.71–7.64 (m, 2H); 7.61 (ddd, $J = 8.4, 6.8, 1.5$ Hz, 1H); 7.58–7.49 (m, 4H); 7.42–7.28 (m, 8H); 6.55 (d, $J = 9.1$ Hz, 1H); 5.20 (s, 2H); 5.17 (s, 2H). ^{13}C NMR (126 MHz, CDCl_3): $\delta = 206.9, 192.3, 158.9, 158.0, 141.6, 137.6, 136.2, 133.7, 132.3, 131.8, 131.0, 128.8, 128.6, 128.6, 128.2, 128.1, 127.9, 127.2, 127.1, 126.4, 126.1, 125.4, 125.2, 123.5, 123.0, 115.7, 104.6, 74.8, 70.8$. HRMS (ESI-FT-ICR) m/z : 509.1727 [M+Na]; calcd. for $\text{C}_{33}\text{H}_{26}\text{NaO}_4$: 509.1729.

5.2.10. (E)-1-(2-(benzyloxy)-6-hydroxyphenyl)-3-(naphthalen-1-yl)prop-2-en-1-one (10)

Bright yellow crystalline solid (80%), mp 145–146 °C. IR (cm^{-1}): 1630, 1555, 1460, 1446, 1353, 1233, 1209, 1169, 1065, 1024, 968, 918, 849. ^1H NMR (500 MHz, CDCl_3): $\delta = 13.41$ (s, 1H); 8.62 (d, $J = 15.4$ Hz, 1H); 8.25 (dd, $J = 8.5, 1.2$ Hz, 1H); 7.95 (d, $J = 15.4$ Hz, 1H); 7.88–7.80 (m, 2H); 7.58–7.49 (m, 2H); 7.49–7.44 (m, 2H); 7.40 (t, $J = 8.4$ Hz, 1H); 7.38–7.34 (m, 1H); 7.32–7.27 (m, 2H); 7.21 (dd, $J = 8.2, 7.2$ Hz, 1H); 7.08 (dt, $J = 7.2, 0.9$ Hz, 1H); 6.68 (dd, $J = 8.4, 1.0$ Hz, 1H); 6.56 (dd, $J = 8.3, 1.0$ Hz, 1H); 5.14 (s, 2H). ^{13}C NMR (126 MHz, CDCl_3): $\delta = 194.5, 165.3, 160.3, 139.6, 136.0, 135.6, 133.6, 132.2, 131.8, 130.3, 130.0, 128.8, 128.6, 128.5, 128.5, 126.8, 126.1, 125.5, 125.0, 123.4, 112.0, 111.3, 102.4, 71.4$. HRMS (ESI-FT-ICR) m/z : 403.1302 [M+Na]; calcd. for $\text{C}_{26}\text{H}_{20}\text{NaO}_3$: 403.1310.

5.3. General procedure for the synthesis of flavanones (11–19)

To a solution of a chalcone (0.12–0.2 mmol) in ethanol (1–2 mL), sodium acetate (10 equiv.) was added. The reaction was heated in refluxing for 24–48 h and then was allowed to cool to room temperature, poured into ice water (10 mL) and extracted with CH_2Cl_2 (3 \times 5 mL). The combined organic phase was washed with brine, dried over Na_2SO_4 , and then concentrated in vacuo. The flavanones were purified by crystallization (MeOH) or column chromatography.

5.3.1. 2-(naphthalen-1-yl)chroman-4-one (11)

Bright yellow crystalline solid (80%), mp 74–75 °C. IR (cm^{-1}): 1678, 1607, 1581, 1474, 1465, 1410, 1339, 1304, 1226, 1147, 1117, 1067, 1027, 984, 918, 901, 856, 840. ^1H NMR (500 MHz, CDCl_3): $\delta = 8.11$ –8.03 (m, 1H); 8.01 (dd, $J = 8.0, 1.8$ Hz, 1H); 7.97–7.86 (m, 2H); 7.79 (d, $J = 7.1$ Hz, 1H); 7.56 (m, 4H); 7.16–7.05 (m, 2H); 6.24 (dd, $J = 13.4, 2.8$ Hz, 1H); 3.28 (dd, $J = 17.0, 13.4$ Hz, 1H); 3.11 (dd, $J = 17.0, 2.8$ Hz, 1H). ^{13}C NMR (126 MHz, CDCl_3): $\delta = 192.3, 161.9, 136.3, 134.3, 134.0, 130.3, 129.5, 129.2, 127.3, 126.8, 126.1, 125.5, 124.0, 122.9, 121.9, 121.2, 118.3, 77.0, 44.1$. HRMS (ESI-FT-ICR) m/z : 297.0901 [M+Na]; calcd. for $\text{C}_{19}\text{H}_{14}\text{NaO}_2$: 297.0891.

5.3.2. 6-methyl-2-(naphthalen-1-yl)chroman-4-one (12)

White crystalline solid (42%), mp 137–138 °C. IR (cm^{-1}): 1687, 1618, 1488, 1417, 1292, 1228, 1181, 1131, 1048, 982, 908. ^1H NMR (500 MHz, CDCl_3): $\delta = 8.09$ –8.02 (m, 1H); 7.96–7.85 (m, 2H); 7.83–7.75 (m, 2H); 7.62–7.47 (m, 3H); 7.35 (dd, $J = 8.4, 2.4$ Hz, 1H);

7.00 (d, $J = 8.4$ Hz, 1H); 6.20 (dd, $J = 13.3, 2.8$ Hz, 1H); 3.25 (dd, $J = 17.0, 13.4$ Hz, 1H); 3.08 (dd, $J = 16.9, 2.9$ Hz, 1H); 2.36 (s, 3H). ^{13}C NMR (126 MHz, CDCl_3): $\delta = 192.5, 159.9, 137.3, 134.3, 133.9, 131.2, 130.2, 129.3, 129.1, 126.7, 126.7, 125.9, 125.4, 123.8, 122.8, 120.7, 118.0, 76.8, 44.0, 20.5$. HRMS (ESI-FT-ICR) m/z : 311.1049 [M+Na]; calcd. for $\text{C}_{20}\text{H}_{16}\text{NaO}_2$: 311.1048.

5.3.3. 6-methoxy-2-(naphthalen-1-yl)chroman-4-one (13)

White crystalline solid (70%); mp 164–165 °C. IR (cm^{-1}): 1682, 1611, 1484, 1429, 1334, 1278, 1209, 1178, 1057, 1027, 982, 892, 866, 818. ^1H NMR (500 MHz, CDCl_3): $\delta = 8.06$ (d, $J = 8.0$ Hz, 1H); 7.92 (d, $J = 8.4$ Hz, 1H); 7.89 (d, $J = 8.1$ Hz, 1H); 7.78 (d, $J = 7.1$ Hz, 1H); 7.55 (m, 3H); 7.43 (d, $J = 3.2$ Hz, 1H); 7.15 (dd, $J = 9.0, 3.2$ Hz, 1H); 7.04 (d, $J = 9.0$ Hz, 1H); 6.19 (dd, $J = 13.4, 2.8$ Hz, 1H); 3.85 (s, 3H); 3.25 (dd, $J = 17.1, 13.4$ Hz, 1H); 3.09 (dd, $J = 17.0, 2.8$ Hz, 1H); ^{13}C NMR (126 MHz, CDCl_3): $\delta = 192.3, 156.5, 154.4, 134.3, 133.9, 130.2, 129.3, 129.1, 126.7, 125.9, 125.4, 125.4, 123.8, 122.8, 120.9, 119.5, 107.5, 77.2, 55.9, 43.9$. HRMS (ESI-FT-ICR) m/z : 327.0999 [M+Na]; calcd. for $\text{C}_{20}\text{H}_{16}\text{NaO}_3$: 327.0997.

5.3.4. 7-methoxy-2-(naphthalen-1-yl)chroman-4-one (14)

White amorphous solid (48%). IR (cm^{-1}): 1697, 1671, 1611, 1600, 1578, 1443, 1379, 1360, 1292, 1259, 1202, 1159, 1121, 1053, 1041, 1013, 991, 949, 892, 873, 828. ^1H NMR (500 MHz, CDCl_3): $\delta = 8.11$ –8.03 (m, 1H); 7.98–7.85 (m, 3H); 7.77 (d, $J = 7.2$ Hz, 1H); 7.55 (dd, $J = 8.5, 6.6$ Hz, 3H); 6.67 (dd, $J = 8.8, 2.4$ Hz, 1H); 6.54 (d, $J = 2.4$ Hz, 1H); 6.23 (dd, $J = 13.3, 2.9$ Hz, 1H); 3.85 (s, 3H); 3.23 (dd, $J = 16.9, 13.3$ Hz, 1H); 3.04 (dd, $J = 17.0, 2.9$ Hz, 1H). ^{13}C NMR (126 MHz, CDCl_3): $\delta = 190.9, 166.2, 163.7, 134.2, 133.9, 130.2, 129.4, 129.1, 128.9, 126.7, 126.0, 125.4, 123.9, 122.8, 115.0, 110.4, 101.0, 77.2, 55.7, 43.6$. HRMS (ESI-FT-ICR) m/z : 327.1007 [M+Na]; calcd. for $\text{C}_{20}\text{H}_{16}\text{NaO}_3$: 327.0997.

5.3.5. 6-chloro-2-(naphthalen-1-yl)chroman-4-one (15)

Bright yellow crystalline solid (80%), mp 137–138 °C; IR (cm^{-1}): 1687, 1604, 1467, 1424, 1408, 1337, 1275, 1221, 1209, 1171, 1131, 982, 911, 901, 892, 852, 833. ^1H NMR (500 MHz, CDCl_3): $\delta = 8.06$ –8.00 (m, 1H); 7.96 (d, $J = 2.6$ Hz, 1H); 7.95–7.87 (m, 2H); 7.76 (dt, $J = 7.3, 1.0$ Hz, 1H); 7.61–7.51 (m, 3H); 7.48 (dd, $J = 8.8, 2.7$ Hz, 1H); 7.06 (d, $J = 8.8$ Hz, 1H); 6.23 (dd, $J = 13.2, 2.9$ Hz, 1H); 3.26 (dd, $J = 17.1, 13.2$ Hz, 1H); 3.12 (dd, $J = 17.1, 2.9$ Hz, 1H). ^{13}C NMR (126 MHz, CDCl_3): $\delta = 191.2, 160.3, 136.2, 134.0, 133.8, 130.3, 129.7, 129.3, 127.5, 126.9, 126.6, 126.2, 125.5, 124.0, 122.8, 122.0, 120.1, 77.2, 43.7$. HRMS (ESI-FT-ICR) m/z : 331.0505 [M+Na]; calcd. for $\text{C}_{19}^{35}\text{ClH}_{13}\text{NaO}_2$: 331.0502; m/z : 333.0463 [M+Na]; calcd. for $\text{C}_{19}^{37}\text{ClH}_{13}\text{NaO}_2$: 333.0472.

5.3.6. 6-benzyloxy-2-(naphthalen-1-yl)chroman-4-one (16)

White crystalline solid (46%), mp 159–160 °C. IR (cm^{-1}): 1682, 1484, 1453, 1431, 1382, 1337, 1271, 1181, 1155, 1131, 1062, 1039, 1027, 982, 963, 894, 861, 837. ^1H NMR (500 MHz, CDCl_3): $\delta = 8.05$ (d, $J = 7.8$ Hz, 1H); 7.97–7.83 (m, 2H); 7.78 (d, $J = 7.1$ Hz, 1H); 7.61–7.50 (m, 4H); 7.46 (d, $J = 7.4$ Hz, 2H); 7.41 (dd, $J = 8.4, 6.6$ Hz, 2H); 7.37–7.29 (m, 1H); 7.23 (dd, $J = 9.0, 3.2$ Hz, 1H); 7.05 (d, $J = 8.9$ Hz, 1H); 6.19 (dd, $J = 13.5, 2.8$ Hz, 1H); 5.10 (s, 2H); 3.25 (dd, $J = 17.1, 13.5$ Hz, 1H); 3.09 (dd, $J = 17.1, 2.8$ Hz, 1H). ^{13}C NMR (126 MHz, CDCl_3): $\delta = 192.2, 156.6, 153.5, 136.6, 134.2, 133.9, 130.2, 129.3, 129.1, 128.6, 128.1, 127.6, 126.7, 126.0, 126.0, 125.4, 123.8, 122.8, 121.0, 119.6, 109.0, 77.0, 70.6, 43.9$. HRMS (ESI-FT-ICR) m/z : 403.1310 [M+Na]; calcd. for $\text{C}_{26}\text{H}_{20}\text{NaO}_3$: 403.1310.

5.3.7. 7-benzyloxy-2-(naphthalen-1-yl)chroman-4-one (17)

Pale yellow amorphous solid (50%). IR (cm^{-1}): 1668, 1607, 1571, 1500, 1443, 1377, 1353, 1334, 1294, 1252, 1185, 1166, 1119, 1060, 1034, 998, 984, 930, 828. ^1H NMR (500 MHz, CDCl_3): $\delta = 7.98$ (d, $J = 7.7$ Hz, 1H); 7.90–7.79 (m, 3H); 7.72–7.66 (m, 1H); 7.52–7.43 (m,

3H); 7.37–7.25 (m, 5H); 6.67 (dd, $J = 8.8, 2.4$ Hz, 1H); 6.55 (d, $J = 2.3$ Hz, 1H); 6.15 (dd, $J = 13.2, 2.8$ Hz, 1H); 5.04 (s, 2H); 3.16 (dd, $J = 17.0, 13.3$ Hz, 1H); 2.97 (dd, $J = 17.0, 2.9$ Hz, 1H). ^{13}C NMR (126 MHz, CDCl_3): $\delta = 190.8, 165.3, 163.7, 135.8, 134.2, 133.9, 130.2, 129.4, 129.1, 128.9, 128.7, 128.3, 127.5, 126.7, 126.0, 125.4, 123.9, 122.8, 115.2, 110.9, 102.0, 77.3, 70.3, 43.6$. HRMS (ESI-FT-ICR) m/z : 403.1313 [M+Na]; calcd. for $\text{C}_{26}\text{H}_{20}\text{NaO}_3$: 403.1310.

5.3.8. 6,8-dichloro-2-(naphthalen-1-yl)chroman-4-one (18)

Pale yellow crystalline solid (56%), mp 172–173 °C. IR (cm^{-1}): 1694, 1592, 1455, 1337, 1266, 1254, 1233, 1214, 1181, 1166, 1003, 982, 968, 878, 852, 809. ^1H NMR (500 MHz, CDCl_3): $\delta = 7.96$ (d, $J = 8.2$ Hz, 1H); 7.89–7.82 (m, 2H); 7.80 (d, $J = 2.6$ Hz, 1H); 7.71 (d, $J = 7.2$ Hz, 1H); 7.56–7.44 (m, 4H); 6.23 (dd, $J = 12.2, 3.5$ Hz, 1H); 3.20 (dd, $J = 17.2, 12.2$ Hz, 1H); 3.13 (dd, $J = 17.2, 3.5$ Hz, 1H). ^{13}C NMR (126 MHz, CDCl_3): $\delta = 190.3, 155.9, 135.7, 133.9, 133.0, 130.1, 129.7, 129.1, 126.9, 126.8, 126.1, 125.3, 125.2, 124.4, 123.9, 122.7, 122.6, 77.6, 43.2$. HRMS (ESI-FT-ICR) m/z : 365.0109 [M+Na]; calcd. for $\text{C}_{19}^{35}\text{Cl}_2\text{H}_{12}\text{O}_2$: 365.0112; m/z : 367.0089 [M+Na]; calcd. for $\text{C}_{19}^{35}\text{Cl}^{37}\text{ClNaH}_{12}\text{O}_2$: 367.0083.

5.3.9. 7,8-bis(benzyloxy)-2-(naphthalen-1-yl)chroman-4-one (19)

White amorphous solid (40%). IR (cm^{-1}): 1686, 1641, 1592, 1505, 1446, 1384, 1312, 1293, 1261, 1194, 1120, 1090, 1073, 1013. ^1H NMR (500 MHz, CDCl_3): $\delta = 8.05$ (dd, $J = 6.1, 3.3$ Hz, 1H); 7.93 (dd, $J = 6.3, 3.4$ Hz, 1H); 7.90 (d, $J = 8.3$ Hz, 1H); 7.77 (d, $J = 7.2$ Hz, 1H); 7.73 (d, $J = 8.9$ Hz, 1H); 7.59–7.49 (m, 3H); 7.45–7.31 (m, 5H); 7.27 (m, 2H); 7.18 (dd, $J = 8.4, 6.3$ Hz, 1H); 7.15–7.06 (m, 2H); 6.74 (d, $J = 8.9$ Hz, 1H); 6.14 (dd, $J = 12.3, 3.4$ Hz, 1H); 5.21 (s, 2H); 5.01 (s, 2H); 3.16 (dd, $J = 17.1, 12.3$ Hz, 1H); 3.08 (dd, $J = 17.0, 3.4$ Hz, 1H). ^{13}C NMR (126 MHz, CDCl_3): $\delta = 205.9, 190.2, 157.3, 155.0, 136.2, 135.3, 135.1, 133.3, 132.7, 129.1, 128.1, 128.0, 127.6, 127.5, 127.1, 127.0, 126.8, 126.2, 125.6, 124.9, 124.3, 122.7, 122.0, 121.8, 115.4, 106.5, 74.2, 69.9, 42.8$. HRMS (ESI-FT-ICR) m/z : 509.1729 [M+Na]; calcd. for $\text{C}_{33}\text{H}_{26}\text{NaO}_4$: 509.1732.

5.4. Cell culture and cytotoxicity assays

U-937, HL-60, NALM-6 and MOLT-3 cells were from DSMZ (German Collection of Microorganisms and Cell Cultures, Braunschweig, Germany). U-937/Bcl-2 cells were kindly provided by Dr. Jacqueline Bréard (INSERM U749, Faculté de Pharmacie Paris-Sud, Châtenay-Malabry, France). The U-937 is a pro-monocytic, human myeloid leukaemia cell line which was isolated from a histiocytic lymphoma. HL-60 is an acute myeloid leukaemia cell line. NALM-6 is a human B cell precursor leukaemia. MOLT-3 is an acute lymphoblastic leukaemia cell line.

Cells were cultured in RPMI 1640 medium containing 10% (v/v) heat-inactivated fetal bovine serum, 100 $\mu\text{g}/\text{ml}$ streptomycin and 100 U/ml penicillin, incubated at 37 °C in a humidified atmosphere containing 5% CO_2 as described [17]. The doubling times of the cell lines were 30 h for U-937 and U-937/Bcl-2, 24 h for HL-60 and 40 h for NALM-6 and MOLT-3. Human peripheral blood mononuclear cells (PBMC) were isolated from heparin-anticoagulated blood of healthy volunteers by centrifugation with Ficoll-Paque Plus (GE Healthcare Bio-Sciences AB, Uppsala, Sweden). PBMC were also stimulated with phytohemagglutinine (2 $\mu\text{g}/\text{mL}$) for 48 h before the experimental treatment. The trypan blue exclusion method was used for counting the cells by a hemacytometer and the viability was always greater than 95% in all experiments. The cytotoxicities of chalcones and flavanones were evaluated by colorimetric 3-(4,5-dimethyl-2-thiazolyl)-2,5-diphenyl-2H-tetrazolium bromide (MTT) assays as previously described [34]. Chalcones and flavanones were dissolved in DMSO and kept under dark conditions at 25 °C. Before each experiment, compounds were dissolved in culture media at 37 °C. The final concentration of DMSO did not exceed 0.3% (v/v).

5.5. Fluorescent microscopy analysis

Cells were washed with PBS and fixed in 3% paraformaldehyde for 10 min at room temperature. The paraformaldehyde was removed by centrifugation (12,000g, 1 min, 25 °C) and the samples were stained with 20 µg/mL of bisbenzimidazole trihydrochloride (Hoechst 33258) in PBS at 25 °C during 15 min. An aliquot of 10 µL of the mixture was used to observe the stained nuclei with fluorescent microscopy (Zeiss-Axiovert).

5.6. Quantification of hypodiploid cells and flow cytometry analysis of annexin V-FITC and propidium iodide-stained cells

Flow cytometric analysis of propidium iodide-stained cells was performed as previously described [35]. Briefly, cells were centrifuged for 10 min at 500g, washed with cold PBS, fixed with ice-cold 75% ethanol and stored at −20 °C for at least 1 h. Samples were then centrifuged at 500g for 10 min at 4 °C, washed with PBS, resuspended in 200 µL of PBS containing 100 µg/mL RNase A and 50 µg/mL propidium iodide and incubated for 1 h in the dark. The DNA content was analyzed by flow cytometry with a BD FACSVerse™ cytometer (BD Biosciences, San Jose, CA, USA). Flow cytometric analysis of annexin V-FITC and propidium iodide-stained cells was performed as described [35].

5.7. Assay of caspase activity

Caspase activity was determined by measuring proteolytic cleavage of the chromogenic substrates Ac-DEVD-pNA (for caspase-3 like protease activity), Ac-IETD-pNA (for caspase-8 activity) and Ac-LEHD-pNA (for caspase-9 activity) as previously described [35].

5.8. Western blot analysis

Cells were harvested by centrifugation (500g, 10 min, 4 °C) and pellets were resuspended in lysis buffer [1% Triton X-100, 10 mM sodium fluoride, 2 mM EDTA, 20 mM Tris-HCl (pH 7.4), 2 mM tetrasodium pyrophosphate, 10% glycerol, 137 mM NaCl, 20 mM sodium β-glycerophosphate], with the protease inhibitors phenylmethylsulfonyl fluoride (PMSF, 1 mM), aprotinin, leupeptin, and pepstatin A (5 µg/mL each) and kept on ice during 15 min. Cells were sonicated on ice five times (5 s each, with intervals between each sonication of 5 s) with a Braun Labsonic 2000 microtip sonifier and centrifuged (11,000g, 10 min, 4 °C). Bradford's method was used to determine protein concentration. The samples that were loaded in sodium dodecyl sulphate-polyacrylamide gel (from 7.5 to 15% depending on the molecular weight of interest) were prepared with the same amount of protein and boiled for 5 min. The proteins were transferred to a poly(vinylidene difluoride) membrane for 20 h at 20 V. The membrane was blocked with 10% nonfat milk in Tris-buffered saline [50 mM Tris-HCl (pH 7.4), 150 mM NaCl] containing 0.1% Tween-20 (TBST) for 1 h, followed by incubation with specific antibodies against caspase-3, caspase-4, caspase-6, caspase-7, caspase-8, caspase-9, Bax, Bcl-2, Bid, DR4, DR5, TRAIL, MAPKs, β-actin and poly(ADP-ribose)polymerase overnight at 4 °C. Membranes were washed three times with TBST and incubated for 1 h with the specific secondary antibody and the antigen-antibodies complexes were visualized by enhanced chemiluminescence using the manufacturer's protocol.

5.9. Subcellular fractionation

Cells were harvested by centrifugation (500g, 10 min, 4 °C) and washed twice with cold PBS at 4 °C. The pellets were resuspended in buffer [20 mM HEPES (pH 7.5), 1 mM EDTA, 0.1 mM phenylmethylsulfonyl fluoride, 1.5 mM MgCl₂, 1 mM EGTA, 10 mM KCl, 1 mM dithiothreitol, and 5 µg/mL leupeptin, aprotinin, and pepstatin A] with 250 mM sucrose. The samples were incubated for 15 min on ice

and lysed 10 times with a 22-gauge needle. The lysates were centrifuged (1000g, 5 min, 4 °C). The supernatants were centrifuged at 105,000g for 45 min at 4 °C, and the resulting supernatant was used as the soluble cytosolic fraction and analysed by immunoblotting with specific antibodies against Smac/DIABLO and cytochrome c.

5.10. Intracellular reactive oxygen species (ROS) determination

Intracellular ROS were detected by flow cytometry using the probe 2',7'-dichlorodihydrofluorescein diacetate (H₂-DCF-DA). Flow cytometric analysis was carried out using a BD FACSVerse™ cytometer (BD Biosciences, San Jose, CA, USA) and has been described in detail elsewhere [36].

5.11. Statistical methods

Statistical differences between means were tested using (i) Student's *t*-test (two samples) or (ii) one-way analysis of variance (ANOVA) (3 or more samples) with Tukey's test used for *a posteriori* pairwise comparisons of means. A significance level of *P* < 0.05 was used.

Acknowledgements

We thank Dr. Jacqueline Bréard (INSERM U749, Faculté de Pharmacie Paris-Sud., Châtenay-Malabry, France) for supplying U-937/Bcl-2 cells.

Funding

This work was supported in part by the Spanish Ministry of Science, Innovation and Universities and the European Regional Development Fund (PGC2018-094503-B-C21).

Conflict of interest

The authors declare that there is no conflict of interest.

Appendix A. Supplementary material

Supplementary data to this article can be found online at <https://doi.org/10.1016/j.bioorg.2019.103450>.

References

- [1] R.L. Siegel, K.D. Miller, A. Jemal, Cancer statistics, 2018, *CA Cancer J. Clin.* 68 (2018) 7–30, <https://doi.org/10.3322/caac.21442>.
- [2] F. Bray, J. Ferlay, I. Soerjomataram, R.L. Siegel, L.A. Torre, A. Jemal, Global cancer statistics GLOBOCAN estimates of incidence and mortality worldwide for 36 cancers in 185 countries, *CA Cancer J. Clin.* 68 (2018) 394–424, <https://doi.org/10.3322/caac.21492>.
- [3] D.J. Newman, G.M. Cragg, Natural products as sources of new drugs from 2014, *J. Nat. Prod.* 79 (2016) 629–661, <https://doi.org/10.1021/acs.jnatprod.5b01055>.
- [4] D. Ravishanker, A.K. Rajora, F. Greco, H.M. Osborn, Flavonoids as prospective compounds for anti-cancer therapy, *Int. J. Biochem. Cell Biol.* 45 (2013) 2821–2831, <https://doi.org/10.1016/j.biocel.2013.10.004>.
- [5] D. Raffa, B. Maggio, M.V. Raimondi, F. Plescia, G. Daidone, Recent discoveries of anticancer flavonoids, *Eur. J. Med. Chem.* 142 (2017) 213–228, <https://doi.org/10.1016/j.ejmech.2017.07.034>.
- [6] S. Shalini, L. Dorstyn, S. Dawar, S. Kumar, Old, new and emerging functions of caspases, *Cell Death Differ.* 22 (2015) 526–539, <https://doi.org/10.1038/cdd.2014.216>.
- [7] E.A. Meyer, R.K. Castellano, F. Diederich, Interactions with aromatic rings in chemical and biological recognition, *Angew. Chem. Int. Ed. Engl.* 42 (2003) 1210–1250, <https://doi.org/10.1002/anie.200390319>. Erratum. In: *Angew Chem Int Ed Engl.* 42 (2003) 4120.
- [8] L.M. Salonen, M. Ellermann, F. Diederich, Aromatic rings in chemical and biological recognition: energetics and structures, *Angew. Chem. Int. Ed. Engl.* 50 (2011) 4808–4842, <https://doi.org/10.1002/anie.201007560>.
- [9] J.L. Asensio, A. Ardá, F.J. Cañada, J. Jiménez-Barbero, Carbohydrate-aromatic interactions, *Acc. Chem. Res.* 46 (2013) 946–954, <https://doi.org/10.1021/ar300024d>.


- [10] S. Makar, T. Saha, S.K. Singh, Naphthalene, a versatile platform in medicinal chemistry: sky-high perspective, *Eur. J. Med. Chem.* 161 (2019) 252–276, <https://doi.org/10.1016/j.ejmech.2018.10.018>.
- [11] P. Harris, P. Ralph, Human leukemic models of myelomonocytic development: a review of the HL-60 and U937 cell lines, *J. Leukoc. Biol.* 37 (1985) 407–422, <https://doi.org/10.1002/jlb.37.4.407>.
- [12] W. Chanput, V. Peters, H. Wichers, THP-1 and U937 cells, in: K. Verhoeckx, P. Cotter, I. López-Expósito, C. Kleiveland, T. Lea, A. Mackie, T. Requena, D. Swiatecka, H. Wichers (Eds.), *The Impact of Food Bioactives on Health: In Vitro and Ex Vivo Models*, Springer, 2015, pp. 147–159.
- [13] B.M. Muller, J. Mai, R.A. Yocum, M.J. Adler, Impact of mono- and disubstitution on the colorimetric dynamic covalent switching chalcone/flavanone scaffold, *Org. Biomol. Chem.* 12 (2014) 5108–5114, <https://doi.org/10.1039/C4OB00398E>.
- [14] A.A. Sy-Cordero, T.N. Graf, S.P. Runyon, M.C. Wani, D.J. Kroll, R. Agarwal, S.J. Brantley, M.F. Paine, S.J. Polyak, N.H. Oberlies, Enhanced bioactivity of silybin B methylation products, *Bioorg. Med. Chem.* 21 (2013) 742–747, <https://doi.org/10.1016/j.bmc.2012.11.035>.
- [15] F. Grande, O.I. Parisi, R.A. Mordocco, C. Rocca, F. Puoci, L. Scrivano, A.M. Quintieri, P. Cantafio, S. Ferla, A. Brancale, C. Saturnino, M.C. Cerra, M.S. Sinicropi, T. Angelone, Quercetin derivatives as novel antihypertensive agents: synthesis and physiological characterization, *Eur. J. Pharm. Sci.* 82 (2016) 161–170, <https://doi.org/10.1016/j.ejps.2015.11.021>.
- [16] M.K. Kim, K.S. Park, C. Lee, H.R. Park, H. Choo, Y. Chong, Enhanced stability and intracellular accumulation of quercetin by protection of the chemically or metabolically susceptible hydroxyl groups with a pivaloxymethyl (POM) promoiety, *J. Med. Chem.* 53 (2010) 8597–8607, <https://doi.org/10.1021/jm101252m>.
- [17] E. Saavedra, H. Del Rosario, I. Brouard, J. Quintana, F. Estévez, 6'-Benzyloxy-4-bromo-2'-hydroxychalcone is cytotoxic against human leukaemia cells and induces caspase-8- and reactive oxygen species-dependent apoptosis, *Chem. Biol. Interact.* 298 (2019) 137–145, <https://doi.org/10.1016/j.cbi.2018.12.010>.
- [18] J.A. Beutler, E. Hamel, A.J. Vlietinck, A. Haemers, P. Rajan, J.N. Roitman, J.H. Cardellina 2nd, M.R. Boyd, Structure-activity requirements for flavone cytotoxicity and binding to tubulin, *J. Med. Chem.* 41 (1998) 2333–2338, <https://doi.org/10.1021/jm970842h>.
- [19] F. Estévez-Sarmiento, M. Said, I. Brouard, F. León, C. García, J. Quintana, F. Estévez, 3'-Hydroxy-3,4'-dimethoxyflavone blocks tubulin polymerization and is a potent apoptotic inducer in human SK-MEL-1 melanoma cells, *Bioorg. Med. Chem.* 25 (2017) 6060–6070, <https://doi.org/10.1016/j.bmc.2017.09.043>.
- [20] S. Rubio, J. Quintana, J.L. Eiroa, J. Triana, F. Estévez, Betuletol 3-methyl ether induces G₂-M phase arrest and activates the sphingomyelin and MAPK pathways in human leukemia cells, *Mol. Carcinog.* 49 (2010) 32–43, <https://doi.org/10.1002/mc.20574>.
- [21] F. Torres, J. Quintana, F. Estévez, 5,7,3'-trihydroxy-3,4'-dimethoxyflavone-induced cell death in human leukemia cells is dependent on caspases and activates the MAPK pathway, *Mol. Carcinog.* 49 (2010) 464–475, <https://doi.org/10.1002/mc.20619>.
- [22] S. Inoue, G. Browne, G. Melino, G.M. Cohen, Ordering of caspases in cells undergoing apoptosis by the intrinsic pathway, *Cell Death Differ.* 16 (2009) 1053–1061, <https://doi.org/10.1038/cdd.2009.29>.
- [23] O. Julien, J.A. Wells, Caspases and their substrates, *Cell Death Differ.* 24 (2017) 1380–1389, <https://doi.org/10.1038/cdd.2017.44>.
- [24] D.C. Gray, S. Mahrus, J.A. Wells, Activation of specific apoptotic caspases with an engineered small-molecule-activated protease, *Cell* 142 (2010) 637–646, <https://doi.org/10.1016/j.cell.2010.07.014>.
- [25] O. Julien, M. Zhuang, A.P. Wiita, A.J. O'Donoghue, G.M. Knudsen, C.S. Craik, J.A. Wells, Quantitative MS-based enzymology of caspases reveals distinct protein substrate specificities, hierarchies, and cellular roles, *Proc. Natl. Acad. Sci. USA* 113 (2016) E2001–E2010, <https://doi.org/10.1073/pnas.1524900113>.
- [26] P. Li, D. Nijhawan, I. Budihardjo, S.M. Srinivasula, M. Ahmad, E.S. Alnemri, X. Wang, Cytochrome c and dATP-dependent formation of Apaf-1/caspase-9 complex initiates an apoptotic protease cascade, *Cell* 91 (1997) 479–489, [https://doi.org/10.1016/S0092-8674\(00\)80434-1](https://doi.org/10.1016/S0092-8674(00)80434-1).
- [27] G.S. Salvesen, C.S. Duckett, IAP proteins: blocking the road to death's door, *Nat. Rev. Mol. Cell Biol.* 3 (2002) 401–410, <https://doi.org/10.1038/nrm830>.
- [28] R.W. Birkinshaw, P.E. Czabotar, The BCL-2 family of proteins and mitochondrial outer membrane permeabilisation, *Semin. Cell Dev. Biol.* 72 (2017) 152–162, <https://doi.org/10.1016/j.semcdb.2017.04.001>.
- [29] Q. Peng, Z. Deng, H. Pan, L. Gu, O. Liu, Z. Tang, Mitogen-activated protein kinase signaling pathway in oral cancer, *Oncol. Lett.* 15 (2018) 1379–1388, <https://doi.org/10.3892/ol.2017.7491>.
- [30] Y. Sun, W.Z. Liu, T. Liu, X. Feng, N. Yang, H.F. Zhou, Signaling pathway of MAPK/ERK in cell proliferation, differentiation, migration, senescence and apoptosis, *J. Recept. Signal Transduct. Res.* 35 (2015) 600–604, <https://doi.org/10.3109/10799893.2015.1030412>.
- [31] S. Rubio, J. Quintana, J.L. Eiroa, J. Triana, F. Estévez, Betuletol 3-methyl ether induces G₂-M phase arrest and activates the sphingomyelin and MAPK pathways in human leukemia cells, *Mol. Carcinog.* 49 (2010) 32–43, <https://doi.org/10.1002/mc.20574>.
- [32] F. Torres, J. Quintana, J.G. Díaz, A.J. Carmona, F. Estévez, Trifolin acetate-induced cell death in human leukemia cells is dependent on caspase-6 and activates the MAPK pathway, *Apoptosis* 13 (2008) 716–728, <https://doi.org/10.1007/s10495-008-0202-0>.
- [33] D. Wang, Q. Sun, J. Wu, W. Wang, G. Yao, T. Li, X. Li, L. Li, Y. Zhang, W. Cui, S. Song, A new Prenylated Flavonoid induces G₀/G₁ arrest and apoptosis through p38/JNK MAPK pathways in Human Hepatocellular Carcinoma cells, *Sci. Rep.* 7 (2017) 5736, <https://doi.org/10.1038/s41598-017-05955-0>.
- [34] T. Mosmann, Rapid colorimetric assay for cellular growth and survival: application to proliferation and cytotoxicity assays, *J. Immunol. Methods* 65 (1983) 55–63, [https://doi.org/10.1016/0022-1759\(83\)90303-4](https://doi.org/10.1016/0022-1759(83)90303-4).
- [35] S. Estévez, M.T. Marrero, J. Quintana, F. Estévez, Eupatorin-induced cell death in human leukemia cells is dependent on caspases and activates the mitogen-activated protein kinase pathway, *PLoS One* 9 (2014) e112536, <https://doi.org/10.1371/journal.pone.0112536>.
- [36] F. Estévez-Sarmiento, E. Hernández, I. Brouard, F. León, C. García, J. Quintana, F. Estévez, 3'-Hydroxy-3,4'-dimethoxyflavone-induced cell death in human leukaemia cells is dependent on caspases and reactive oxygen species and attenuated by the inhibition of JNK/SAPK, *Chem. Biol. Interact.* 288 (2018) 1–11, <https://doi.org/10.1016/j.cbi.2018.04.006>.

3. Cytotoxicity of the sesquiterpene lactone spiciformin and its acetyl derivative against the human leukemia cell lines U-937 and HL-60



Article

Cytotoxicity of the Sesquiterpene Lactone Spiciformin and Its Acetyl Derivative against the Human Leukemia Cell Lines U-937 and HL-60

Ester Saavedra ¹, Francisco Estévez-Sarmiento ¹, Mercedes Said ¹, José Luis Eiroa ², Sara Rubio ¹, José Quintana ¹  and Francisco Estévez ^{1,*}

¹ Departamento de Bioquímica y Biología Molecular, Instituto Universitario de Investigaciones Biomédicas y Sanitarias (IUIBS), Universidad de Las Palmas de Gran Canaria, 35016 Las Palmas de Gran Canaria, Spain; saavedradiazestergloria@gmail.com (E.S.); festevez1985@gmail.com (F.E.-S.); mercedessaid@gmail.com (M.S.); sara.rubio@ulpgc.es (S.R.); jose.quintana@ulpgc.es (J.Q.)

² Departamento de Química, Instituto Universitario de Investigaciones Biomédicas y Sanitarias (IUIBS), Universidad de Las Palmas de Gran Canaria, 35017 Las Palmas de Gran Canaria, Spain; joseluis.eiroa@ulpgc.es

* Correspondence: francisco.estevez@ulpgc.es; Tel.: +34-928-451443

Received: 27 March 2020; Accepted: 14 April 2020; Published: 16 April 2020



Abstract: Spiciformin (**1**) is a sesquiterpene lactone with a germacrane skeleton that is found in two *Tanacetum* species endemic to the Canary Islands. In this study, the cytotoxicities of **1** and its acetyl derivative (**2**) were evaluated against human tumor cells. These sesquiterpene lactones were cytotoxic against human acute myeloid leukemia (U-937 and HL-60) cells, even in cells over-expressing the pro-survival protein Bcl-2, but melanoma (SK-MEL-1) and human mononuclear cells isolated from blood of healthy donors were more resistant. Both compounds are apoptotic inducers in human leukemia U-937 cells. Cell death was mediated by the processing and activation of initiator and effector caspases and the cleavage of poly(ADP-ribose) polymerase, and it was blocked by a broad-spectrum caspase inhibitor and (in the case of sesquiterpene lactone **2**) by the selective caspase-3/7, -8, and -9 inhibitors. In addition, certainly in the case of compound **2**, this was found to be associated with a decrease in mitochondrial membrane potential, downregulation of the anti-apoptotic protein Bcl-2, activation of the mitogen-activated protein kinases signaling pathway, and generation of reactive oxygen species. It will, therefore, be relevant to continue characterization of this class of compounds.

Keywords: apoptosis; cytotoxicity; caspase; poly(ADP-ribose) polymerase; sesquiterpene lactone

1. Introduction

The discovery of new anticancer agents is of great interest since the currently available drugs against cancer exhibit several critical problems, including serious adverse effects, insufficient effectiveness, and the development of multidrug resistance [1]. Acute myeloid leukemia is a lethal form of hematologic malignancy and is the most usual type of acute leukemia in adults and accounts for 15%–20% of all tumors diagnosed in children aged 1 to 14 years [2]. Despite recent advances to treat and cure acute myeloid leukemia, mortality rates are still very high [3].

Many small molecules approved as anticancer drugs are based on natural products [4]. Sesquiterpene lactones are naturally occurring compounds formed from the condensation of three isoprene units and contain one or more lactone rings. A large number of sesquiterpene lactones exhibit cancer cell cytotoxicity, which depends on the presence of the α -methylene- γ -lactone moiety. This functional group acts as an alkylating agent in a Michael-type reaction with biomolecules

containing nucleophilic groups [5,6]. Sesquiterpene lactones target multiple signal transduction pathways involved in survival and cell death. It has been shown that sesquiterpene lactones inhibit nuclear factor κ B, phosphatidylinositol-3-kinase, Janus kinase/signal transducer, and activator of transcription and mitogen-activated protein kinase signaling, as well as epigenetic factors such as DNA methyltransferase 1 and histone deacetylase 1, together with activation of c-Jun N-terminal kinases and reactive oxygen species generation (reviewed in Reference [6]). The effect of sesquiterpene lactones on multiple targets triggers the blocking of cancer development and progression and might sensitize cancer cells to conventional chemotherapy. Interest in this kind of natural product has emerged mainly because they are selective toward tumor and cancer stem cells [7].

Several sesquiterpene lactones have been evaluated in cancer clinical trials [8]. Specific sesquiterpene lactones are apoptotic inducers in different types of cancer cells [9]. This type of regulated cell death is characterized by cytoplasmic shrinkage, plasma membrane blebbing, phosphatidylserine exposure at the cell surface, loss of mitochondrial membrane potential, chromatin condensation, nuclear fragmentation, and formation of apoptotic vesicles [10,11]. It can occur with or without the activation of a class of aspartate-specific cysteine proteases known as caspases [12–14]. Two main apoptotic pathways have been described, namely the extrinsic and intrinsic pathways [15]. The intrinsic or mitochondrial pathway is controlled by pro-apoptotic and anti-apoptotic proteins of the B-cell lymphoma 2 (Bcl-2) family and involves mitochondrial outer membrane permeabilization, which promotes the cytosolic release of apoptogenic factors including cytochrome *c* [16]. Cytosolic cytochrome *c* is involved in the assembly of apoptosome and pro-caspase-9 stimulation, which activates the executioner caspase-3 and -7. The death receptor or extrinsic pathway is mediated by plasma membrane receptors and induces activation of caspase-8, which mainly activates caspase-3 [17,18]. In addition, most of the anticancer drugs trigger apoptosis induction in malignant cells and reactivation of this pathway is critical for more effective treatments [19].

Two *Tanacetum* species endemic of the Canary Islands, *Tanacetum ptarmiciflorum* and *T. ferulaceum* var. *latipinnum* contain spiciformin (1) (Figure 1), a sesquiterpene lactone with a germacrane skeleton [20]. Its potential antiproliferative activity against human cancer cells has not been investigated to date. The justification for studying the cytotoxic effects of spiciformin against human cancer cells is two-fold: (1) it has the same skeleton as parthenolide, a sesquiterpene lactone with potent anti-cancer and anti-inflammatory activity, and (2) its chemical structure allows the addition of new substituents to improve its cytotoxicity. The present study explores the potential cytotoxicity of spiciformin (1) and its acetyl derivative (2) against human tumor cells and their underlying mechanisms of cell death, including the disruption of mitochondrial membrane potential, the activation of the caspase cascade and the mitogen-activated protein kinase pathway, the changes in the Bcl-2 family proteins expression, and the generation of reactive oxygen species.

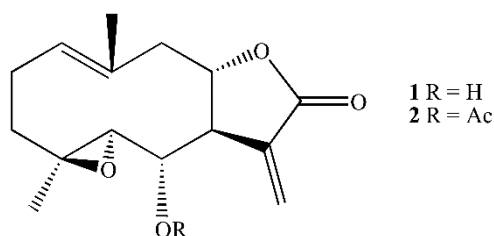


Figure 1. Structure of spiciformin (1) and its acetate (2).

2. Results and Discussion

2.1. Spiciformin Acetate (2) is More Cytotoxic Than Spiciformin (1) Against Human Tumor Cells

In the present study, the effects of the naturally occurring spiciformin (1), an epoxylated germacranolide, and its acetyl derivative (2) on the growth of human acute myeloid leukemia (U-937 and HL-60) and melanoma (SK-MEL-1) cells were evaluated. Spiciformin acetate (2) was

synthesized and evaluated for cytotoxicity against human tumor cells since its higher hydrophobicity can facilitate diffusion through the plasma membrane and, therefore, enhance cytotoxicity in vitro. No studies have yet addressed the cytotoxicity of these germacranolides against human acute myeloid leukemia and melanoma cell lines.

To evaluate the potential antiproliferative effect of both sesquiterpene lactones, cells were treated with increasing concentrations and viability was determined by the 3-(4,5-dimethyl-2-thiazolyl)-2,5-diphenyl-2H-tetrazolium bromide (MTT) assay. These compounds were found to inhibit the cell viability in a concentration-dependent manner and displayed cytotoxic effects against the human leukemia cell lines (Figure 2a). The IC_{50} (concentrations inducing a 50% inhibition of cell growth) values for spiciformin (**1**) were similar in both leukemia cells (IC_{50} values of ca. 5 μ M), while in SK-MEL-1 the IC_{50} value was approximately four-fold higher (Table 1). The human tumor U-937 cells were more sensitive than SK-MEL-1 melanoma cells to the cytotoxic effects of spiciformin (**1**). The IC_{50} values for spiciformin acetate (**2**) were lower than spiciformin (**1**) in all cell lines assayed, except in HL-60 cells. In these experiments, etoposide, which is an agent commonly used for the treatment of acute leukemia, was included as a positive control. The IC_{50} values of etoposide were 1.2 ± 0.4 μ M, 0.4 ± 0.1 μ M, and 10 ± 4 μ M, for U-937, HL-60, and SK-MEL-1, respectively.

Table 1. Effects of sesquiterpene lactones on cell viability of human tumor cell lines.

	IC_{50} (μ M)			
	U-937	HL-60	SK-MEL-1	U-937/Bcl-2
Spiciformin (1)	5.0 ± 0.8	4.7 ± 1.3	22.5 ± 4.1	5.5 ± 1.4
Spiciformin acetate (2)	1.2 ± 0.5	3.8 ± 1.5	11.5 ± 4.0	1.6 ± 1.0

U-937, U-937/Bcl-2, HL-60: acute myeloid leukemia; SK-MEL-1: melanoma. The IC_{50} values were calculated using the methodology described in the Materials and Methods section from cells treated for 72 h. The data shown represent the mean \pm SEM (standard error of the mean) of 3–5 independent experiments with three determinations each.

Over-expression of the pro-survival protein Bcl-2 did not suppress the cytotoxicity induced by sesquiterpene lactones **1** and **2** since the IC_{50} values were similar for U-937 and U-937/Bcl-2 cells (Figure 2b, Table 1). This result is very interesting since Bcl-2 protein confers resistance to apoptosis by antagonizing the mitochondrial outer membrane permeability and exerts anti-apoptotic functions through the binding of pro-apoptotic members of the Bcl-2 family [21].

Treatment with both sesquiterpene lactones induced profound morphological changes as well as a marked reduction in the number of cells. Representative images obtained with an inverted phase-contrast microscope of U-937 cells treated with increasing concentrations of spiciformin (**1**) and spiciformin acetate (**2**) for 24 h are shown in Figure 2c. It was also investigated whether both sesquiterpene lactones were likewise cytotoxic for human mononuclear cells isolated from peripheral blood of healthy donors (PBMC). As shown in Figure 2d, a pronounced reduction was detected in the proliferation of U-937 cells while quiescent PBMC showed higher resistance than leukemia cells, even at 30 μ M sesquiterpene lactones. The IC_{50} values determined at 24 h for **1** and **2** were 30.4 ± 3.6 μ M and 41.0 ± 3.8 μ M against PBMC, while the IC_{50} values against U-937 cells were 10 ± 4.0 μ M and 12.2 ± 2.6 μ M, respectively. Interestingly, the IC_{50} values in U-937 cells for both compounds were similar at 24 h. These results suggest that both sesquiterpene lactones affected viability of peripheral blood mononuclear cells (PBMC) to a lesser extent than U-937 cells. Control experiments with the fibroblast-like Vero cell line showed no appreciable toxicity even at 100 μ M spiciformin or spiciformin acetate for 24 h. As a positive control, doxorubicin (3 μ M) was included in the experiment and there was a 50% decrease in the viability of these cells (Figure 2e). Future studies addressing the selectivity and efficacy of in vivo concentrations of these compounds are necessary to determine their potential for human health.

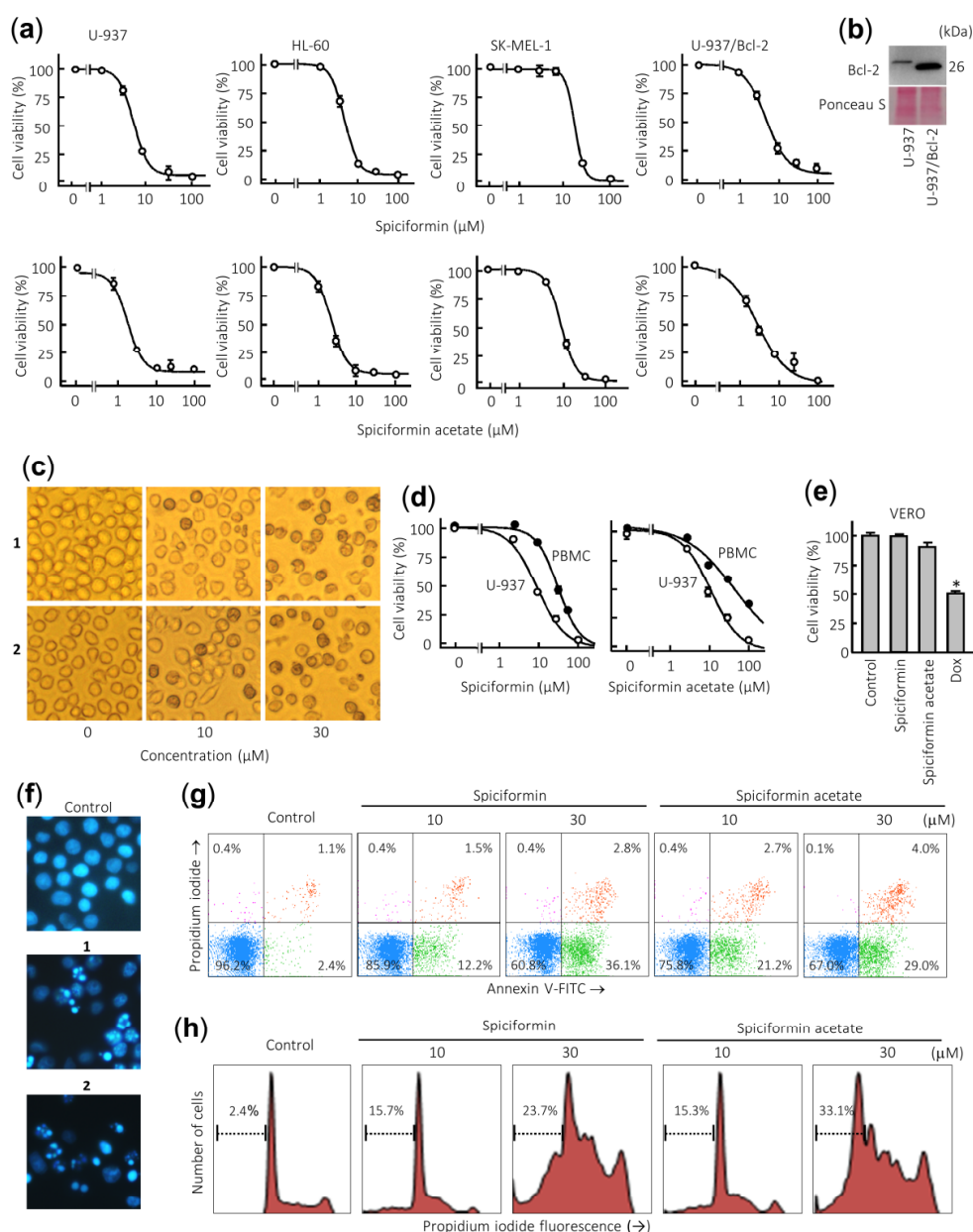


Figure 2. Effects of sesquiterpene lactones **1** and **2** on human tumor cells. (a) Dose–response study on human cancer cell lines. Cells were cultured in the presence of increasing concentrations of spiciformin or spiciformin acetate for 72 h, and then the cell viability was determined by the 3-(4,5-dimethyl-2-thiazolyl)-2,5-diphenyl-2H-tetrazolium bromide (MTT) assay. (b) Immunoblot analysis of Bcl-2 protein in U-937 and U-937/Bcl-2. The membrane was stained with Ponceau S to control equal protein loading. (c) U-937 cells were incubated with the indicated concentrations of the specified compounds for 24 h and visualized with an inverted phase-contrast microscope. Original magnification 40×. (d) Differential effects of sesquiterpene lactones on viability of normal mononuclear cells from peripheral blood (PBMCs) versus U-937 cells. Quiescent PBMC from healthy human origin and human leukemia cells were treated with increasing concentrations of **1** and **2** for 24 h. (e) Effect of 100 μM sesquiterpene lactones on Vero cells viability determined by the MTT assay after treatment for 24 h. Doxorubicin (Dox, 3 μM) was included as a positive control. The results are means ± SE of three independent experiments performed in triplicate (* $p < 0.05$, significantly different from untreated control). (f) Morphological analysis after staining with Hoechst 33,258 to assess nuclear chromatin fragmentation and condensation (i.e., apoptosis) after treatment with 30 μM sesquiterpene lactones **1** and **2**. Cells were observed under a fluorescence microscope and representative fields were photographed

with a digital camera. Original magnification 63×. (g) Cells were incubated with the specified concentrations of germacranolides **1** and **2** for 24 h, stained with annexin V-FITC and propidium iodide and analyzed by flow cytometry. Shown data are representative out of three independent experiments with similar results. (h) Cells were incubated as in (e), fixed, and analyzed by flow cytometry. Representative histograms of flow cytometry after propidium iodide labeling and the percentages of hypodiploid cells (apoptotic cells) are shown.

2.2. *Spiciformin (1) and Spiciformin Acetate (2) Induce Apoptosis in Human Acute Myeloid Leukemia Cells*

To elucidate whether growth inhibition mediated by sesquiterpene lactones was caused by apoptosis, fluorescence microscopy using Hoechst 33258 staining and flow cytometry experiments were performed in U-937 cells. To this end, cells were treated with 30 µM of compounds for 24 h, and morphological aspects were visualized by fluorescent microscopy. As shown in Figure 2f, control cells showed round nuclei with uncondensed and dispersed chromatin, while treated cells with sesquiterpene lactones showed fragmented and condensed nuclei. The evaluation of the number of annexin V-fluoresceine isothiocyanate (FITC) positive cells by flow cytometry revealed that the percentage of apoptosis increased about five and nine times in cells treated with 10 µM sesquiterpene lactones **1** and **2** for 24 h, respectively (Figure 2g). In accordance with the annexin V-FITC studies, the percentage of hypodiploid cells (i.e., sub-G₁ fraction) increased about 10-fold and 14-fold in cells treated with compounds **1** and **2**, respectively, compared with control cells after 24 h exposure at a concentration of 30 µM. Representative histograms obtained after treatment with both sesquiterpene lactones and subjected to flow cytometric analysis of nuclei stained with propidium iodide are shown (Figure 2h). These results indicate that sesquiterpene lactones **1** and **2** induce apoptosis in human U-937 cells.

2.3. *Spiciformin (1) and Spiciformin Acetate (2) Induce Cell Death by a Caspase-Dependent Pathway*

To determine whether compounds **1** and **2** activate the caspase cascade, U-937 cells were incubated in the absence or presence of both sesquiterpene lactones and poly(ADP-ribose) polymerase (PARP), as well as the initiator (caspase-8 and -9) and executioner (caspase-3 and -7) caspases were determined by immunoblotting using specific antibodies. Dose–response and time–course experiments revealed that both compounds induce PARP cleavage and the processing of pro-caspases-3, -7, and -9 (Figure 3a,b). The processing of pro-caspase-8 (detected as a reduction of this zymogen) was evident even with the lower concentration of compound **2** (10 µM) and PARP cleavage was detected at concentrations as low as 10 µM of each sesquiterpene lactone (Figure 3a). Caspase-4, which is involved in the endoplasmic reticulum stress, was also cleaved in U-937 cells treated with **1** and **2**. In these experiments, Ponceau S staining prior to antibody detection was used as an alternative loading control.

Enzymatic assays were also performed to confirm caspase activation. To this end, U-937 cells were incubated in the presence of 30 µM sesquiterpene lactones **1** and **2** for 24 h and cell lysates were analyzed for cleavage of the tetrapeptide substrates DEVD-pNA, IETD-pNA, and LEHD-pNA as specific substrates of caspase-3/7, -8 and -9, respectively. The results revealed that both sesquiterpene lactones stimulate the activity of the initiator caspases, caspase-8 and -9, as well as the effector caspases-3/7. In addition, compound **2** was a more potent caspase activator than compound **1** (Figure 3c). To determine whether caspases are involved in sesquiterpene lactones-induced cell death, it was investigated the effects of the pancaspase inhibitor Z-VAD-FMK, as well as the following selective caspase inhibitors: the caspase-3/7 inhibitor Z-DEVD-FMK, the caspase-4 inhibitor Ac-LEVD-CHO, the caspase-8 inhibitor Z-IETD-FMK, and the caspase-9 inhibitor Z-LEHD-FMK. Pretreatment of cells with Z-VAD-FMK completely blocked the increase in the percentage of sub-G₁ cells (Figure 3d) as well as the increase in the percentage of annexin V-FITC positive cells (Figure 3e) induced by compounds **1** and **2**. In addition, the selective caspase inhibitors Z-DEVD-FMK, Z-IETD-FMK, and Z-LEHD-FMK significantly reduced the percentage of sub-G₁ cells and almost completely stopped annexin V-FITC

positive cells from being induced by compound **2** (Figure 3d,e). Nonetheless, the pretreatment of cells with the selective caspase-4 inhibitor Ac-LEVD-CHO did not reduce the percentage of annexin V-FITC positive cells induced by compound **2** (results not shown).

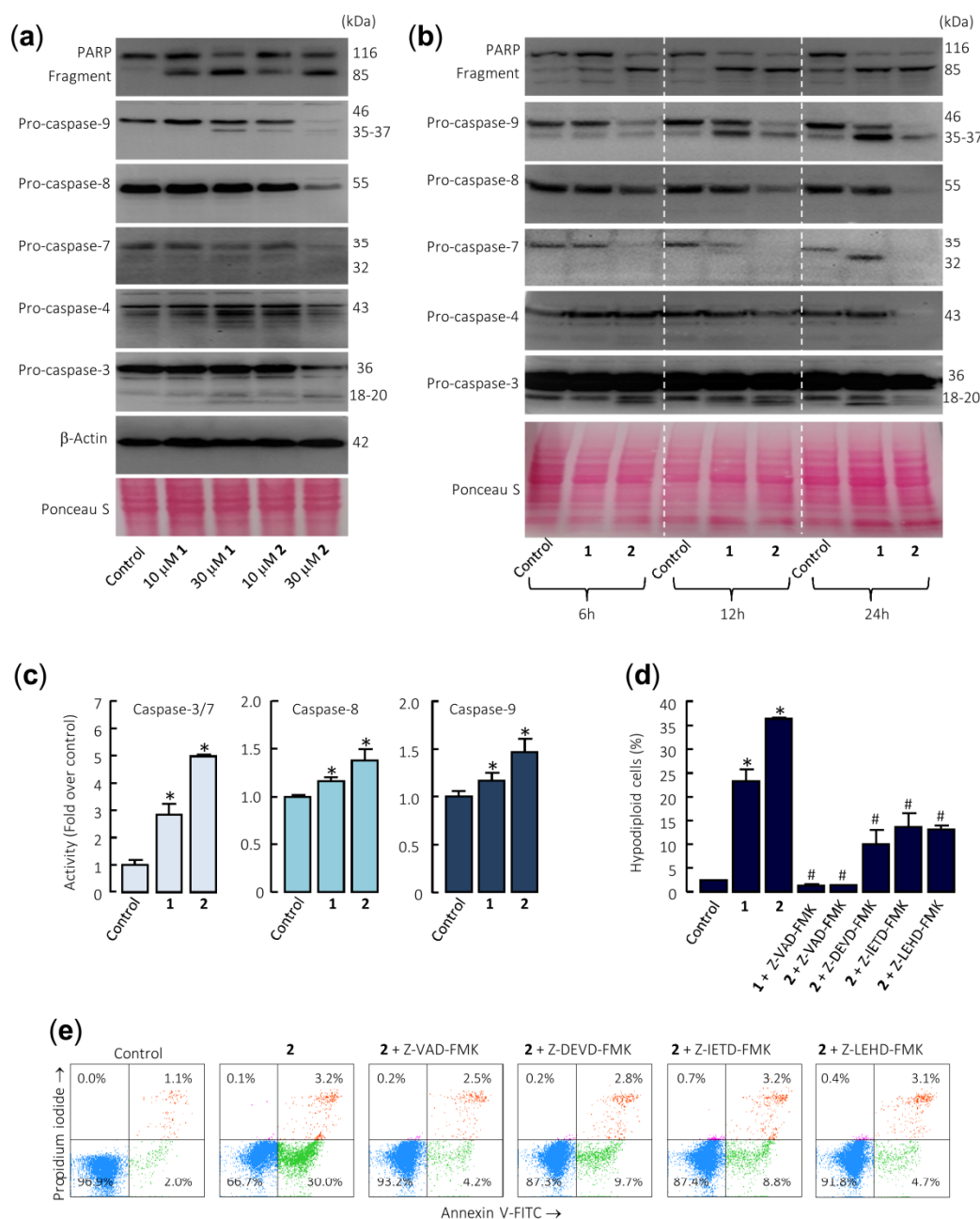


Figure 3. Caspase cascade is involved in apoptosis induction by sesquiterpene lactones in U-937 cells. (a) The cells were cultured for 24 h in control conditions or in the presence of the indicated concentrations of the specified compounds, and the cell lysates were analyzed by Western blots for the cleavage of poly(ADP-ribose) polymerase (PARP) and pro-caspases-3, -4, -7, -8, and -9. β -Actin was used as a loading control. Total protein loading was also controlled by Ponceau S staining (a representative stained membrane is shown). (b) Representative Western blots show the time-dependent PARP cleavage and pro-caspases processing in response to sesquiterpene lactones **1** and **2**. Cells were incubated with 30 μ M of compounds for the indicated time points, and protein extracts were prepared and analyzed by immunoblotting using specific antibodies. The membrane was stained with Ponceau S to control equal protein loading. (c) Cells were cultured in control conditions or in the presence of 30 μ M sesquiterpene lactones for 24 h and lysates were assayed for caspase-3/7, -8, and -9 activities. Results are expressed as

fold increase in caspase activity compared with control. Values represent means \pm SE of three independent experiments, each performed in triplicate (* $p < 0.05$, significantly different from untreated control). (d) Effects of caspase inhibitors on the percentage of hypodiploid cells. The cells were pretreated in the absence or presence of Z-VAD-FMK (100 μ M) or the selective caspase inhibitors Z-DEVD-FMK (50 μ M), Z-IETD-FMK (50 μ M), or Z-LEHD-FMK (50 μ M) for 1 h before the addition of sesquiterpene lactones (30 μ M). The percentages of hypodiploid cells were determined by flow cytometry. The data represent means \pm SE of two independent experiments with three determinations each (* $p < 0.05$, significantly different from untreated control, # $p < 0.05$, significantly different from sesquiterpene lactone treatment alone). (e) Cells were pretreated with the indicated caspase inhibitors and then with 30 μ M compound **2**, harvested, stained with annexin V-FITC and propidium iodide, and analyzed by flow cytometry.

Taken together, these results demonstrate that both sesquiterpene lactones induce apoptosis by a mechanism dependent on caspase since cell death was completely inhibited by the broad-spectrum caspase inhibitor Z-VAD-FMK. In addition, the selective caspase inhibitors for caspase-3 and -7, -8, and -9 were effective at blocking the increase in the percentage of annexin V positive cells and the increase in the percentage of hypodiploid cells induced by these sesquiterpene lactones. This result suggests that the mechanism of cytotoxicity is dependent on caspase-8 and caspase-9 activation. Although pro-caspase-4 was also processed by these sesquiterpene lactones, the selective caspase-4 inhibitor did not block cell death, suggesting a minor role of the endoplasmic reticulum stress signaling pathway in the mechanism of cell death.

The mechanism of cytotoxicity exhibited by spiciformin (**1**) and spiciformin acetate (**2**) is different from the previously described sesquiterpene lactones depending on the cell types. For example, parthenolide, a sesquiterpene lactone isolated from the plant *Tanacetum parthenium*, induces cell death that is not dependent on caspases in human osteosarcoma MG63 and melanoma SK-MEL-28, because cell death was not blocked by the pan-caspase inhibitor Z-VAD-FMK [22]. Parthenolide cytotoxicity has also been described to be partly caspase-dependent, as the broad-spectrum caspase inhibitor Z-VAD-FMK could partially protect multiple myeloma cells [23].

Since the intrinsic pathway of apoptosis involves release of mitochondrial proteins such as cytochrome *c* into the cytosol, it was explored whether this crucial protein is involved in the cell death induced by both sesquiterpene lactones. Dose–response experiments revealed an increase in cytochrome *c* in the cytosol after 24 h of treatment with 10 μ M of compound **2** (Figure 4a). This was accompanied by a decrease in cytochrome *c* in the mitochondria-enriched fraction. However, results at earlier time points (6 h or 12 h; Figure 4b) remain largely elusive for both compounds. Control determinations using anti-cytochrome *c* oxidase (COX IV) antibody revealed that the supernatants of the cytosolic fraction were free of mitochondrial contamination. Therefore, sesquiterpene lactones have reasonably been shown to induce late release of cytochrome *c* as well as activation of multiple caspases, including caspase-3, -4, -7, -8, and -9, emphasizing that both the extrinsic and the intrinsic pathways play a role in the observed cell death. In addition, there were no changes in Bax levels (whole cell lysates) after treatment with both sesquiterpene lactones (Figure 4a), but there was a decrease in Bax levels in the cytosolic fraction after treatment with 30 μ M sesquiterpene lactone **2** for 24 h. This was associated with the increase of Bax in mitochondria-enriched fraction. This Bcl-2 family protein is characterized by its ability to form pores across the outer mitochondrial membrane [16]. An interesting result of these experiments was that both sesquiterpene lactones downregulate the Bcl-2 levels (Figure 4a) and this could be the mechanism by which these germacranolides block the protection conferred by Bcl-2. This anti-apoptotic protein plays a crucial role in apoptosis induction by antagonizing the mitochondrial outer membrane permeability. In addition, the inhibition of Bcl-2 in acute myeloid leukemia may overcome chemoresistance without affecting normal hematopoietic stem cells.

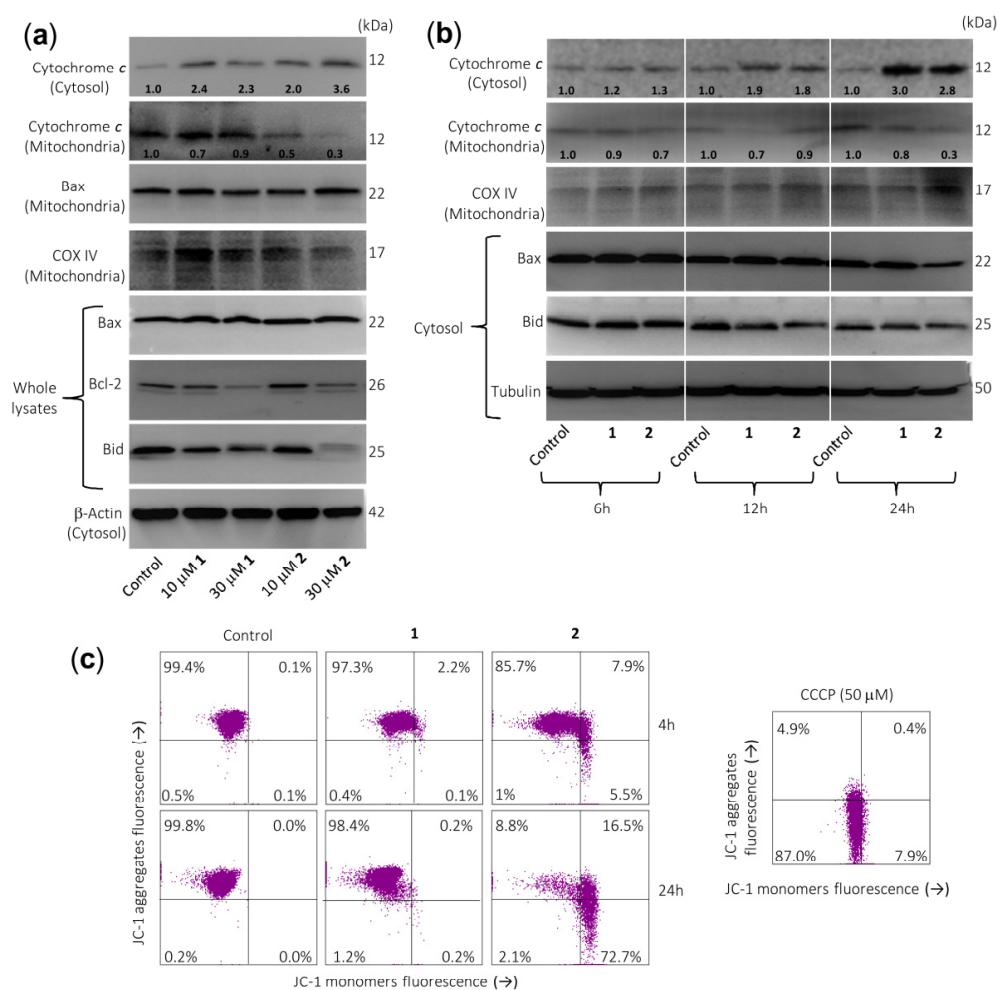


Figure 4. Sesquiterpene lactones induce the release of cytochrome *c* and changes on Bcl-2 family members' expression in U-937 cells. **(a)** Cells were cultured in control conditions or in the presence of the indicated concentrations of sesquiterpene lactones for 24 h and cytosolic and mitochondrial extracts were analyzed by immunoblotting to detect mitochondrial cytochrome *c* release and Bcl-2 family proteins, except for Bcl-2 and Bax, which were analyzed in whole extracts. Bax was also analyzed in the mitochondrial fraction. β -Actin and COX IV (cytochrome *c* oxidase) were used as loading controls in cytosol and mitochondria, respectively. **(b)** Cells were incubated in control conditions or in the presence of 30 μ M compounds **1** or **2** for the indicated times and cytosolic or mitochondrial fractions were prepared and analyzed by immunoblotting using specific antibodies described in the Material and Methods section. Tubulin and COX IV (cytochrome *c* oxidase) were used as loading controls in cytosol and mitochondria, respectively. The cytosolic and mitochondria-enriched fractions were prepared and Western blot analyses were performed as described in the Materials and Methods. Numbers below each panel of cytochrome *c* indicate fold differences after normalization to the corresponding loading control (β -actin, tubulin, or COX IV). **(c)** Sesquiterpene lactone **2** reduces the mitochondrial membrane potential ($\Delta\Psi$ m). Cells were incubated in control conditions or in the presence of 30 μ M compounds **1** or **2** for 4 h or 24 h, and $\Delta\Psi$ m were analyzed by flow cytometry using the fluorescent probe JC-1. The results are representative of three separate experiments. Carbonyl cyanide *m*-chlorophenylhydrazone (CCCP, 50 μ M) was used as a positive control.

Activation of caspase-8 may result in the proteolytic cleavage of Bid, a Bcl-2 family protein, which translocates to mitochondria to release cytochrome *c* [24]. A significant decrease in full-length Bid after treatment was observed for both sesquiterpene lactones, in accordance with the processing and activation of caspase-8.

To determine whether cell death was associated with significant changes in mitochondrial membrane potential ($\Delta\Psi_m$), U-937 cells were treated with these compounds for 4 h or 24 h and analyzed by flow cytometry after staining with JC-1. The results indicated an important loss of $\Delta\Psi_m$ at 4 h of treatment with compound **2** (Figure 4c), suggesting that the alteration of $\Delta\Psi_m$ contributed to apoptosis induced by this sesquiterpene lactone. In these experiments, the protonophore carbonyl cyanide *m*-chlorophenylhydrazone (CCCP) was used as a positive control.

2.4. Spiciformin (**1**) and Spiciformin Acetate (**2**) Activate Mitogen-Activated Protein Kinases (MAPKs) and Induce Reactive Oxygen Species (ROS) Generation

The effects of sesquiterpene lactones **1** and **2** on the activation of the mitogen-activated protein kinases (MAPKs) were investigated because these enzymes play a crucial role in survival and cell death. To this end, U-937 cells were treated for different time periods and phosphorylation of the three major protein kinases of this signal transduction pathway were determined by Western blot. In an attempt to identify the primary targets and early mechanism of action of sesquiterpene lactones, we interrogated the MAPK pathway activation by using high concentrations of the drugs ($>$ antiproliferative IC_{50} values). The results showed that sesquiterpene lactones induce fast phosphorylation (0.5 h) of JNK/SAPK (c-Jun *N*-terminal kinases/stress-activated protein kinases) and $p38^{MAPK}$ (p38 MAPKs) and the activation of ERK (extracellular signal-regulated kinases) 1/2 took place after 4–6 h under identical experimental conditions (Figure 5a). These results indicate that both sesquiterpene lactones induce activation of the three main mitogen-activated protein kinases following different kinetics. Fast activation of JNK/SAPK and $p38^{MAPK}$ has been reported to trigger cell death in response to several cellular stressors including oxidative stress [25,26].

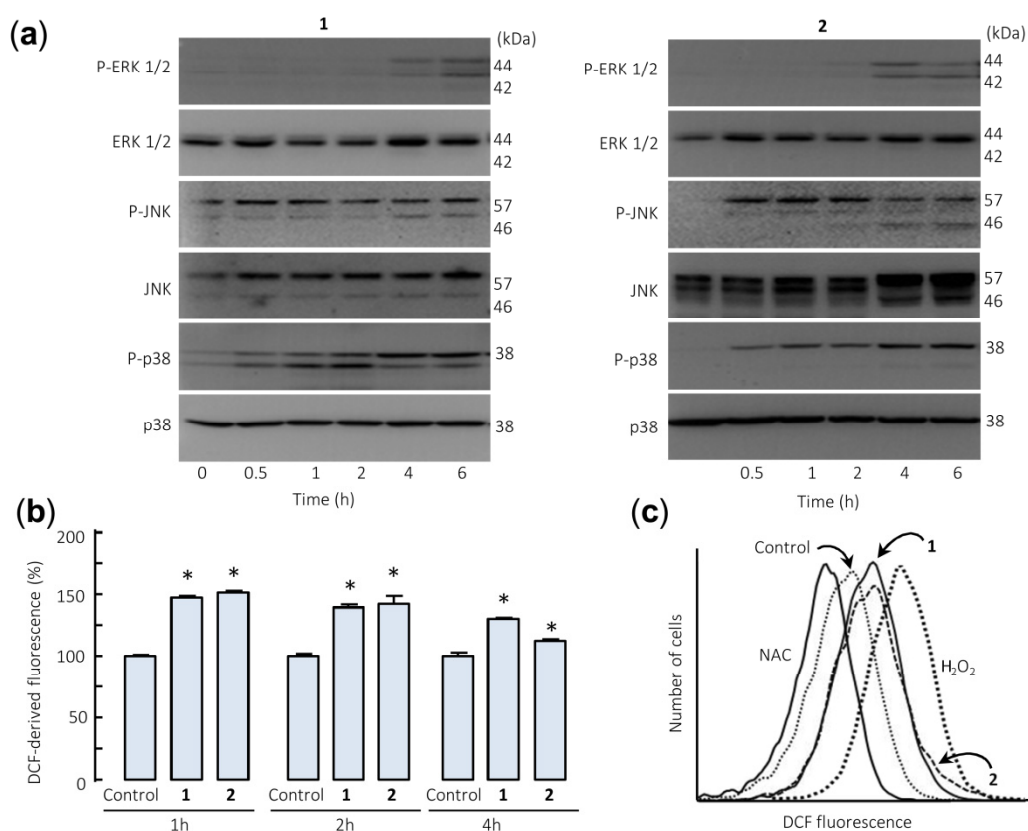


Figure 5. Sesquiterpene lactones induce phosphorylation of mitogen-activated protein kinases (MAPKs) and reactive oxygen species generation in U-937 cells. **(a)** Representative immunoblots show the kinetics of phosphorylation of MAPKs by the sesquiterpene lactones. Cells were incubated with the specified compound (30 μ M) for the indicated times and protein extracts were prepared and analyzed

by immunoblotting with specific antibodies. Blots were subsequently stripped and reprobed for the expression of total MAPKs, as indicated, to ensure equivalent loading and transfer of protein. (b) Cells were treated with compounds **1** or **2** (30 μ M) for the indicated times (b) or for 1 h (c) and the fluorescence obtained by the oxidation of 2',7'-dichlorodihydrofluorescein diacetate (H₂-DCF-DA) was determined by flow cytometry. The data in (b) represent means \pm SE of three independent experiments, each performed in triplicate (* $p < 0.05$, significantly different from untreated control). The free radical scavenger *N*-acetyl-L-cysteine (NAC, 5 mM) and H₂O₂ (200 μ M) were used as negative and positive controls of reactive oxygen species, respectively.

The involvement of reactive oxygen species (ROS) in the apoptosis induced by germacranolides **1** and **2** was investigated because they are considered important mediators and are generated by many apoptosis-inducing agents. To this end, U-937 cells treated with both sesquiterpene lactones were stained with 2',7'-dichlorodihydrofluorescein diacetate (H₂-DCF-DA) and analyzed by flow cytometry. The results revealed a fast increase (1 h) in ROS levels in sesquiterpene lactones-treated cells (Figure 5b,c). In these experiments, the antioxidant *N*-acetyl-L-cysteine (NAC, 5 mM) and hydrogen peroxide (200 μ M) were used as negative and positive controls.

3. Materials and Methods

3.1. Sesquiterpene Lactones Evaluated

The extraction and isolation of spiciformin (**1**) from the aerial parts of *Tanacetum ptarmiciflorum* and *Tanacetum ferulaceum* var. *latipinnum* was performed as previously described [20]. The acetyl derivative of spiciformin (**2**) was obtained by treatment with acetic anhydride and pyridine and purified by column chromatography over silica gel using *n*-hexane-ethyl acetate as eluent. Known compounds spiciformin and spiciformin acetate were identified by HR-MS (high resolution mass spectrometry) as well as ¹H- and ¹³C-NMR spectrometry. The previously unreported ¹³C-NMR data of spiciformin acetate were obtained on a Bruker model AMX-500 spectrometer with standard pulse sequences operating at 126 MHz. ¹³C-NMR (126 MHz, CDCl₃) δ = 127.8 (C-1), 23.5 (C-2), 35.2 (C-3), 62.3 (C-4), 55.6 (C-5), 75.6 (C-6), 57.3 (C-7), 76.3 (C-8), 34.8 (C-9), 127.5 (C-10), 134.3 (C-11), 124.3 (C-12), 167.3 (C-13), 15.9 (C-14), 16.5 (C-15), 173.1 (CH₃-C=O), 22.4 (CH₃-C=O).

3.2. Cell Culture and Cytotoxicity Assays

The U-937 (ACC 5) and HL-60 (ACC 3) human acute myeloid leukemia and SK-MEL-1 (ACC 303) human melanoma cells were obtained from the German Collection of Microorganisms and Cell Cultures (Braunschweig, Germany) and cultured in RPMI-1640 medium containing 2 mM L-glutamine supplemented with 10% heat-inactivated fetal bovine serum and 100 μ g/mL streptomycin and 100 U/mL penicillin in 5% CO₂ at 37 °C [27,28]. The U-937 cell line overexpressing human Bcl-2 (kindly provided by Dr. Jacqueline Bréard, INSERM U749, Faculté de Pharmacie Paris-Sud., Châtenay-Malabry, France) was cultured as described [28]. The functioning of U-937/Bcl-2 cells was checked with the cytotoxic agent 1- β -D-arabino furanosylcytosine (1 μ M, 24 h) as previously described [29]. Mononuclear cells from peripheral blood were isolated from heparin-anticoagulated blood of healthy donors by centrifugation using a Ficoll-Paque Plus density gradient (GE Healthcare Bio-Sciences AB, Uppsala, Sweden). All donors gave informed consent (CEIC-CHUIMI-2015/780, 13 August 2015. Ethics committee of clinical research of the C.H.U. Insular-Materno Infantil of Gran Canaria). The Vero cell line (ATCC, CCL81) was cultured in Dulbecco's modified Eagle's medium containing 10% (v/v) fetal bovine serum, 2 mM L-glutamine, 100 U/mL penicillin, and 100 μ g/mL streptomycin.

The cytotoxicity of sesquiterpene lactones on human tumor, human mononuclear cells, and Vero cells was determined by colorimetric 3-(4,5-dimethyl-2-thiazolyl)-2,5-diphenyl-2H-tetrazolium bromide (MTT) assay [30]. Cells (5000) were seeded in 96-well microculture plates with increasing concentrations of germacranolides for 24 or 72 h at 37 °C. The IC₅₀ values were determined graphically for each

experiment as described previously [27]. Values are means \pm standard errors of the means S.E.M. from at least three independent experiments, with three determinations each.

3.3. Evaluation of Apoptosis

Fluorescent microscopy, flow cytometric analysis of annexin V-FITC and propidium iodide-stained nuclei were performed as described [28]. Briefly, for fluorescent microscopy, cells were washed with phosphate buffered saline PBS, fixed in 3% paraformaldehyde, and stained with 20 μ g/mL Hoechst 33258. For flow cytometry of propidium iodide-stained cells, cells were fixed in 70% ethanol overnight at -20°C and then washed in PBS, incubated in the dark with 1 U/mL RNase A (DNase free) and 10 μ g/mL of propidium iodide at room temperature. Double staining with annexin V-fluoresceine isothiocyanate (FITC) and propidium iodide was performed using an Annexin V-FITC apoptosis detection kit (BD PharMingen, San Diego, CA, USA) according to the manufacturer's protocol. All flow cytometry assays were performed using a BD FACSVerser cytometer (BD Biosciences, San Jose, CA, USA).

3.4. Western Blot Analysis and Subcellular Fractionation

Western blot analyses of caspases, PARP, Bcl-2 family members, and MAPKs and cytochrome *c* release from mitochondria were performed as described previously [28]. Briefly, for whole-cell lysates cells were resuspended in lysis buffer (20 mM Tris-HCl (pH 7.4) containing 1% Triton X-100, 20 mM sodium β -glycerophosphate, 10 mM NaF, 2 mM EDTA, 2 mM tetrasodium pyrophosphate, 10% glycerol, 137 mM NaCl, 2 mM sodium orthovanadate, and protease inhibitors (1 mM phenylmethylsulfonyl fluoride and 1 μ g/mL leupeptin and aprotinin)), sonicated, and centrifuged. For the subcellular fractionation to determine cytochrome *c* release, cells were resuspended in ice-cold buffer [20 mM HEPES (pH 7.5), 250 mM sucrose, 10 mM KCl, 1.5 mM MgCl_2 , 1 mM EGTA, 1 mM EDTA, 1 mM dithiothreitol, 0.1 mM phenylmethylsulfonyl fluoride, and 1 μ g/mL aprotinin, leupeptin, and pepstatin A], lysed by being pushed them several times through a 22-gauge needle, and the lysate was centrifuged at $1000\times g$ for 5 min at 4°C to eliminate nuclei and unbroken cells. The resulting supernatant was centrifuged to $10,000\times g$ at 4°C for 20 min to obtain the mitochondrial fraction. The supernatant was centrifuged again at $105,000\times g$ for 45 min at 4°C and the resulting supernatant was used as the soluble cytosolic fraction.

Samples containing equal amounts of proteins were separated by electrophoresis, transferred to poly(vinylidene difluoride) membranes, and probed with specific antibodies. The primary antibodies used for Western blots were purchased from the following companies: anti-caspase-3 (ADI-AAP-113), -7 (ADI-AAM-137), -8 (ADI-AAM-118), and -9 (ADI-AAM-139) from Enzo (Plymouth Meeting, PA, USA); anti-caspase-4 monoclonal antibody (M029-3) from Medical and Biological Laboratories (Nagoya, Japan); anti-poly(ADP-ribose) polymerase (PARP) (551024) and anti-cytochrome *c* (556433) from BD Pharmingen (San Diego, CA, USA); anti-Bcl-2 (#2872), anti-Bax (#2772), anti-Bid (#2002), anti-JNK/SAPK (#9252), antiphospho-JNK/SAPK (phosphor T183 + Y185) (#9251), anti-ERK1/2 (#9102), antiphospho-ERK1/2 (T202/Y204) (#9101), anti-p38^{MAPK} (#9212), and anti-phospho-p38^{MAPK} (T180/Y182) (#9211) antibodies from Cell Signaling Technology (Beverly, MA, USA); anti- β -actin (clone AC-74, A2228) and anti- α -tubulin (clone B-5-1-2, T6074) from Sigma-Aldrich (Saint Louis, MO, USA); mouse monoclonal COX IV antibody (mAbcam33985) from Abcam (Cambridge, UK). Secondary antibodies (NA9310 and NA9340) were from GE Healthcare (Little Chalfont, UK). Polyvinylidene difluoride (PVDF) membranes were from Millipore (Temecula, CA, USA).

3.5. Assays of Caspase Activity

Caspase-3/7, caspase-8, and caspase-9 activities were determined by measuring proteolytic cleavage of specific colorimetric substrates. Specifically labeled substrates for caspase-3 like protease, -8 and -9 activities were DEVD-*p*NA (*N*-acetyl-Asp-Glu-Val-Asp-*p*-nitroaniline), IETD-*p*NA (*N*-acetyl-Ile-Glu-Thr-Asp-*p*-nitroaniline), and LEHD-*p*NA (*N*-acetyl-Leu-Glu-His-Asp-*p*-nitroaniline),

respectively. Equal amounts of protein were used and absorbance was recorded at 405 nm as previously described [28].

3.6. Analysis of Mitochondrial Transmembrane Potential ($\Delta\psi_m$) and Determination of Intracellular Reactive Oxygen Species (ROS) Levels

The mitochondrial membrane potential and ROS levels were determined by flow cytometry using the fluorochromes JC-1 (5,5',6,6'-tetrachloro-1,1',3,3'-tetraethylbenzimidazolylcarbocyanine iodide) and H₂-DCF-DA (2',7'-dichlorodihydrofluorescein diacetate), respectively. Fluorescence of JC-1 was detected at excitation and emission wavelengths of 527 and 590 nm, respectively. Fluorescence of 2',7'-dichlorofluorescein was detected at excitation and emission wavelengths of 488 and 530 nm, respectively. Internal controls using unlabeled cells indicated that spiciformin (1) and spiciformin acetate (2) autofluorescence was null at all assayed conditions. All of the methods have been described in detail elsewhere [28].

3.7. Statistical Analysis

Statistical differences between means of control and treated samples were tested using Student's *t*-test (two samples) or one-way ANOVA (3 or more samples) with Tukey's test used for *a posteriori* pairwise comparisons of means. *P*-values below 0.05 were considered as statistically significant.

4. Conclusions

In conclusion, spiciformin (1) and spiciformin acetate (2) are cytotoxic against the human acute myeloid leukemia cells, including cells that overexpress Bcl-2, and display less cytotoxicity against the melanoma cell line SK-MEL-1 and mononuclear cells isolated from healthy volunteers. Human U-937 cells responding to germacranolides 1 and 2 manifested a great reduction in the levels of the anti-apoptotic protein Bcl-2. The mechanism of cytotoxicity triggered by these sesquiterpene lactones was due to caspase-dependent apoptosis and associated with mitogen-activated protein kinase pathway activation and reactive oxygen species generation. The results support that these sesquiterpene lactones have an impact in at least two cellular hallmarks of cancer, such as resistance to apoptosis and sustained proliferative signaling. However, the early mode of action of these compounds and relative signaling cascade remains to be elucidated in more detail.

Author Contributions: E.S., F.E.-S., M.S., and S.R. performed biological experiments. J.L.E. prepared and characterized the compounds. J.Q. and F.E. analyzed the data. F.E. designed the experiments and wrote the paper. All authors have read and agreed to the published version of the manuscript.

Funding: This research was funded by FEDER and AGENCIA CANARIA DE INVESTIGACIÓN, INNOVACIÓN Y SOCIEDAD DE LA INFORMACIÓN (PROID2017010095 FEDER/ACIISI).

Acknowledgments: The authors would like to thank J. Bréard for supplying U-937/Bcl-2 cells.

Conflicts of Interest: The authors declare no conflict of interest. The funders had no role in the design of the study; in the collection, analyses, or interpretation of data; in the writing of the manuscript, or in the decision to publish the results.

References

1. Carugo, A.; Draetta, G.F. Academic discovery of anticancer drugs: Historic and future perspectives. *Annu. Rev. Cancer Biol.* **2019**, *3*, 385–408. [\[CrossRef\]](#)
2. Lai, C.; Doucette, K.; Norsworthy, K. Recent drug approvals for acute myeloid leukemia. *J. Hematol. Oncol.* **2019**, *12*, 100. [\[CrossRef\]](#) [\[PubMed\]](#)
3. Döhner, H.; Weisdorf, D.J.; Bloomfield, C.D. Acute myeloid leukemia. *N. Engl. J. Med.* **2015**, *373*, 1136–1152. [\[CrossRef\]](#)
4. Newman, D.J.; Cragg, G.M. Natural products as sources of new drugs from 1981 to 2014. *J. Nat. Prod.* **2016**, *79*, 629–661. [\[CrossRef\]](#) [\[PubMed\]](#)

5. Merfort, I. Perspectives on sesquiterpene lactones in inflammation and cancer. *Curr. Drug Targets* **2011**, *12*, 1560–1573. [\[CrossRef\]](#)
6. Quintana, J.; Estévez, F. Recent advances on cytotoxic sesquiterpene lactones. *Curr. Pharm. Des.* **2018**, *24*, 4355–4361. [\[CrossRef\]](#)
7. Guzman, M.L.; Rossi, R.M.; Karnischky, L.; Li, X.; Peterson, D.R.; Howard, D.S.; Jordan, C.T. The sesquiterpene lactone parthenolide induces apoptosis of human acute myelogenous leukemia stem and progenitor cells. *Blood* **2005**, *105*, 4163–4169. [\[CrossRef\]](#)
8. Ghantous, A.; Gali-Muhtasib, H.; Vuorela, H.; Saliba, N.A.; Darwiche, N. What made sesquiterpene lactones reach cancer clinical trials? *Drug Discov. Today* **2010**, *15*, 668–678. [\[CrossRef\]](#)
9. da Silva Castro, E.; Alves Antunes, L.A.; Revoredo Lobo, J.F.; Ratcliffe, N.A.; Borges, R.M.; Rocha, L.; Burth, P.; Fonte Amorim, L.M. Antileukemic properties of sesquiterpene lactones: A systematic review. *Anticancer Agents Med. Chem.* **2018**, *18*, 323–334. [\[CrossRef\]](#)
10. Fuchs, Y.; Steller, H. Live to die another way: Modes of programmed cell death and the signals emanating from dying cells. *Nat. Rev. Mol. Cell Biol.* **2015**, *16*, 329–344. [\[CrossRef\]](#)
11. Green, D.R.; Llamby, F. Cell death signaling. *Cold Spring Harb. Perspect. Biol.* **2015**, *7*, a006080. [\[CrossRef\]](#) [\[PubMed\]](#)
12. Hensley, P.; Mishra, M.; Kyprianou, N. Targeting caspases in cancer therapeutics. *Biol. Chem.* **2013**, *394*, 831–843. [\[CrossRef\]](#) [\[PubMed\]](#)
13. Shalini, S.; Dorstyn, L.; Dawar, S.; Kumar, S. Old, new and emerging functions of caspases. *Cell Death Differ.* **2015**, *22*, 526–539. [\[CrossRef\]](#) [\[PubMed\]](#)
14. Julien, O.; Wells, J.A. Caspases and their substrates. *Cell Death Differ.* **2017**, *24*, 1380–1389. [\[CrossRef\]](#)
15. Tait, S.W.; Green, D.R. Mitochondrial regulation of cell death. *Cold Spring Harb. Perspect. Biol.* **2013**, *5*, a008706. [\[CrossRef\]](#)
16. Czabotar, P.E.; Lessene, G.; Strasser, A.; Adams, J.M. Control of apoptosis by the BCL-2 protein family: Implications for physiology and therapy. *Nat. Rev. Mol. Cell Biol.* **2014**, *15*, 49–63. [\[CrossRef\]](#)
17. Ashkenazi, A. Targeting the extrinsic apoptotic pathway in cancer: Lessons learned and future directions. *J. Clin. Invest.* **2015**, *125*, 487–489. [\[CrossRef\]](#)
18. Flusberg, D.A.; Sorger, P.K. Surviving apoptosis: Life-death signaling in single cells. *Trends Cell Biol.* **2015**, *25*, 446–458. [\[CrossRef\]](#)
19. Fulda, S. Targeting apoptosis for anticancer therapy. *Semin. Cancer Biol.* **2015**, *31*, 84–88. [\[CrossRef\]](#)
20. Triana, J.; Eiroa, J.L.; Morales, M.; Pérez, F.J.; Brouard, I.; Marrero, M.T.; Estévez, S.; Quintana, J.; Estévez, F.; Castillo, Q.A.; et al. A chemotaxonomic study of endemic species of genus *Tanacetum* from the Canary Islands. *Phytochemistry* **2013**, *92*, 87–104. [\[CrossRef\]](#)
21. Warren, C.F.A.; Wong-Brown, M.W.; Bowden, N.A. BCL-2 family isoforms in apoptosis and cancer. *Cell Death Dis.* **2019**, *10*, 177. [\[CrossRef\]](#) [\[PubMed\]](#)
22. D'Anneo, A.; Carlisi, D.; Lauricella, M.; Emanuele, S.; Di Fiore, R.; Vento, R.; Tesoriere, G. Parthenolide induces caspase-independent and AIF-mediated cell death in human osteosarcoma and melanoma cells. *J. Cell. Physiol.* **2013**, *228*, 952–967. [\[CrossRef\]](#) [\[PubMed\]](#)
23. Suvannasankha, A.; Crean, C.D.; Shanmugam, R.; Farag, S.S.; Abonour, R.; Boswell, H.S.; Nakshatri, H. Antimyeloma effects of a sesquiterpene lactone parthenolide. *Clin. Cancer Res.* **2008**, *14*, 1814–1822. [\[CrossRef\]](#) [\[PubMed\]](#)
24. Kantari, C.; Walczak, H. Caspase-8 and bid: Caught in the act between death receptors and mitochondria. *Biochim. Biophys. Acta* **2011**, *1813*, 558–563. [\[CrossRef\]](#) [\[PubMed\]](#)
25. Tobiume, K.; Matsuzawa, A.; Takahashi, T.; Nishitoh, H.; Morita, K.; Takeda, K.; Minowa, O.; Miyazono, K.; Noda, T.; Ichijo, H. ASK1 is required for sustained activations of JNK/p38 MAP kinases and apoptosis. *EMBO Rep.* **2001**, *2*, 222–228. [\[CrossRef\]](#) [\[PubMed\]](#)
26. Liu, M.; Zhao, G.; Cao, S.; Zhang, Y.; Li, X.; Lin, X. Development of certain protein kinase inhibitors with the components from traditional chinese medicine. *Front. Pharmacol.* **2017**, *7*, 523. [\[CrossRef\]](#)
27. Estévez-Sarmiento, F.; Said, M.; Brouard, I.; León, F.; García, C.; Quintana, J.; Estévez, F. 3'-Hydroxy-3,4'-dimethoxyflavone blocks tubulin polymerization and is a potent apoptotic inducer in human SK-MEL-1 melanoma cells. *Bioorg. Med. Chem.* **2017**, *25*, 6060–6070. [\[CrossRef\]](#)

28. Estévez-Sarmiento, F.; Hernández, E.; Brouard, I.; León, F.; García, C.; Quintana, J.; Estévez, F. 3'-Hydroxy-3,4'-dimethoxyflavone-induced cell death in human leukaemia cells is dependent on caspases and reactive oxygen species and attenuated by the inhibition of JNK/SAPK. *Chem. Biol. Interact.* **2018**, *288*, 1–11. [[CrossRef](#)]
29. Rubio, S.; Quintana, J.; Eiroa, J.L.; Triana, J.; Estévez, F. Acetyl derivative of quercetin 3-methyl ether-induced cell death in human leukemia cells is amplified by the inhibition of ERK. *Carcinogenesis* **2007**, 2105–2113. [[CrossRef](#)]
30. Mosmann, T. Rapid colorimetric assay for cellular growth and survival: Application to proliferation and cytotoxicity assays. *J. Immunol. Methods* **1983**, *65*, 55–63. [[CrossRef](#)]



© 2020 by the authors. Licensee MDPI, Basel, Switzerland. This article is an open access article distributed under the terms and conditions of the Creative Commons Attribution (CC BY) license (<http://creativecommons.org/licenses/by/4.0/>).

Conclusiones

1. La chalcona sintética 6'-benciloxi-4-bromo-2'-hidroxichalcona (CHAL) presenta mayor citotoxicidad y estabilidad que los análogos ensayados; y exhibe propiedades citotóxicas potentes frente a distintas líneas celulares de leucemia humana, incluidas las células que expresan niveles elevados de Bcl-2 y la glicoproteína P implicadas en la multiresistencia a fármacos; por el contrario exhibe menor grado de citotoxicidad en células mononucleares de sangre periférica.
2. La inhibición del crecimiento de las células U-937 inducida por CHAL está causada por la activación de la muerte celular apoptótica y depende de la generación de especies reactivas de oxígeno, está asociada con la activación de múltiples caspasas y es bloqueada por los inhibidores de las caspasas -3/7, -6 y -8, por los inhibidores de las catepsinas B/L y por la expresión de niveles elevados de Bcl-2.
3. Se han establecido las relaciones estructura-actividad de un grupo de naftilchalconas y sus correspondientes flavanonas. Determinadas naftilchalconas son más potentes que sus correspondientes flavanonas, indicando que la flexibilidad estructural es importante en la citotoxicidad. La presencia de un grupo metoxi en la posición 5' en el anillo A de la naftilchalcona, o en la posición 6 en el anillo A de la correspondiente naftilflavanona, potencia la citotoxicidad frente a las células U-937.
4. La flavanona sintética 6-metoxi-2-naftilcroman-4-ona es citotóxica frente a cuatro líneas celulares de leucemia humana, con valores de IC₅₀

comparables con los del compuesto antitumoral etopósido, pero no lo es frente a células mononucleares de sangre periférica humana de donantes sanos.

5. La citotoxicidad inducida por la naftilflavanona implica apoptosis por activación y procesamiento de las caspasas iniciadoras -8 y -9 y las caspasas ejecutoras -3, -6, y -7, y es atenuada por el inhibidor general de las caspasas z-VAD-fmk. Además, está asociada con la fosforilación de las proteínas activadas por mitógenos ERK 1/2, JNK 1/2 y p38^{MAPK} y la apoptosis se reduce por la inhibición de MEK 1/2 y JNK1/2.
6. La lactona sesquiterpénica acetil-espiciformina es más citotóxica que el su precursor frente a las células tumorales humanas. Ambas son citotóxicas frente a las células de leucemia mieloide aguda humana, incluidas las células que expresan niveles elevados de Bcl-2, y son menos tóxicas frente a las células de melanoma humano SK-MEL-1 y sobre las células mononucleares sanguíneas aisladas de voluntarios sanos.
7. La citotoxicidad desencadenada por la espiciformina y el acetato de espiciformina implica la estimulación de la apoptosis dependiente de caspasas y está asociada con la activación de la vía de las proteínas quinasas activadas por mitógenos y con la generación de especies reactivas de oxígeno.

Referencias

- [1] Kartal-Yandim M, Adan-Gokbulut A, Baran Y. Molecular mechanisms of drug resistance and its reversal in cancer. *Crit Rev Biotechnol*. 2016; 36:716-26. doi: 10.3109/07388551.2015.1015957.
- [2] Maioral MF, Gaspar PC, Rosa Souza GR, Mascarello A, Chiaradia LD, Licínio MA, Moraes AC, Yunes RA, Nunes RJ, Santos-Silva MC. Apoptotic events induced by synthetic naphthylchalcones in human acute leukemia cell lines. *Biochimie*. 2013; 95:866-74. doi: 10.1016/j.biochi.2012.12.001.
- [3] Ren Y, Yu J, Kinghorn AD. Development of Anticancer Agents from Plant-Derived Sesquiterpene Lactones. *Curr Med Chem*. 2016; 23:2397-420. doi: 10.2174/0929867323666160510123255.
- [4] Loa J, Chow P, Zhang K. Studies of structure-activity relationship on plant polyphenol-induced suppression of human liver cancer cells. *Cancer Chemother Pharmacol*. 2009; 63:1007-16. doi: 10.1007/s00280-008-0802-y.
- [5] da Silva Castro E, Alves Antunes LA, Revoredo Lobo JF, Ratcliffe NA, Borges RM, Rocha L, Burth P, Fonte Amorim LM. Antileukemic Properties of Sesquiterpene Lactones: A Systematic Review. *Anticancer Agents Med Chem*. 2018; 18:323-334. doi: 10.2174/1871520617666170918130126.
- [6] Adewole KE. Nigerian antimalarial plants and their anticancer potential: A review. *J Integr Med*. 2020; 18:92-113. doi: 10.1016/j.joim.2020.01.001.
- [7] Rengarajan T, Rajendran P, Nandakumar N, Balasubramanian MP, Nishigaki I. Cancer preventive efficacy of marine carotenoid fucoxanthin: cell cycle arrest and apoptosis. *Nutrients*. 2013; 5:4978-89. doi: 10.3390/nu5124978.

- [8] Cabrera J, Saavedra E, Del Rosario H, Perdomo J, Loro JF, Cifuentes DA, Tonn CE, García C, Quintana J, Estévez F. Gardenin B-induced cell death in human leukemia cells involves multiple caspases but is independent of the generation of reactive oxygen species. *Chem Biol Interact.* 2016; 256:220-7. doi: 10.1016/j.cbi.2016.07.016.
- [9] Newman DJ, Cragg GM. Natural Products as Sources of New Drugs from 1981 to 2014. *J Nat Prod.* 2016; 79:629-61. doi: 10.1021/acs.jnatprod.5b01055.
- [10] Liu RH. Health-promoting components of fruits and vegetables in the diet. *Adv Nutr.* 2013; 4:384S-92S. doi: 10.3945/an.112.003517.
- [11] Chikara S, Nagaprashantha LD, Singhal J, Horne D, Awasthi S, Singhal SS. Oxidative stress and dietary phytochemicals: Role in cancer chemoprevention and treatment. *Cancer Lett.* 2018; 413:122-134. doi: 10.1016/j.canlet.2017.11.002.
- [12] Gonçalves CFL, de Freitas ML, Ferreira ACF. Flavonoids, Thyroid Iodide Uptake and Thyroid Cancer-A Review. *Int J Mol Sci.* 2017; 18:1247. doi: 10.3390/ijms18061247.
- [13] Spatafora C, Tringali C. Natural-derived polyphenols as potential anticancer agents. *Anticancer Agents Med Chem.* 2012; 12:902-18. doi: 10.2174/187152012802649996.

- [14] Loa J, Chow P, Zhang K. Studies of structure-activity relationship on plant polyphenol-induced suppression of human liver cancer cells. *Cancer Chemother Pharmacol*. 2009; 63:1007-16. doi: 10.1007/s00280-008-0802-y.
- [15] Raffa D, Maggio B, Raimondi MV, Plescia F, Daidone G. Recent discoveries of anticancer flavonoids. *Eur J Med Chem*. 2017; 142:213-228. doi: 10.1016/j.ejmech.2017.07.034.
- [16] Chang H, Lei L, Zhou Y, Ye F, Zhao G. Dietary Flavonoids and the Risk of Colorectal Cancer: An Updated Meta-Analysis of Epidemiological Studies. *Nutrients*. 2018; 10:950. doi: 10.3390/nu10070950.
- [17] Saikali M, Ghantous A, Halawi R, Talhouk SN, Saliba NA, Darwiche N. Sesquiterpene lactones isolated from indigenous Middle Eastern plants inhibit tumor promoter-induced transformation of JB6 cells. *BMC Complement Altern Med*. 2012; 12:89. doi: 10.1186/1472-6882-12-89.
- [18] Sak K. Cytotoxicity of dietary flavonoids on different human cancer types. *Pharmacogn Rev*. 2014; 8:122-46. doi: 10.4103/0973-7847.134247.
- [19] Ravishankar D, Rajora AK, Greco F, Osborn HM. Flavonoids as prospective compounds for anti-cancer therapy. *Int J Biochem Cell Biol*. 2013; 45:2821-31. doi: 10.1016/j.biocel.2013.10.004.
- [20] Orlikova B, Tasdemir D, Golais F, Dicato M, Diederich M. Dietary chalcones with chemopreventive and chemotherapeutic potential. *Genes Nutr*. 2011; 6:125-47. doi: 10.1007/s12263-011-0210-5.

[21] Cabrera M, Simoens M, Falchi G, Lavaggi ML, Piro OE, Castellano EE, Vidal A, Azqueta A, Monge A, de Ceráin AL, Sagrera G, Seoane G, Cerecetto H, González M. Synthetic chalcones, flavanones, and flavones as antitumoral agents: biological evaluation and structure-activity relationships. *Bioorg Med Chem.* 2007; 5;15:3356-67. doi: 10.1016/j.bmc.2007.03.031.

[22] Quintana J, Estévez F. Recent Advances on Cytotoxic Sesquiterpene Lactones. *Curr Pharm Des.* 2018; 24:4355-4361. doi: 10.2174/1381612825666190119114323.

[23] Duronio RJ, Xiong Y. Signaling pathways that control cell proliferation. *Cold Spring Harb Perspect Biol.* 2013; 5:a008904. doi: 10.1101/cshperspect.a008904.

[24] Mens MMJ, Ghanbari M. Cell Cycle Regulation of Stem Cells by MicroRNAs. *Stem Cell Rev Rep.* 2018; 14:309-322. doi: 10.1007/s12015-018-9808-y.

[25] Wenzel ES, Singh ATK. Cell-cycle Checkpoints and Aneuploidy on the Path to Cancer. *In Vivo.* 2018; 32:1-5. doi: 10.21873/in vivo.11197.

[26] Harashima H, Dissmeyer N, Schnittger A. Cell cycle control across the eukaryotic kingdom. *Trends Cell Biol.* 2013; 23:345-56. doi: 10.1016/j.tcb.2013.03.002.

[27] Stafman LL, Beierle EA. Cell Proliferation in Neuroblastoma. *Cancers (Basel).* 2016; 8:13. doi: 10.3390/cancers8010013.

[28] Liu G, Pei F, Yang F, Li L, Amin AD, Liu S, Buchan JR, Cho WC. Role of Autophagy and Apoptosis in Non-Small-Cell Lung Cancer. *Int J Mol Sci.* 2017; 18:367. doi: 10.3390/ijms18020367.

[29] Fujita K, Iwama H, Oura K, Tadokoro T, Samukawa E, Sakamoto T, Nomura T, Tani J, Yoneyama H, Morishita A, Himoto T, Hirashima M, Masaki T. Cancer Therapy Due to Apoptosis: Galectin-9. *Int J Mol Sci.* 2017; 18:74. doi: 10.3390/ijms18010074.

[30] Derakhshan A, Chen Z, Van Waes C. Therapeutic Small Molecules Target Inhibitor of Apoptosis Proteins in Cancers with Deregulation of Extrinsic and Intrinsic Cell Death Pathways. *Clin Cancer Res.* 2017; 23:1379-1387. doi: 10.1158/1078-0432.CCR-16-2172.

[31] Wong RS. Apoptosis in cancer: from pathogenesis to treatment. *J Exp Clin Cancer Res.* 2011; 30:87. doi: 10.1186/1756-9966-30-87.

[32] Stevens M, Oltean S. Modulation of the Apoptosis Gene Bcl-x Function Through Alternative Splicing. *Front Genet.* 2019; 10:804. doi: 10.3389/fgene.2019.00804.

[33] Pistritto G, Trisciuglio D, Ceci C, Garufi A, D'Orazi G. Apoptosis as anticancer mechanism: function and dysfunction of its modulators and targeted therapeutic strategies. *Aging (Albany NY).* 2016; 8:603-19. doi: 10.18632/aging.100934.

[34] Ding J, Mooers BH, Zhang Z, Kale J, Falcone D, McNichol J, Huang B, Zhang XC, Xing C, Andrews DW, Lin J. After embedding in membranes

antiapoptotic Bcl-XL protein binds both Bcl-2 homology region 3 and helix 1 of proapoptotic Bax protein to inhibit apoptotic mitochondrial permeabilization. *J Biol Chem.* 2014; 289:11873-96. doi: 10.1074/jbc.M114.552562.

[35] Burke PJ. Mitochondria, Bioenergetics and Apoptosis in Cancer. *Trends Cancer.* 2017; 3:857-870. doi: 10.1016/j.trecan.2017.10.006.

[36] D'Arcy MS. Cell death: a review of the major forms of apoptosis, necrosis and autophagy. *Cell Biol Int.* 2019; 43:582-592. doi: 10.1002/cbin.11137.

[37] Fu TM, Li Y, Lu A, Li Z, Vajjhala PR, Cruz AC, Srivastava DB, DiMaio F, Penczek PA, Siegel RM, Stacey KJ, Egelman EH, Wu H. Cryo-EM Structure of Caspase-8 Tandem DED Filament Reveals Assembly and Regulation Mechanisms of the Death-Inducing Signaling Complex. *Mol Cell.* 2016; 64:236-250. doi: 10.1016/j.molcel.2016.09.009.

[38] Sung ES, Park KJ, Lee SH, Jang YS, Park SK, Park YH, Kwag WJ, Kwon MH, Kim YS. A novel agonistic antibody to human death receptor 4 induces apoptotic cell death in various tumor cells without cytotoxicity in hepatocytes. *Mol Cancer Ther.* 2009; 8:2276-85. doi: 10.1158/1535-7163.MCT-09-0235.

[39] Pizzino G, Irrera N, Cucinotta M, Pallio G, Mannino F, Arcoraci V, Squadrito F, Altavilla D, Bitto A. Oxidative Stress: Harms and Benefits for Human Health. *Oxid Med Cell Longev.* 2017; 2017:8416763. doi: 10.1155/2017/8416763.

[40] Redza-Dutordoir M, Averill-Bates DA. Activation of apoptosis signalling pathways by reactive oxygen species. *Biochim Biophys Acta.* 2016; 1863:2977-2992. doi: 10.1016/j.bbamcr.2016.09.012.

- [41] Sinha K, Das J, Pal PB, Sil PC. Oxidative stress: the mitochondria-dependent and mitochondria-independent pathways of apoptosis. *Arch Toxicol*. 2013; 87:1157-80. doi: 10.1007/s00204-013-1034-4.
- [42] Cabukusta B, Neeffes J. Mechanisms of lysosomal positioning and movement. *Traffic*. 2018; 19:761-769. doi: 10.1111/tra.12587.
- [43] Linder S, Shoshan MC. Lysosomes and endoplasmic reticulum: targets for improved, selective anticancer therapy. *Drug Resist Updat*. 2005; 8:199-204. doi: 10.1016/j.drug.2005.06.004.
- [44] Fennelly C, Amaravadi RK. Lysosomal Biology in Cancer. *Methods Mol Biol*. 2017; 1594:293-308. doi: 10.1007/978-1-4939-6934-0_19.
- [45] Cirman T, Oresić K, Mazovec GD, Turk V, Reed JC, Myers RM, Salvesen GS, Turk B. Selective disruption of lysosomes in HeLa cells triggers apoptosis mediated by cleavage of Bid by multiple papain-like lysosomal cathepsins. *J Biol Chem*. 2004; 279:3578-87. doi: 10.1074/jbc.M308347200.
- [46] Oakes SA, Papa FR. The role of endoplasmic reticulum stress in human pathology. *Annu Rev Pathol*. 2015; 10:173-94. doi: 10.1146/annurev-pathol-012513-104649.
- [47] Wang M, Kaufman RJ. Protein misfolding in the endoplasmic reticulum as a conduit to human disease. *Nature*. 2016; 529:326-35. doi: 10.1038/nature17041.

- [48] Oakes SA. Endoplasmic reticulum proteostasis: a key checkpoint in cancer. *Am J Physiol Cell Physiol.* 2017; 312:C93-C102. doi: 10.1152/ajpcell.00266.2016.
- [49] Cubillos-Ruiz JR, Bettigole SE, Glimcher LH. Tumorigenic and Immunosuppressive Effects of Endoplasmic Reticulum Stress in Cancer. *Cell.* 2017; 168:692-706. doi: 10.1016/j.cell.2016.12.004.
- [50] Soustek MS, Balsa E, Barrow JJ, Jedrychowski M, Vogel R, Jan Smeitink, Gygi SP, Puigserver P. Inhibition of the ER stress IRE1 α inflammatory pathway protects against cell death in mitochondrial complex I mutant cells. *Cell Death Dis.* 2018; 9:658. doi: 10.1038/s41419-018-0696-5.
- [51] Kang SJ, Lee YJ, Kang SG, Cho S, Yoon W, Lim JH, Min SH, Lee TH, Kim BM. Caspase-4 is essential for saikosaponin a-induced apoptosis acting upstream of caspase-2 and γ -H2AX in colon cancer cells. *Oncotarget.* 2017; 8:100433-100448. doi: 10.18632/oncotarget.22247.
- [52] Moon HW, Han HG, Jeon YJ. Protein Quality Control in the Endoplasmic Reticulum and Cancer. *Int J Mol Sci.* 2018; 19:3020. doi: 10.3390/ijms19103020.
- [53] Ou L, Lin S, Song B, Liu J, Lai R, Shao L. The mechanisms of graphene-based materials-induced programmed cell death: a review of apoptosis, autophagy, and programmed necrosis. *Int J Nanomedicine.* 2017; 12:6633-6646. doi: 10.2147/IJN.S140526.

[54] Lu M, Wang Y, Zhan X. The MAPK Pathway-Based Drug Therapeutic Targets in Pituitary Adenomas. *Front Endocrinol (Lausanne)*. 2019; 10:330. doi: 10.3389/fendo.2019.00330.

[55] Kim EK, Choi EJ. Compromised MAPK signaling in human diseases: an update. *Arch Toxicol*. 2015; 89:867-82. doi: 10.1007/s00204-015-1472-2.

[56] Low HB, Zhang Y. Regulatory Roles of MAPK Phosphatases in Cancer. *Immune Netw*. 2016; 16:85-98. doi: 10.4110/in.2016.16.2.85.

